TRANSPORT PROPERTIES OF CONCRETE WITH LIGHTWEIGHT AGGREGATES

LIU XUEMEI

NATIONAL UNIVERSITY OF SINGAPORE

2009

TRANSPORT PROPERTIES OF CONCRETE WITH LIGHTWEIGHT AGGREGATES

LIU XUEMEI

(*M.Eng. Tianjin University*)
(*B.Eng., Shandong Jianzhu University*)

A THESIS SUBMITTED
FOR THE DEGREE OF DOCTOR OF PHILOSOPHY
DEPARTMENT OF CIVIL ENGINEERING
NATIONAL UNIVERSITY OF SINGAPORE

2009

Dedicated to my parents...

ACKNOWLEDGEMENTS

First and foremost I offer my sincere appreciation and deep gratitude to my supervisor, Associate Professor Zhang Min-Hong for her supervision, invaluable guidance, continuous encouragement, constructive advices and ultimate patience throughout the entire course of this research. She offers advices and suggestions whenever I need. Without her, this thesis would not be possible.

Associate Professor Ong Khim Chye and Dr Tam Chat Tim deserve special thanks as my thesis committee members for their helpful suggestions, constructive comments, and valuable discussions.

Research scholarship awarded by National University of Singapore is gratefully acknowledged. The heartfelt appreciation is dedicated to Dr. Chia Kok Seng for his valuable advices, suggestions and help. I gratefully acknowledge Dr. Brouwers H.J.H. and Dr. Michelle R. Nokken for their help and valuable comments. Great appreciation goes to Sun Dao Jun, Dr. Kyaw Miynt Lay, Dr. Wang Zeng Rong, Lado Riannevo Chandra, and Xiao Hua Wen for their sharing, help and discussions.

This research would not have been successfully completed without the kind assistance from lab technicians at Structural and Concrete Laboratory. Special thanks go to Mr. Ang Beng Oon, Mr. Choo Peng Kin, and Ms. Tan Annie for their generous and kind support for experimental work. Appreciation also goes to Mr. Lim Huay Bak,

Mr. Koh Yian Kheag, and Mr. Yong Tat Fah. Thanks also go to Qi Feng who helped with sample preparation for SEM.

I would like to express my gratitude to the undergraduate students who contributed to the experimental work. They are Yap Miin Kai, Allen Fong Hui Seng, Lui Wing Fai, and Dang Yang. Acknowledgements are also given to those who have in one way or another contributed to this research and to the authors of various papers and materials quoted in the references.

Great appreciations go to my dear friends Wang ShaSha, Rupika Swarnamala, Patria Kusumaningrum, Thanuja Krishanthi Kulathunga, Lee Siew Chin, Zhang SuFen, Gan ChengTi, Cheng Yong Gang, Ali Akbarnezhad, Fu Hongxia, Ma Wei, Du Hong Jian etc. for their help, friendship, and great encouragement. Great thanks go to those friends and colleagues, seniors and juniors, from both structural and geotechnical labs for their help and encouragement. Without all of you, the study life in NUS would not be so enjoyable.

This study would not be possible without the unconditioned love, incredible moral support and encouragement from my family for these years. Great appreciation goes to my mother and my sister.

Lastly, I offer my regards and blessings to all of those who supported me in any respect during the completion of this thesis and my study life in NUS.

TABLE OF CONTENT

SUMMARY

Literature review indicates that information on the transport properties of concrete with lightweight aggregate (LWA) for internal curing is limited. There are also contradicting opinions on the effect of LWA on the transport properties of concrete. In addition, there is a lack of information for predicting the transport properties of lightweight concrete (LWC). For structures exposed to severe environment, such information is essential. Therefore, this research is carried out.

This research investigates the effect of LWA on transport properties of concrete including water absorption, water permeability, and resistance to chloride ion penetration. It covers normal weight concretes (NWCs) in which LWA is used for internal curing, LWC where only coarse LWA is used, and LWC where all aggregates are lightweight. Effects of the cumulative LWA content, porosities and surface textures of LWA, and w/c of concrete on the transport properties of concrete are also investigated. Control NWCs and concrete with a shrinkage reducing admixture are also included for relative comparisons. Rapid chloride penetrability test (ASTM C 1202), rapid migration test (NT Build 492), and salt ponding test (AASHTO T 259) are conducted to evaluate the concrete resistance to chloride-ion penetration.

In general, concretes with LWA had water absorption and permeability similar to or lower than those of the NWC and concrete with shrinkage reducing admixture (SRA) with the same w/c 0.38. The charges passed, chloride migration coefficient and

chloride diffusion coefficient of such concretes were in the same order as those of the NWC and the concrete with SRA. When high-performance lightweight concrete, shrinkage reducing admixture or pre-soaked LWA can be used to reduce/eliminate autogenous shrinkage of concrete. Comparing LWAs of different sizes for internal curing, the increase in the more porous crushed lightweight particles in concrete seems to increase the penetration of chloride ions in the concrete.

The resistance of LWC to chloride ion penetration decreased with increase in the cumulative LWA content. The water penetration depth under pressure and water sorptivity showed, in general, similar trends. The increase in porosity of coarse LWA in concrete increased the sorptivity and permeability slightly compared to NWC of similar w/c. Fine LWA has more influence on the transport properties of concrete than coarse ones. For a given type of LWA, coarse LWA did not influence the water sorptivity and permeability significantly compared to NWC of similar w/c and mix proportion. Fine LWA has more influence on the transport properties than coarse LWA. For given size and content of coarse LWA, the more porous coarse LWA tends to reduce the resistance to water and chloride ion penetration of concrete.

In addition, LWC with very low unit weight about 1300 kg/m^3 but high resistance to water and chloride ion penetration was developed by using low w/cm, silica fume, and LWA with very low density. Such low unit weight has opened up a new avenue for potential use of LWC in marine environment for floating structures.

Based on the experimental results and regression analyses, empirical relationships of sorptivity, charge passed, and chloride migration coefficient versus the water accessible porosity and oven dry unit weight of the concrete are established. For both LWC and NWC, physical properties of water accessible porosity and unit weight can be easily determined in the laboratory. Using the empirical equations, the transport

properties of concrete can be estimated for quality control and for estimating durability of concrete.

Keywords: Absorption, Cement Paste, Chloride, Concrete, Diffusion, Interface Transition Zone, Internal curing, Lightweight aggregate, Migration, Permeability, Porosity, Sorptivity

LIST OF TABLES

LIST OF FIGURES

NOMENCLATURES

A	cross-sectional surface area/area of inflow surface;
B	weight of pycnometer and water (g);
BSE	back scattered electron;
c_d	chloride concentration at which the color changes (≈ 0.07 N for OPC concrete);
c_0	chloride concentration in the catholyte solution, and $c_0 \approx 2$ N;
C	chloride concentration (kg/m^3)/ concentration (mol/m^3).
C_f	cement factor (content) for concrete mixtures (kg/m^3);
C_T	total charge passed;
$C(x, t)$	chloride concentration at depth x and time t;
C_0	surface chloride concentration;
CS	chemical shrinkage of cement (g of water/g of cement);
d	depth of water penetration in concrete (m);
d_{cap}	diameter of the capillary;
d_0	a constant;
dh	head loss (m);
dL	flow path of length (m);
Δp	pressure difference;
D	oven dry unit weight of concrete (kg/m^3);
D_m	migration coefficient (m^2/s);

erf	error function;
f	mass flux (kg/m^{2}s);
f_a	total porosity of aggregate (%, by volume);
F	Faraday constant (9.648×10^4 J/(V mol));
$\mathbf{F_C}$	capillary force;
h	hydraulic head of water (m);
HPC	high performance concrete
i	cumulative mass absorbed per unit area of inflow surface (g/ mm^2);
ITZ	interface transition zone;
K	hydraulic diffusivity;
K_{d}	diffusion coefficient (or diffusivity) (m^2/s);
K_{u}	generalized or unsaturated permeability (or liquid conductivity);
K_P	water permeability coefficient (or hydraulic conductivity) (m/s);
K_{sd}	Steady state diffusion coefficient or diffusivity (m^2/s);
L	specimen thickness (m);
LWA	lightweight aggregate;
LWC	lightweight concrete;
m	gain in mass (g);
m_{a}	apparent weight of the saturated specimen immersed in water (kg);
m_e	empirical coefficient;
m_{o}	oven dry mass of the specimen in air (kg);
m_{s}	'saturated surface-dry mass' of the specimen in air (kg);
M	mass of water absorbed (g);
M_{LWA}	mass of (dry) fine LWA needed per unit volume of concrete (kg/m^3);
MIP	mercury intrusion porosimetry;

n	a tortuosity factor reflecting the devious path around hydrated and unhydrated material in cementitious materials, >1;
NWC	normal weight concrete;
P	injection pressure;
P_w	water accessible porosity;
Δp	pressure difference;
Q	flow rate (m^3/s);
r	pore radius;
R	gas constant (8.314 J/(V mol));
s	degree of saturation of aggregate (0 to 1);
S	water sorptivity ($g/mm^2/s^{0.5}$);
S_0	a constant, representing the initial disturbance of the water absorption (g/mm^2);
S'	penetration coefficient of the concrete;
SEM	scanning electron micrograph;
SRA	shrinkage reducing admixture;
t	time/ time under pressure /elapsed time (s);
T	average value of the initial and final temperatures in the anolyte solution (K);
u	flow velocity;
U	absolute value of the applied voltage (V);
v	apparent velocity of flow
V	a unit volume of pores in hardened cement paste;
W	weight of pycnometer, water and “saturated” aggregate (g);
W_0	weight of dry particle (g);

W_m	weight of "saturated" surface dry particle (g);
w/c	water to cement ratio;
w/cm	water to cementitious material ratio;
x	depth;
x_d	average value of the penetration depths (m);
z	absolute value of ion valence, for chloride z=1;
α	degree of cement hydration;
α_{max}	maximum expected degree of hydration of cement;
ϕ	Boltzmann variable;
ϕ_{cap}	porosity of capillary pores;
ϕ_{gel}	porosity of gel pores;
ϕ_{LWA}	absorption of lightweight aggregates (kg water/kg dry LWA);
γ	surface tension of the liquid;
η	viscosity;
μ	transport properties such as sorptivity, total charge passed, and migration coefficient;
θ	ratio of liquid to bulk volume
θ_s	volume fraction of the liquid content at saturation;
θ_d	volume fraction of the liquid content in nominal dry state;
θ_m	contact angle of the mercury;
ρ	density of water (about 1000 kg/m^3).
ρ_s	density of solid material (kg/m^3);
ρ_b	bulk density of aggregate particles (kg/m^3);

v	porosity of the concrete;
ψ	capillary potential;

CHAPTER 1 INTRODUCTION

1.1 Background

1.1.1 History of Lightweight Concrete

The word ‘concrete’ comes from the Latin ‘concretus’ which means compound. The development of concrete as a construction material dates back several thousand years to the days of the ancient Egyptians, the Greeks and the Romans. These early concrete compositions were based on pozzolana and lime. The roof of the Pantheon is testimony to the durability of this material. Today concrete is understood to consist of aggregates of different sizes bound together by hardened cement paste.

Concrete has an extensive role to play both in construction and improvement of buildings, roads, bridges, airports, railways, tunnels, ports and harbors and many other structures and infrastructures. When used for structures which require low unit weight of materials such as buildings with poor soil conditions, high-rise buildings, long-span bridges, and floating structures, lightweight aggregate concrete (LWC) has advantages due to its low unit weight compared with normal weight concrete (NWC). For structural applications, the concretes are usually designed based on equivalent 28-day compressive strength. By reducing the unit weight of concrete with given strength, the strength/weight ratio of the concrete can be increased. Low unit weight concrete also reduces self-weight of the structure, thus reduces requirements for foundation and construction costs of the structures.

The historical application of LWA and LWC is introduced in ACI 213R-03. Lightweight aggregates were first used in buildings over 2000 years ago. Sumerians used LWC in building Babylon in the 3rd millennium B.C. The Greeks and the Romans used natural pumice aggregate in concrete for such notable edifices as LWC St. Sofia Cathedral of Hagia Sofia in Istanbul, Turkey, built in the 4th century A.D.; the Pantheon, erected in the years of A.D. 118 to 128; the Roman aqueduct, pont du Gard, built in A.D. 14; and Colosseum, built between A.D. 70 and 82. Lightweight aggregate was also used in the construction of Pyramids during the Mayan period in Mexico. The industrial use of natural lightweight aggregates was started in 1845 in Germany by Ferdinand Nebel from Koblenz who produced masonry blocks from pumice, with burnt lime as binder. The lightweight aggregates have low particle density because of the cellular pore structure within the particles normally developed by heating certain raw materials to incipient fusion. At this fusion temperature, gases are evolved within the pyroplastic mass, causing expansion, which is retained upon cooling. The use of lightweight aggregates contributes to the low unit weight of LWC.

However, the lightweight aggregates (LWA) are porous compared with rock based normal weight aggregates (NWA). Higher porosity of LWA may affect transport of water and ions in concrete. Most LWC used for long-span bridges and floating structures built in the last 30 years incorporated only coarse LWA.

1.1.2 Classification of Lightweight Aggregate and Lightweight Aggregate Concrete

1.1.2.1 Lightweight aggregate

Most types of the LWAs that are used by the construction industry today are manufactured materials, made from natural resources like clay and slate or from industrial by-products such as fly ash and glass. The products are commercially

available LWAs such as Leca, Solite (USA), Liapor, and Lytag. Naturally occurring lightweight aggregates are mined from volcanic deposites that include pumice and scoria. Pyroprocessing methods include the rotary kiln process (a long, slowly rotating, slightly inclined lined with refractory materials similar to cement kilns); the sintering process wherein a bed of was materials, including fuel, is carried by a traveling grate under an ignition hood; and the rapid agitation of molten slag with controlled amounts of air or water.

The increased usage of processed LWAs is evidence of environmentally sound planning, as theses products require less trucking and use of materials that have limited structural applications in their natural state, thus minimizing construction industry demands on finite resources of natural sands, stones, and gravels.

1.1.2.2 Lightweight aggregate concrete

According to ACI 213R-03 [2003], Guide for Structural Lightweight Aggregate Concrete, structural lightweight aggregate concretes are defined as those made with lightweight aggregate as defined in ASTM C 330, and with a minimum 28-day compressive strength of 17 MPa and equilibrium density between 1120 and 1920 kg/m^2. In some LWC, coarse lightweight aggregate (LWA) and normal weight fine aggregate are used (referred to as sand-LWC), whereas in others, both coarse and fine LWA are used (referred to as all-LWC).

1.1.3 Features of Lightweight Aggregate Concrete

1.1.3.1 Transport properties of concrete

Durability of concrete is determined by its ability to resist weathering action, chemical attack, abrasion, or any other process of deterioration according to ACI

201.2R-08 [2008]. There are many forms of concrete deterioration, but they take two primary forms, chemical or physical, or sometimes a combination of the both. Mechanisms of deterioration have something in common – water. Moisture and its transport within the pores and cracks of concrete control the physical and chemical processes that lead to structural deterioration. It enters by, e.g. absorption, diffusion, condensation, run off from roof and façade and/or capillary rise of ground water. If wet, the material can become susceptible to freezing damage. It may also act as a substrate for the growth of bacteria, fungi, or algae with possible physical damage, chemical damage, and possible health risks. Water will transport contaminants such as soluble salts and harmful ions. Mechanisms for penetration of aggressive substances into concrete generally include (1) diffusion, driven by concentration gradient, (2) permeation, driven by pressure gradients, and (3) absorption, driven by moisture gradients under the effect of capillary force.

The transport of deleterious agents into and within hardened concrete has an important influence on the durability of concrete structures. For these kinds of transport properties, two very simple ideas control how the spatial geometry of the microstructure affects transport properties. The ideas can be expressed in terms of tube theory [Kropp and Hilsdorf, 1995]: (1) large-diameter tubes have higher transport rates than small-diameter tubes, and (2) tubes that are blocked have zero transport rates. These ideas, phrased more rigorously as pore size and connectivity, provide the theoretical framework necessary for describing how the transport properties of concrete depend on pore structure. The rate, extent, and effect of the transport are largely dependent on the pore structure of the concrete (amount, shape, size and connectivity of pores, and pore-size distribution), presence of cracks in concrete, and microclimate at the concrete surface. A variety of different mechanisms may govern

the transport of aggressive substances into the concrete, depending on its local concentration, environmental conditions, and pore structure of concrete.

When exposed to aggressive environments such as in marine environment, the durability of concrete is to a large extent controlled by its permeability which determines how quickly harmful substances such as chloride ions, water, and oxygen will reach the steel reinforcement [Samples and Ramirez, 1999]. The time to corrosion initiation and subsequent corrosion induced damage is related to the time that it takes chloride ions to reach a critical level at the steel bars in reinforced concrete structures [Berke and Hicks, 1992]. Therefore, the resistance of concrete to the penetration of harmful substances such as chloride-ions is of great concern.

Because of the potential corrosion of steel reinforcement, most design codes set strict limits on the chloride that may be included in the raw materials of the concrete. Therefore, the consideration is mainly for the chloride which has penetrated into the concrete from external sources such as seawater or de-icing salts.

Lightweight aggregates are generally more porous than cement paste matrices. For sand-LWC with only coarse LWA, harmful substances may not be able to penetrate into the concrete easily if the porous coarse aggregate particles are evenly distributed and embedded in dense mortar matrix (Fig. 1.1). However, when porous fine LWA are added in concrete in addition to the coarse ones, the total porosity of the all-LWC will be increased (Fig. 1.2) and harmful substances may penetrate into the concrete more easily assuming everything else is equal.

1.1.3.2 Differences of LWC in comparison to NWC of the same w/c that may affect transport of water and ions in concrete

Comparing LWC and NWC of the same w/c, there are some differences in resisting water and chloride ion penetration.

Porosity – Comparing LWC and NWC of the same water to cement ratio (w/c), the differences are mainly aggregate and interface transition zone (ITZ) between the aggregate and cement paste. Lightweight aggregates are porous and have the ability to absorb water. However, some pores are closed depending on the type and size of LWA. Assuming that the cement paste matrix in NWC and LWC with equivalent w/c was the same, porosity of LWC would be increased significantly due to the incorporation of porous aggregates compared to that of NWC (Fig. 1.1 (a) and (b)). As water and ions can penetrate through porous substances, the porous LWA may reduce the concrete resistance to water and chloride-ion penetration.

Interface transition zone – Penetration of water and ions in concrete depends not only on concrete porosity but also on pore size distribution, pore connectivity, and pore tortuosity. Figure 1.3 shows the schematic differences between porosity and permeability [EuroLightCon, 1998]. It is clear that connectivity of the pore system is essential for water and chloride-ion penetration. A material can be porous but still has low permeability as long as the pores are not interconnected. On the other hand, a material can have lower porosity but higher permeability if the pores are interconnected.

For NWC, the ITZ between aggregate and paste matrix is generally more porous than bulk paste matrix. It is due to "wall effect" near the large surface of an aggregate where the cement particles are not packed in an ideal manner, thereby leading to more porosity than in the bulk paste. Moreover, as the aggregate surface is inert, the C-H-S gel (formed on the cement grain) grows only in one direction and not towards the aggregate faces. In principal, high porosity of the ITZ would facilitate the penetration of water and ions in concrete. For LWC, the water absorption of LWA reduces the "wall effect" and improves the quality of ITZ compared with that in NWC.

The improved ITZ for LWC would have a positive effect in resisting water and chloride-ion penetration [Zhang and Gjørv, 1990]. Detailed literature reviews in ion diffusion in ITZ compared with that in the bulk paste matrix is presented in Section 2.2.3.

Internal curing effect – Porous structure of LWA allows absorption of water into the aggregate particles, and the water can later be used for "internal curing" in the hardening process of concrete. Thus there would be increased cement hydration which reduces capillary pores and their connectivity and increases their tortuosity in concrete. This is another positive effect to resist water and chloride-ion penetration in LWC.

Microcracks – In LWC, differences in modulus of elasticity between aggregate and cement paste is typically small compared with that in NWC. Thus, frequency of microcrackings in the ITZ caused by drying shrinkage or under loading is generally lower in LWC than that in NWC. Reduced microcracking is also positive to resist water and chloride-ion penetration in LWC.

The overall resistance of LWC to water and chloride-ion penetration depends on all the factors discussed above and depends on which factor(s) is/are more dominant. The transport properties of both NWC and LWC are further reviewed in Chapter 2.

1.1.4 Applications of Lightweight Aggregate Concrete

The reduced unit weight compared with NWC can contribute to a reduction in dead loads of structures which make savings for foundations and reinforcement. Therefore, LWCs have been used for structural applications in long-span bridges, high-rise buildings, buildings where soil conditions are poor, and floating structures. It has also been proposed that lightweight concrete may be used in steel-concrete-steel composite plates for ship structures [Eyres, 2007].

Most LWC used for long-span bridges and floating structures built in the last 30 years incorporated only coarse LWA. For example, the LWC used for Heidrun tension leg platform in the North Sea and the Nordhordland floating bridge in Norway mentioned in reference [FIB, 2000] used natural sand and coarse LWA with concrete density of more than 1800 kg/m^3. For structures with design requirement for much lower unit weight of concrete, both coarse and fine LWA may be used to further reduce the self weight of structures. When such a structure is exposed to aggressive environments such as marine environment, long-term durability of the structure is to a large extent controlled by concrete resistance to the penetration of water and chloride-ions. For those exposed to marine atmospheric environment, carbonation may be another concern.

Nowadays, there is an increased use of high-performance concrete (HPC) in structures exposed to severe environments for durability considerations. Such concrete typically has lower water-to-cement (w/c) ratios and higher autogenous shrinkage at early age compared with ordinary concrete. Various approaches have been proposed to reduce the autogenous shrinkage and cracking of such concrete, for example incorporating presoaked or saturated lightweight aggregates for internal curing or incorporating shrinkage reducing admixture (SRA) in concrete.

The term “internal curing” implies the introduction of a component into the concrete mixture that serves as a curing agent. According to ACI 213R-03, internal curing refers to the process by which the hydration of cement continues because of the availability of internal water that is not part of the mixing water. The internal water is made available by the pore system in structural lightweight aggregate that absorbs and releases water.

Self-desiccation and autogenous shrinkage of HPC is one of their drawbacks which cannot be readily accommodated by conventional curing. The concept of internal curing using lightweight soaked aggregates, to provide internal reservoirs of water necessary to accommodate that consumed by cement hydration and to reduce autogenous shrinkage and cracking has been advanced by several authors [Philleo, 1991; Vaysburd, 1996; Weber and Reinhardt, 1997]. Such porous LWA particles in concrete are uniformly distributed throughout the matrix and act as an internal water reservoir. As soon as the hydration process leads to shortage of water in the cement paste there is a humidity gradient. Water from the LWA is transported from the LWA to cement paste, thereby supporting continuous hydration.

1.2 Research Objectives, Scope, and Significance

As mentioned above, information on the transport properties of concrete with LWA for internal curing is limited. There are contradicting opinions on the effect of LWA on the transport properties of concrete. In addition, there is a lack of information on estimating the transport properties of LWC. Therefore, this study was carried out with the following objectives, scope, and significance:

1. Pre-soaked LWA is commonly incorporated into concrete for internal curing to reduce/eliminate autogeneous shrinkage and potential cracking. Based on published information, the efficiency of the internal curing and reduction in the autogenous shrinkage was affected by the size of LWA incorporated. Smaller size LWAs are more efficient in reducing autogenous shrinkage. However, no information is available on how the use of such porous LWA affects the transport properties of concrete and how the fine LWAs influence the concrete permeability compared with coarse ones. Only limited information on charge

passed determined by ASTM C 1202 [2006e] is available for concrete with w/c of 0.35. For structures exposed to severe environment, such information is essential to design structures with good long term durability.

Therefore the objective of this part of the research is to study the effect of different sizes of LWA on the permeability and resistance to chloride ion penetration of high performance concrete where LWAs are used for internal curing.

The lower the w/c, the more significant the autogenous shrinkage. According to literature review by Hoff [2003], autogenous shrinkage due to self-desiccation occurs when w/c below 0.4. Therefore, a w/c of 0.38 was selected to investigate the internal curing effect on the autogenous shrinkage. Crushed lightweight sand less than 1.18mm and expanded clay LWA in size fractions 1.18-2.36 mm, 2.36-4.75 mm, and 4.75-9.5mm are used for internal curing. The results are compared with control concrete and concrete with shrinkage reducing admixture to reduce shrinkage.

This study provides the information that allows engineers and designers to select concrete mixtures by using LWA with proper type and size for exposure in severe environment to reduce autogenous shrinkage, cracking, and improve long term durability.

2. There are contradicting opinions on the effect of LWA on the transport properties of concrete. By carefully analyzing the published information, it seems that the amount, size, and porosity of LWA and w/c of concrete all play important roles. Therefore, the second objective of this study is to carry out a comprehensive research to investigate the influence of cumulative LWA

contents, porosity and surface textures of LWA on the transport properties of LWC.

A w/c of about 0.38 is used for concrete mixtures with increased cumulative LWA content, different coarse LWA, and different fine LWA. Both expanded clay and expanded glass LWA are used. Coarse LWA made of expanded clay with different densities and porosities are evaluated on their influence on transport properties of concrete in comparison to the granite coarse aggregate. Crushed fine LWA in expanded clay and fine expanded glass particles of spherical shape are used in the comparison with natural sand to evaluate the effects of porosity and surface textures of fine LWA on transport properties. The results were also compared with those of a cement paste and a control NWC with the same w/c of 0.38 and a NWC (w/c=0.54) with 28-day compressive strength similar to some of the LWC and discussed.

The results will clarify the effect of LWA on the transport properties of concrete, and provide general guidelines in selecting different types, sizes, and contents of LWA for design of lightweight and durable concrete.

3. Most LWC used for long-span bridges and floating structures built in the last 30 years incorporated only coarse LWA and had unit weight generally more than 1700 kg/m^3. Therefore the third objective of this study is to develop an all-LWC with very low unit weight but high resistance to water and chloride ion penetration. Both expanded clay and expanded glass LWA are used in the concrete. Water to cementitious material (w/cm) ratio of 0.20 and 10% silica fume are used. Such LWC with low unit weight may open up a new avenue for potential use of LWC in marine environment for floating structures.

4. There has been considerable interest in the relationship between pore structure and transport properties such as water absorption, resistance to chloride ion penetration in concrete as many of the tests that directly measure the transport properties require specialized equipments and long durations of time. Lightweight aggregate concrete differs from normal weight aggregate concrete in a number of aspects that may influence the penetration of chloride ions in the concrete. Therefore, the fourth objective of this research is to establish empirical relationships between transport properties of lightweight concrete and basic physical properties such as water accessible porosity and unit weight which can be easily determined. Using the empirical equations, the transport properties of concrete such as sorptivity, charge passed, and chloride migration coefficient can be estimated which can be used for quality control and for estimating durability of concrete. The charge passed and chloride migration coefficient have been found to be related to the diffusion coefficient which is a critical parameter used for life cycle prediction of concrete.

1.3 Thesis Organization

Chapter 1 introduces LWC and concrete with LWA for internal curing, transport properties of concrete as well as the differences of LWC in comparison to NWC of the same w/c in resisting water and chloride ion penetration. Research objectives, scope, and significance are put forward at the end of this chapter.

Chapter 2 provides a review of the mechanisms of transport of water and harmful substances in concrete. Those factors influencing the resistance of concrete to water and chloride ion penetration are compared for concretes with

NWA and LWA. Permeability of LWC and concrete with LWA for internal curing are reviewed. Finally, methods for testing concrete resistance to water and chloride ion penetration are reviewed.

Chapter 3 describes the experimental details including the design of mixture proportions, materials used, mixture preparation and test methods used to achieve the objectives.

Chapter 4 presents and discusses the results on the transport properties of concrete incorporating presoaked LWA of different sizes for internal curing.

Chapter 5 evaluates the effect of cumulative LWA content, porosities and surface textures of LWA, and w/cm on the resistance of concrete to water and chloride ion penetration.

Chapter 6 analyses the effect of basic physical properties of concrete on the transport properties of concrete and establishes empirical relationships of transport properties including water absorption, charge passed, and migration coefficient vs water accessible porosity and oven dry unit weight of concretes.

Chapter 7 summarizes and draws conclusions based on the results obtained in this research and makes recommendations for future research.

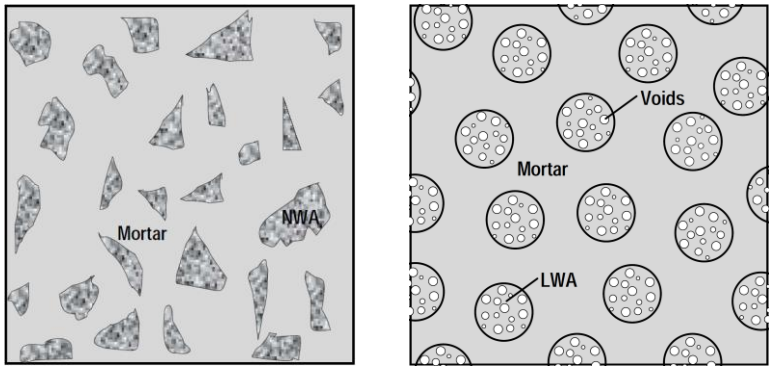

(a) (b)

Fig. 1.1 Schematic graphs of concrete with the same mortar matrix but different coarse aggregate (a) granite and (b) LWA

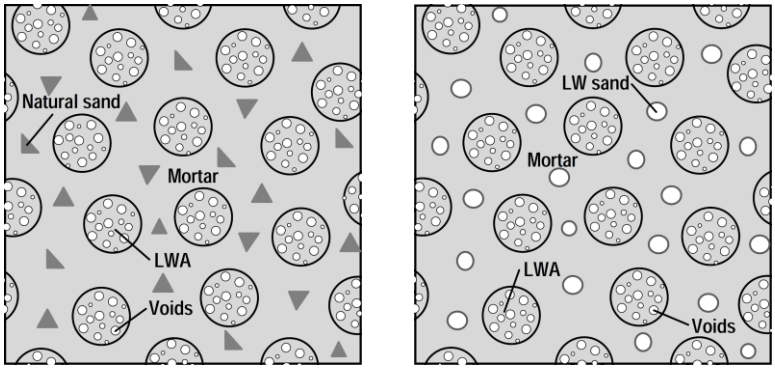

(a) (b)

Fig. 1.2 Schematic graphs of concrete (a) with only coarse LWA, and (b) with both coarse and fine LWA.

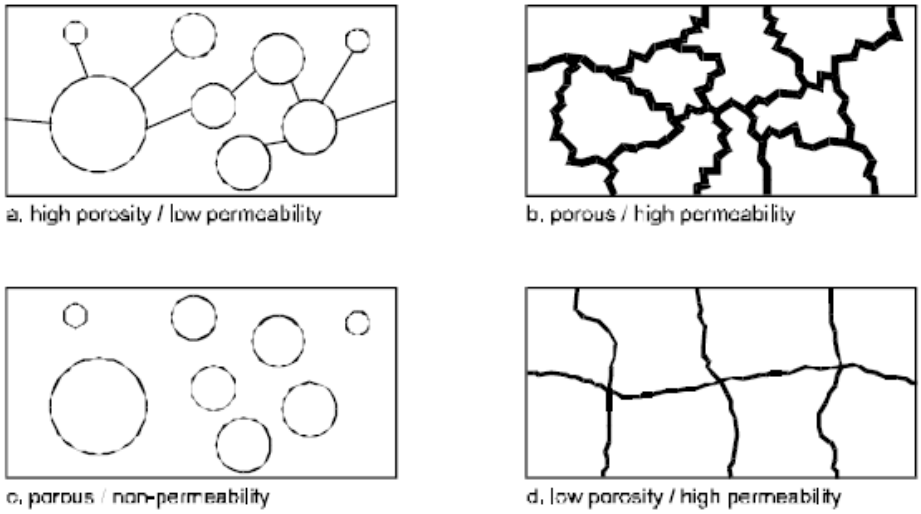

Fig. 1.3 Porosity vs. permeability, Schematic representation of the difference [EuroLightCon, 1998]

CHAPTER 2 LITERATURE REVIEW

2.1 Mechanisms of Transport of Water and Harmful Substances into Concrete

Movement of gases, liquids and ions through concrete is important because of their possible interactions with concrete constituents or pore water which affect the integrity of concrete and structures. Depending on exposure conditions and driving forces, deleterious substances may penetrate into concrete by mechanisms of absorption, permeability, or diffusion.

2.1.1 Absorption

Concrete is often unsaturated during their service life. In unsaturated concrete, the penetration and transport of water is initiated by a surface tension within capillary network. The process is known as capillary suction or absorption.

According to Hall [1989], the flow processes in unsaturated concrete can be described by extended Darcy equation

$$\mathbf{u} = K_u(\theta)\mathbf{F}_C \tag{2.1}$$

where

u – vector flow velocity;

$K_u(\theta)$ – generalized or unsaturated permeability;

$\mathbf{F_C}$ – capillary force;

θ – ratio of liquid to bulk volume.

$\mathbf{F_C}$ is defined as the negative gradient of the capillary potential ψ, so that

$$\mathbf{u} = -K_u(\theta)\nabla\psi \tag{2.2}$$

Here ψ is capillary potential per unit weight of liquid, and it is coherent with the pressure potential. The continuity equation can be expressed as:

$$\frac{\partial\theta}{\partial t} = -\nabla\mathbf{u} \tag{2.3}$$

Combining Eq. (2.2) with the continuity equation (2.3) leads to the fundamental equation of flow in unsaturated concrete, i.e. the Richard equation:

$$\frac{\partial\theta}{\partial t} = \nabla\left(K_u(\theta)\nabla\psi\right) \tag{2.4}$$

If a quantity $K = K_u(d\psi/d\theta)$ is defined, Eq. (2.4) becomes:

$$\frac{\partial\theta}{\partial t} = \nabla\left(K\nabla\theta\right) \tag{2.5}$$

where

K – hydraulic diffusivity (if the fluid is water),

t – elapsed time.

However, the strong dependence of K on water content presents difficulties in solving this equation. Hence the one-dimensional flow in unsaturated media is defined from Eq. (2.5) by

$$\frac{\partial\theta}{\partial t} = \frac{\partial}{\partial x}\left(K\frac{\partial\theta}{\partial x}\right) \tag{2.6}$$

If we consider first the case of the absorption of liquid under the action of a potential gradient, Eq. (2.6) is subject to the boundary condition $\theta = \theta_s$, for $x = 0$ and $t \geq 0$ and initial condition $\theta = \theta_d$, for $x > 0$ and $t = 0$; let $\theta = f(\phi)$ which is a function of x and t given by

$$\phi = xt^{-1/2} \tag{2.7}$$

Then the solution of the flow in the unsaturated material is

$$x(\theta,t) = \phi(\theta)t^{\frac{1}{2}} \ . \tag{2.8}$$

where

θ_s – volume fraction of the liquid content at saturation;

θ_d – volume fraction of the liquid content in a nominal dry state.

Eq.(2.8) shows that as water is absorbed horizontally into an initially dry porous solid all points on the advancing wetting profile advance as $t^{1/2}$. It's clear from Eq. (2.8) that the total amount of water absorbed in time t is given by

$$\int_{\theta_d}^{\theta_s} x d\theta = t^{1/2} \int_{\theta_d}^{\theta_s} \phi(\theta) d\theta = St^{1/2} \tag{2.9}$$

Equation (2.9) defines the sorptivity S which is considered as a material property and is important in understanding the flow in unsaturated media in characterizing porous materials. Sorptivity is a property which expresses the tendency of a material to absorb and transmit water and other liquids by capillarity [Hall and Hoff, 2002]. Philip [1957] introduced this term in the field of soil physics and hydrology. The theoretical equation (2.9) has been amply confirmed by experiment for many materials and it is suggested that flow theory in unsaturated media reasonably describes the processes of capillary flow in porous materials such as brick, stone, plaster, mortar and concrete [Basheer, 1991; Gummerson et al., 1979; Olorunsogo and Padayachee, 2002].

For concrete, its absorption is related not only to the pore geometry, but also to the moisture condition of the concrete. Since the filling of capillary channels and voids and advancing of water occur almost simultaneously during absorption, only a combined effect can be measured.

Water absorption and desorption caused by wetting and drying of concrete is important near the surface, but becomes less significant with an increase in depth [Bouguerra et al., 2002; Olorunsogo and Padayachee, 2002]. However, the water absorption can measure fluid transport into unsaturated concrete, the condition typical of concrete bridge decks, and thus provides a unique method for assessing this important aspect of concrete quality.

2.1.2 Permeability

According to ACI committee 116, permeability is defined as the rate of discharge of water under laminar flow conditions through a unit cross-sectional area of a porous medium under a unit hydraulic gradient and standard temperature conditions. In general, the rate at which water permeates through the concrete under a given pressure head is regarded as a fundamental material property. Darcy's law states that the steady-state rate of flow is directly proportional to the hydraulic gradient [Darcy, 1856].

$$\mathrm{v} = \frac{Q}{A} = -K_P \frac{dh}{dL} \tag{2.10}$$

where

v – apparent velocity of flow;

Q – flow rate (m^3/s);

A – cross-sectional area of flow (m^2);

K_P –water permeability coefficient (hydraulic conductivity) (m/s);

dh/dL – head loss dh (m) over a flow path of length dL (m).

Although water permeability of concrete is rarely the predominant transport mechanism in practical situations, the permeability coefficient can provide information on the connectivity of the pore structure. The term "permeability" is often used for

overall movement of fluids into and through concrete except where distinctions between the various types of flow are necessary.

2.1.3 Diffusion

In saturated or near-saturated concrete where no pressure head exists, diffusion under a concentration gradient is a principal mechanism of transport of e.g. chloride ions in concrete exposed to sea water.

Under steady state conditions, diffusion coefficient is determined from Fick's First Law:

$$f = K_{sd} \frac{\partial C}{\partial x} \tag{2.11}$$

where

f – mass flux (kg/m^2/s);

K_{sd} – Steady state diffusion coefficient or diffusivity (m^2/s);

C – chloride concentration (kg/m^3).

For most applications, the diffusion of chloride ions is under non-steady state conditions and the diffusion can be described by Fick's Second Law:

$$\frac{\partial C}{\partial t} = K_d \frac{\partial^2 C}{\partial x^2} \tag{2.12}$$

where

t – time (s);

K_d – diffusion coefficient (or diffusivity) (m^2/s);

x – depth (m).

The solution to this equation for a semi-finite slab with boundary conditions $C_{(x = 0,\, t > 0)} = C_0$, and $C_{(x = \infty,\, t > 0)} = 0$, and initial condition $C_{(x = 0,\, t = 0)} = 0$ is

$$C(x,t) = C_0\left[1 - \text{erf}\left(\frac{x}{2\sqrt{K_d t}}\right)\right] \quad (2.13)$$

in which

$C(x, t)$ –chloride concentration at depth x and time t;

C_0 – chloride concentration at the surface;

erf – error function.

Experimental results reported by Berke and Hicks [1996] shows that penetration of chloride ions follows Fick's 2nd Law very closely, as shown in Fig. 2.1.

2.2 Factors that Influence the Concrete Resistance to Water and Chloride-Ion Penetration

Durability of concrete is associated with various liquids, gases, and salts transported into the concrete. The ease of the transport may be affected by the permeability of concrete. It is well recognized that the transport occurs through a continuous network of pores, which exist in the cement-based matrix and ITZ in NWC. For LWC, the continuous network of pores also exists in porous LWA. Unfortunately, concrete has highly heterogeneous and complex structures. It is very difficult to establish realistic constitutive models with the consideration of its microstructure from which the behavior of the material can be reliably predicted. However, knowledge on the microstructure and properties of individual components of concrete and their correlation is useful for prediction of different properties of concrete. In terms of the transport properties, the microstructure of concrete inevitably plays a dominant role. Concrete has been considered as a three-phase composite material consisting of inert aggregate particles of different sizes embedded in a matrix of hydrated cement paste,

and the ITZ between these two components. The permeability of concrete depends on the quality of these three phases and their relative proportions.

2.2.1 Cement Paste Matrix

The flow of water through concrete is similar to that through any porous body. Hence, the permeability of concrete is a function of its porosity, pore size distribution and pore connectivity. The permeability of concrete is affected substantially by the cement paste. The permeability coefficient K_p of cement paste depends on both the w/c ratio and the degree of cement hydration as the total capillary porosity decreases with the decrease in w/c and/or with the increase in the degree of cement hydration (Table 2.1).

As the w/c decreases, the capillary porosity of the paste is decreased and the concrete becomes more impermeable (Fig. 2.2). Powers-Brownyard's model introduces a relationship between w/c and porosity of cement paste [Taylor, 1990]:

$$\phi_{cap} = 1 - (1 + 1.3\alpha)/\big(1 + 3.2(w/c)\big) \tag{2.14}$$

and

$$\phi_{gel} = 0.21\alpha/\big(0.313 + (w/c)\big) \tag{2.15}$$

Where

ϕ_{cap} – porosity of capillary pores;

ϕ_{gel} – porosity of gel pores;

α – degree of cement hydration;

w/c – water to cement ratio.

However, the exponential relationship (Fig. 2.3) between permeability and w/c indicates that permeability will not be reduced significantly when w/c is below a certain level.

The permeability is affected not only by the porosity but also by pore size distribution, and the continuity of pores. According to Mindess et al. [2003], pores in cement based materials are classified as capillary pores and gel pores. As presented in Table 2.2, the pores from 10 – 50 nm are medium capillary pores and those from 50 – 1000 nm are large capillary pores. Those pores with diameter less than 10 nm are classified as gel pores. More importantly, large and medium capillary pores have an influence on permeability or diffusivity of cement paste according to Mindess et al. [2003] (Table 2.3).

Brown et al. [1991] reviewed the relationship between porosity and permeability of cement based materials and also noted that the variation in permeability is dominated by large capillary pores rather than gel pores. Water can flow more easily through the capillary pores than through gel pores. Cement paste as a whole is 20 to 100 times more permeable than the gel itself [Neville, 1995]. A direct relationship was also noted between the permeability of the cement paste and the volume of pores larger than about 100 nm corresponding to large capillary pores [Mehta and Monteiro, 2005]. As cement hydration proceeds, the capillary network becomes increasingly tortuous as interconnected pores are blocked by the formation of C-S-H [Mindess et al., 2003]. Even after the capillary pores are completely isolated by regions of C-S-H, the porosity of cement paste continues to decrease by several more orders of magnitude. This is not only due to an increase in thickness in the C-S-H between capillary pores, but also due to the fact that calcium hydroxide continues to grow within the residual capillary pores, thus forming impermeable regions. A limiting

value of K_p should occur when all capillary porosity has been eliminated, and this is believed to be less than 10^{-22} m/s [Mindess et al., 2003].

It has also been reported that there is a good correlation between K_p and the critical pore diameter (d_c) determined by mercury intrusion porosimetry (MIP) [Quenard et al., 1998]. The critical pore diameters (d_c) represents the mean size of pore entryways that allows maximum percolation throughout the pore system. The pores with size larger than d_c, are the most important ones in determining the permeability of a porous material [Garboczi, 1990]. The larger value of d_c indicates higher K_p [Mindess et al., 2003].

Hughes [1985] suggests the following equation to emphasize influence of the pore size distribution on water transport:

$$Q = \frac{r^2 \Delta p V}{32 n^2 \eta L} \tag{2.16}$$

where

Q – total flow rate;

Δp – pressure difference;

η – viscosity;

r – pore radius;

V – a unit volume of pores in hardened cement paste;

n – a tortuosity factor reflecting the devious path around hydrated and unhydrated material, $n>1$;

L – general specimen thickness.

The addition of supplementary cementing materials, especially silica fume, results in a significant decrease in permeability of cement pastes and concretes [Banthia and Mindess, 1989; Khan, 2003; Mindess et al., 2003]. This is largely due to the reduction in total porosity (up to 10% replacement level for silica fume) and the

pore size [Khan, 2003]. Scanning electron microscope examination showed that silica fume significantly decreases the number of large capillary pores with diameters between 1 and 10 μm. In addition, mercury intrusion porosimetry shows that the incorporation of silica fume in cement paste or mortar reduces the number of large and medium capillary pores with diameters between 0.01 and 1.0 μm [Mindess et al., 2003].

As part of the cement paste, air content also influences the permeability of concrete. Higher air content results in a pore network with weaker connection in the cement paste, and can cause greater chloride penetration although the entrained air may have little effect on sorptivity [Lo et al., 2006].

2.2.2 Aggregate Characteristics

Aggregates generally occupy 60 to 80% of the volume of concrete and can therefore be expected to have an important influence on the properties of concrete including permeability. As reported by Torgal and Castro-Gomes [2006], the water permeability of concrete is influenced by aggregate geometrical and physical properties. The type, porosity, permeability, size, grading and content of aggregate may influence the permeability of concrete.

2.2.2.1 Normal weight aggregate

For normal weight rock based aggregates, the volume of pores is generally much less than in cement paste, usually less than 3% and rarely exceeds 10% [Mehta and Monteiro, 2005]. It is expected, therefore, that the permeability of aggregate would be much lower than that of the typical cement pastes. If the aggregate has a very low permeability, its presence reduces the effective area over which flow can take place,

thus permeability. However, this may not necessarily be the case. From the permeability data of some natural rocks [Powers, 1958], the permeability coefficient of aggregates is as high as that of hydrated cement pastes with w/c from 0.38 to 0.71 (Table 2.4). The permeability of a mature paste with w/c 0.48 can be between 10 to 0.001 times that of aggregates (Table 2.4).

Different aggregates may have different porosities, and thus different water absorptions. With five different types of normal aggregates of different absorptions in concretes, Dhir et al. [2006] found that the concrete absorption would be reduced by using NWA with lower aggregate absorption capacity by initial surface absorption test. They also found that the diffusion coefficient of concrete (*w/c*: 0.45 – 0.65) increased with increasing water absorption capacity of NWA. According to them, low-absorption aggregate tends to give better performance for NWC in resisting water and chloride ion penetration.

The grading and maximum size of aggregate may also affect concrete permeability. Dhir et al. [1989] found no significant difference in air permeability of concrete made from aggregates with different maximum sizes up to 20 mm. With air permeability test and micro structural analysis, Basheer et al. [2005] found that both coarse aggregate grading and maximum size up to 20 mm affected the permeability of concrete. They found that the air permeability was increased with increasing the size of coarse aggregate from 10 to 20 mm in concrete mixtures. When the effect of coarse aggregate grading is considered, they found that air permeability increased as the proportion of 20 mm aggregate over 10 mm aggregate increased in the concrete.

2.2.2.2 Lightweight aggregate

Lightweight aggregates are produced from a wide variety of raw materials including clay, shale, slate, fly ash, blast-furnace slag, pumice, diatomite, perlite, and vermiculite. Lightweight aggregates have low particle densities because of their cellular pore structure. Properties and characteristics of LWA may vary within wide limits, due to differences in raw materials at production processes.

The LWAs generally have higher porosity than NWAs. Some pores are open and thus susceptible to water absorption, others are closed. The pore size also varies considerably and may vary with the texture of the raw material. The shape of the pores is rather irregular. Different microstructure of LWA may result in different water absorption. The absorption characteristic of LWA results in different interactions of LWA and the matrix compared with that of NWA.

The particle shape and surface texture varies considerably depending on the manufacturing processes. The surface texture of LWA may also contribute to the properties of interfacial transition zone. Some of the aggregate types have a distinct outer shell of dense material which is much less porous than the interior.

Most LWA particles are more porous than NWA particles and this will allow more diffusion of deleterious substances. Zhang [1989] determined chloride diffusion coefficients of several LWA (Table 2.5) and the values varied between 3.6×10^{-11} m^2/s and 8.4×10^{-11} m^2/s depending on pore structure and particle density of the aggregates. It needs to be noticed that the samples used for the diffusion test here were sliced from the middle of LWA particles. Therefore the outer shell of the aggregate was removed and its influence on diffusion was not considered. The diffusion coefficient of the LWA was in the same order as that of a pure cement paste with a w/c ratio of 0.9 (1.91×10^{-11} m^2/s) cured in a sealed condition for at least half a year [Gautefall et al.,

1986]. This indicates that the chloride diffusion coefficient in LWA is higher than that of cement pastes commonly used in concretes exposed to severe environments which typically have w/c of less than 0.5.

2.2.3 Interface Transition Zone

2.2.3.1 In normal weight concrete

For NWC, there is an ITZ between aggregate and cement paste which is generally more porous than bulk cement paste due to "wall effect". In NWC the ITZ is generally the weakest link and is considered as the strength-limiting phase in NWC. A diagrammatic representation of ITZ in NWC is shown in Fig. 2.4 [Mehta and Monteiro, 2005]. As ITZ forms around aggregates in the cement paste matrix, the aggregate properties and content in concrete will influence the quality and quantity of the ITZ which may affect the permeability of concrete. Permeability generally increases with an increase in aggregate content in normal weight mortar and concrete [Nyame, 1985; Watson and Oyeka, 1982].

The ITZ is known to be more porous than the surrounding cement paste and may consist of ink-bottle type pores by comparing the total porosity of cement paste and mortar using mercury intrusion porosimetry with two cycles of mercury intrusion and extrusion [Kaufmann et al., 2009]. Kaufumann et al. [2009] also mentioned that such zones with larger pores may lead to a sub-pore network which increases the connectivity to the external surface. The presence of porous ITZ around the aggregates may allow easier movement of water and ions into concrete.

Bentz [2009] reviewed some research work on ion diffusion in ITZ compared with that in bulk paste. Bretton et al. [1993] conducted model experiments using a cylindrical aggregate surrounded by cement paste and concluded that the ITZ exhibits

a chloride ion diffusion coefficient that is 12-15 times that of bulk paste with w/cm of 0.5 cured for 10 days and with an assumed ITZ thickness of 100 μm. Bourdette [1994] suggested a lower diffusivity ratio of 3 between the ITZ and bulk paste for a mortar with w/cm = 0.4 cured for 3 months, assuming an ITZ thickness of 120 μm. Otsuki et al. [2006] suggested that the diffusion coefficient for the ITZ could be over 100 times that of the bulk paste for concretes with w/cm between 0.4 and 0.7, assuming that an ITZ thickness is a function of aggregate size and varies between 0 and about 80 μm. Based on multi-scale microstructure model, Bentz [2000] found that the average diffusivity ratio of ITZ to bulk cement paste ranges from 0.7 to 21. Larger values near 20 observed for concrete with w/cm of 0.5 [Bentz, 2000] are in reasonable agreement with that of Bretton et al. [1993]. The lower ratio of less than one was obtained for silica fume concrete with w/cm of 0.3.

However, Delagrave et al. [1997] found a significant decrease in diffusion coefficient of mortars compared with cement paste of the same w/cm. They, therefore, concluded that increased pore tortuosity due to the presence of normal weight aggregates is more important to resist chloride-ion penetration than ITZ. The aggregate particles act as obstacles which increase travel length for water and chloride-ions to penetrate into concrete around aggregates. Shane and Jennings [1999] also drew a similar conclusion. To improve the ITZ and reduce permeability in the NWC, reduction of w/cm and incorporation of silica fume in concrete are efficient.

2.2.3.2 In lightweight concrete

As found by Zhang and Gjørv [1990], for high strength lightweight aggregate with a denser layer the nature of the ITZ between aggregate and cement paste is similar to that for normal weight aggregate. For lightweight aggregate with a weaker and more

porous outer layer and for aggregate without any outer layer, the ITZ is denser and more homogeneous. Also for such aggregates the bond appears to be better due to an improved mechanical interlocking between the aggregate and the cement paste. The nature of the ITZ in LWC appears to depend on the microstructural characteristics of the aggregate.

With SEM examination on mortars with a w/c of 0.55 and with dry or prewetted LWAs, Elsharief *et al.* [2005] found that the ITZ around the LWA appears to be about 10 to 50 μm thick for dry and prewetted LWAs, respectively. For mortar with NWA, the ITZ extends beyond 35 μm. The paste located between 10 to 50 μm from the surface of the LWAs seems to be denser than the bulk paste located at 50 μm and farther. They attributed the denser paste around LWA to water absorption by the LWA. They found that the sorptivity and electrical conductivity of lightweight mortar were lower than those of the corresponding normal weight mortar, and attributed those to the dense paste located between 10 to 50 μm from the surface of the LWA. There is no information available on the permeability and diffusion coefficient of ITZ in concrete with LWA.

2.3 Permeability of Lightweight Aggregate Concrete

Generally, LWAs have higher porosity than NWAs. However, the permeability of LWC may not necessarily be higher than that of NWC. It must be noted that there is a difference between porosity and permeability as shown in Fig. 1.3. The connectivity of the pore system is of primary importance for permeability. In order to obtain LWC with low permeability, it is essential to have the porous aggregates embedded in a dense cement paste matrix.

In some LWCs, only coarse LWA is used (referred to as sand-LWC) whereas in others both coarse and fine LWA are used (referred to as all-LWC). In the former, natural sands are included in the mortar matrix, whereas in the latter, porous fine LWA particles are included in the mortar matrix. For concrete with only coarse LWA, if the porous aggregate particles are evenly distributed and embedded in dense mortar matrix (assuming natural sand particles have negligible porosity), harmful substances may not be able to penetrate into the concrete easily. With the introduction and increase in porous fine LWA particles in concrete in addition to the coarse LWA particles, however, the porosity of the mortar is increased. Thus, harmful substance may penetrate into concrete more easily assuming everything else is equal. A schematic difference of the porous aggregates in the concrete for these two cases is shown in Figs. 1.2 (a) and (b). When both coarse and fine LWA are used as shown in Fig. 1.2 (b), the thickness of the dense paste matrix will be reduced. If porous particles are in contact with one another, percolation occurs.

According to Nyame [1985], mortars with a w/c of 0.47 and lightweight sand are about twice as permeable as mortars made with natural sand at a given aggregate volume determined by steady-state permeability test at a pressure of 15 MPa.

Zhang and Gjørv [1991] conducted water permeability test, accelerated chloride permeability test and ASTM 1202 test on high-strength LWC with w/cm from 0.28 to 0.44 and with different types of LWAs. The water permeability of the concretes with different types of LWAs embedded within similar cement paste matrix was approximately in the same order even though the porosity and characteristics of the aggregates were different. They found that the permeability of high-strength LWC was much dependent on the quality of the matrix. They also found that the concrete with

part normal sand and part lightweight sand had lower permeability than the concrete with all lightweight sand.

Chia and Zhang [2002] evaluated water permeability and resistance of concrete to chloride penetration of NWC and LWC with w/c of 0.35 and 0.55. In the LWC, only coarse LWA was used. They found that the water permeability of high-strength LWC and NWC with the same w/cm of 0.35 was of the same order. However, at the strength level of about 30-40 MPa, the water permeability of the LWC with a w/c of 0.55 was lower than that of the corresponding NWC. They also found that the resistance of LWC to the chloride penetration was similar to that of the corresponding NWC. As the compressive strength of LWC was lower than that of the corresponding NWC with the same w/cm ratios, the results indicated that for a given 28-day strength, the LWC would probably have higher resistance to water and chloride-ion penetration than the NWC.

Water permeability and penetration of chloride ions in LWC and NWC with 28-day compressive strengths of 50 and 35 MPa were also studied and compared by Al-Khaiat and Haque [1999]. Lightweight coarse and fine aggregates based on sintered fly ash (Lytag) were used for LWC, and 10% of silica fume was used in all concrete mixtures. Both coarse and fine LWA were presoaked with 30% of mixing water for 10 minutes before concrete mixing. They found that LWCs were more sensitive to the initial curing than the NWCs. At the age of 90 days, the water penetrability of the LWC with the strength of 50 MPa was about 1/3 more than that in the NWC with the same strength. Both LWC and NWC had an initial moist curing of 7 days and were tested in the same condition. The concentrations of the penetrated chloride-ions in the LWC were somewhat higher than that in the NWC.

Thomas [2006] investigated all-LWC (with expanded slate), and found that the use of LWA substantially reduced the electrical conductivity and chloride penetrability of high-performance LWC containing blended silica fume cement. The LWAs used in his experiments had relatively low water absorption of about 6% at 24 hours. At the age of 3 years, the chloride diffusion coefficient of LWC (w/c=0.3 and 0.4) made with silica fume blended cement was between 1/3 and 1/2 that of NWC of the same age and w/cm. Thomas concludes that the LWC may have better durability than NWC.

The above literature review indicates that although lightweight aggregates are more porous than normal weight aggregate, the permeability of LWC may not necessarily be higher than that of NWC with the same w/c. However, there is no agreement on the effect of LWA on permeability and resistance to chloride ion penetration. Some researchers found that LWC had lower resistance to water and chloride ion penetration, whereas others found that LWC may have similar or higher resistance to water and chloride ion penetration compared with NWC with the same w/c.

For floating reinforced concrete structures, great efficiencies in design can be achieved when a material of low unit weight is used. According to Ries and Holm [2004], a 25% reduction of mass in air will result in a 50 % reduction when submerged in water. When such structures are exposed to marine environment, long-term durability of the structure is to a large extent controlled by concrete resistance to the penetration of chloride ions. Very little information on resistance to water and chloride ion penetration of LWC with very low unit weight is available.

2.4 Permeability of Concrete with Lightweight Aggregate Used for Internal Curing

2.4.1 Autogenous deformation

Different definitions have been used to define more or less the same phenomenon of autogenous shrinkage. Kyaw [2007] reviewed those definitions from different literatures. Jensen and Hansen [1996] defined autogenous deformation as bulk deformation of a closed isothermal cement paste system. JCI [1999] defined "autogenous shrinkage as the macroscopic volume reduction of cementitious materials when concrete hydrates after initial setting". In another study, Holt [2004] defined autogenous shrinkage as an external volume change occurring with no moisture being transferred to the surrounding environment.

2.4.2 Internal curing for high performance concrete

There is an increased use of high-performance concrete (HPC) in structures exposed to severe environments for durability considerations. According to American Concrete Institute (ACI), HPC is defined as concrete meeting special combination of performance and uniformity requirements that cannot always be achieved routinely using conventional constituents and normal mixing, placing and curing practices [Russell, 1999]. Such concrete typically has lower water-to-cement (w/c) ratios and higher autogenous shrinkage at early age compared with ordinary concrete. The high autogenous shrinkage of such low w/c concrete is generated mainly due to rapid reduction of internal relative humidity and self-desiccation caused by cement hydration where the volume of hydration products is less than the combined volume of cement and water.

Since concrete is relatively weak at early age, the high autogeneous shrinkage may lead to cracking if concrete members are restrained [Lee et al., 2003; Neville and Aitcin, 1998; Persson, 1997]. Since such undesirable problem may undermine the benefits of using HPC, shrinkage reduction methods are of great interest to both researchers and engineers. Various approaches have been proposed to reduce the autogeneous shrinkage and cracking of such concrete, e.g. incorporating presoaked or saturated LWA or incorporating shrinkage reducing admixture (SRA) in concrete.

Philleo [1991] suggested to incorporate presoaked LWA in concrete to provide an internal source of water necessary to accommodate that consumed by cement hydration and to reduce autogenous shrinkage and cracking in 1991. Since then, a lot of research has been carried out in this area and a comprehensive review was published by Hoff [2003]. Bentz and Snyder [1999] proposed the following formula to estimate the quantity of LWAs required in concrete to control autogenous shrinkage.

$$M_{LWA} = \frac{C_f \times CS \times \alpha_{max}}{s \times \emptyset_{LWA}} \tag{2.17}$$

where

M_{LWA} – mass of (dry) fine LWA needed per unit volume of concrete (kg/m^3);

C_f – cement factor (content) for concrete mixture (kg/m^3);

CS – chemical shrinkage of cement (g of water/g of cement);

α_{max} – maximum expected degree of hydration of cement;

s – degree of saturation of aggregate (0 to 1);

ϕ_{LWA} – absorption of LWA (kg water/kg dry LWA).

For w/c below 0.36, the maximum expected degree of hydration of the cement under saturated conditions can be estimated as (*w/c*)/0.36 and should not vary significantly with curing temperature. For w/c higher than 0.36, the maximum

expected degree of hydration of the cement can be estimated as 1. Because the densities of the dry LWAs and the conventional aggregates are substantially different, the ultimate substitution in the concrete mixture should be performed on a volume basis with the mass of LWA determined from Eq. (2.17) replacing the same volume of conventional aggregates. Knowing the dry densities of the two types of aggregates, a simple calculation can be employed to determine the mass of conventional aggregates that must be removed from the mixture (which will be more than the mass of the LWA determined by Eq. (2.17)).

A procedure to determine *CS* and ϕ_{LWA} more accurately was proposed by Bentz *et al.* [2005]. Several studies have dealt with the experimental evaluation of the presence of LWA on autogenous shrinkage. Most of them assessed the use of coarse aggregates by evaluating the influence of their amount and degree of saturation. Later on, the use of fine LWA has been explored.

2.4.3 Effect of internal curing from LWA on properties of concrete

With sufficient amounts of saturated LWAs incorporated in concrete the autogenous shrinkage and its associated stresses can be eliminated from the concrete.

As LWAs were used to replace part of the NWA in the HPC with low w/c ratios for internal curing, published information concentrated on the effect of LWAs on improving cement hydration and reducing/eliminating shrinkage and cracking. Hammer [1992] demonstrated that autogenous shrinkage was practically eliminated by the use of wet LWA and showed that the compressive strength did not suffer significantly from internal or external drying when a sufficient replacement of NWA with pre-wetted LWA was used [Hammer, 1993]. Hammer used expanded clay LWA, Liapor and Leca, 4-12mm. Their content was about 600 kg/m^3 and the absorbed water

exceeded 40 kg/m^3 when soaked. The LWA were employed in three different states: oven-dried, moist (as delivered), and water-soaked. In concrete with w/cm of 0.30, autogenous shrinkage was eliminated even in the case of dry LWA, suggesting that LWA can absorb part of the mixing water and release it afterwards to the self-desiccating matrix [Lura, 2003]. The influence of the percentage of replacement of coarse NWA with saturated LWA (10, 17.5, and 25% Liapor by volume of coarse aggregate) on the autogenous deformation from setting time was studied by van Breugel and de Vries [1999]. With 25% replacement, the autogenous shrinkage was about half of the reference mixture. When all the coarse aggregates were substituted with Liapor of Lytag, early-age expansion was measured when the saturation of the LWA was 100% or 60%, while some shrinkage followed by expansion was measured when the saturation was 30% [Takada et al., 1999].

The efficiency of internal curing by using LWA is found to be influenced by aggregate size. Smaller size LWA or fine LWA (e.g. 0 to 4 mm) are more efficient than larger ones (e.g. 4 to 8mm) [Bentz et al., 2002; Bentz and Snyder, 1999; Hoff, 2003; Zhutovsky et al., 2004]. Smaller size LWAs are more efficient in reducing autogenous shrinkage as the distances between the smaller particles are shorter so that the water inside the LWA does not have to travel far to contribute to the internal curing. It has also been found [Bentz et al., 2002] that the incorporation of presoaked fine LWAs in the concrete does not appear to have adverse effects on the mechanical properties of the concrete and, in many instances, small improvements have been noted.

2.4.4 Effect of lightweight aggregate used for internal curing on concrete resistance to water and chloride ion penetration

Most of the published research focuses on the use of LWAs to improve cement hydration and to reduce autogenous shrinkage and cracking. Only limited information

is available on how the use of such porous LWAs affects the chloride penetrability in concrete. Results by Lam and Hooton [2005] show that the use of fine LWAs for internal curing of concrete with a w/c of 0.35 reduced the total charge passed in comparison to the control concrete according to the ASTM C 1202 test. The fine LWA used had a 24-hour water absorption of about 17% and a bulk specific gravity of 1590 kg/m^3 and the concrete was moist cured. However, no information is available on how the use of such porous LWA affects water permeability, water absorption, and chloride diffusion in concrete. Nor is information available on how the fine LWAs influence the concrete permeability compared with coarse ones although fine LWAs are known to be more efficient to reduce autogenous shrinkage. Such information is essential to ensure the resistance of concrete to the penetration of harmful substances and thus durability of structures.

2.5 Test Methods for Water Absorption and Sorptivity of Concrete

As discussed before, sorptivity is one of the most important properties of a porous material like concrete when capillary flow in unsaturated concrete is of concern. Sorptivity is increasingly used in the specification of durability [Ballim and Alexander, 2005].

There are generally three types of measurements for water absorption and sorptivity, namely direct gravimetric method, penetration distance method, and measurement of moisture distribution method.

2.5.1 Direct gravimetric method

This is the most straightforward method to determine the sorptivity of a porous solid by monitoring the increase in mass of a specimen over a time interval due to

capillary absorption of liquid of density ρ. A typical arrangement is to place the specimen on rods or other suitable supports in a tray containing the test liquid so that the entire lower surface of the specimen is in contact with the liquid (Fig. 2.5). The sorptivity is determined from the slope of the mass of water absorbed against square root of time. A minimum of 5 points is necessary to define a good sorptivity curve [Hall and Hoff, 2002]. The coefficient of water absorption can be determined according to Eq. (2.18) which is similar to Eq. (2.9):

$$i = \frac{M}{A} = S_0 + St^{1/2} \tag{2.18}$$

where

i – cumulative mass absorbed per unit area of inflow surface (g/ mm^2);

M – mass of water absorbed (g);

A – area of inflow surface (mm^2);

S – water sorptivity (g/mm^2/s$^{0.5}$);

t – elapsed time (s);

S_0 – initial disturbance (g/mm^2) observed by some researchers, which is a constant [Basheer and Nolan, 2001], and is believed to be dependent on the surface condition of specimens.

The higher the moisture content of the concrete, the lower the measured sorptivity. Thus the preconditioning process of concrete specimens should be consistent for comparison. Equation (2.18) has been confirmed by experimental results of many materials such as bricks and cement-based materials [Gummerson et al., 1979; Olorunsogo and Padayachee, 2002].

The test is based on a mechanism relevant to deterioration processes in many field concretes. Furthermore, it is found that this test method yields reproducible results which describe the material behavior with regard to variations in compositions

and curing conditions [Sabir et al., 1998]. The ASTM C 1585 test method is based on this principle where the water absorption *i* and the sorptivity *S* (a term 'rate of absorption' is used in the standard) could be easily obtained.

2.5.2 Methods based on penetration distance

The sorptivity can also be defined in terms of water penetration depth by absorption. Based on this, Ho and Lewis [1984] proposed a technique to estimate sorptivity by allowing a specimen to take up liquid for a fixed period of time and then splitting the specimen to measure the penetration depth inside the specimen. The relationship between the water penetration depth *d* and the elapsed time *t* could be represented by the following equation [McCarter, 1993]:

$$d = d_0 + S^{'} t^{1/2} \tag{2.19}$$

where

d_0 – a constant;

$S^{'}$ – penetration coefficient of the concrete.

In practice, it is much easier and more accurate to determine the mass of liquid absorbed compared to determining the penetration depth. Also an appreciable amount of liquid may exist beyond the visual wet front. It should be noted that the determination of the sorptivity from the cumulative absorbed mass, coupled with knowledge of the porosity, the distance of penetration depth of the wet front may be estimated [Hall and Hoff, 2002].

2.5.3 Methods based on measurement of moisture distribution

The third method is based on measurement of moisture distributions. Nuclear magnetic resonance imaging (NMR), positron emission tomography, neutron

radiography, X-ray absorption and gamma-ray absorption can measure liquid (especially water) penetration front. These techniques are particularly useful for measuring the water penetration front as water advances into an initially dry porous solid [Hall and Hoff, 2002]. However, these equipment may not be available in many laboratories.

2.6 Test Methods for Water Permeability of Concrete

For cement based materials, there are two common methods for measuring their permeabilities, i.e. the steady flow method and the depth of penetration method. Both methods are consistent with the definition of Darcy's Law.

Pressure-induced water flow method is performed on a saturated specimen and involves subjecting one end of the specimen to a pressure head. When a steady flow condition is reached, the measurement of the outflow from the other end of the specimen enables the determination of permeability coefficient by using Darcy's law. Such a steady flow is difficult to achieve in dense concrete. For instance, it could not be achieved in low-permeability concrete specimens even after being exposed to a pressure of 3.85 MPa for 5000 hours (208 days) [Bisaillon and Malhotra, 1988].

Besides, radial flow geometry of a cylindrical specimen with a central core can also be used. The flow is normally established between the outer circumferential face of the core and the central core. The principle of conducting this test is summarized by Hall and Hoff [2002]. It has the same drawbacks with the other steady-state flow methods as mentioned above.

The test of penetration depth involves subjecting one end of unsaturated concrete to a pressure head. The water penetration depth is determined by measuring

the average depth of discoloration due to wetting after splitting the cylinder. BS EN standard 12390-8 [2000c] is based on this principle.

Provided that the flow of water is uniaxial, water penetration depth can be used to estimate the coefficient of permeability according to Valenta's equation [Valenta, 1970]:

$$K_P = \frac{d^2 \cdot v}{2 \cdot h \cdot t} \tag{2.20}$$

where

K_P – coefficient of water permeability (m/s);

d – penetration depth in concrete (mm);

v – porosity of the concrete;

h – hydraulic head of water (m);

t – time under pressure (s).

The value of v represents discrete pores, such as air voids, which are not filled with water except under pressure, and can be calculated from the increase in the mass of concrete during the test [Vuorinen, 1985].

$$v = \frac{m}{Ad\rho} \tag{2.21}$$

where

m – gain in mass (g);

A – cross-sectional area of the specimen (mm^2);

ρ – density of water (about 1000 kg/m^3).

It has been found that the steady state flow method is more applicable to concretes with relatively high permeability, whereas the depth of penetration method is more appropriate for concretes with very low permeability [Khatri and Siriviatnanon, 1997].

2.7 Test Methods Based on Diffusion Mechanism

2.7.1 Salt Ponding Test

AASHTO T259 test (commonly referred to as the salt ponding test) is a test for measuring the penetration of chloride into concrete (Fig. 2.6). It provides a one-dimensional chloride ingress profile used for evaluating the chloride penetration in concrete.

However, the test mechanism for AASHTO T259 encompasses a combination of surface absorption and diffusion. Analytical models currently available are not able to describe such complex mechanisms. In addition, a substantial period of drying can exaggerate the effect of initial surface absorption [McGrath and Hooton, 1998]. Hence, the use of well controlled saturated specimens can improve the precision of the chloride penetration profile and may reflect the extent of long-term penetration of chloride into concrete more accurately than specified by AASHTO T259 test. In such a case, the chloride diffusion coefficient can be reasonably obtained based on Fick's Second Law (Eq. (2.11)). To obtain more accurate results, smaller thickness of each layer from the exposure surface is needed to determine the chloride profile [McGrath and Hooton, 1998].

It is well documented that the rate of chloride ingress into concrete decreases with time. Thus the diffusion coefficient obtained by this method is not a constant, but a time-dependent parameter [Buenfeld and Newman, 1987]. To take the time-dependent factor into consideration when calculating the diffusion coefficient, a power function of time has been assumed by Mangat and Molly [1994], and the modified

Fick's 2nd Law after incorporation of the time dependence of the diffusion is proposed.

$$C = C_0 \left\{ 1 - \text{erf} \left[\frac{x}{2\sqrt{\frac{K_d}{1-m_e} t^{1-m_e}}} \right] \right\} \quad (2.22)$$

where

C – chloride concentration at distance x and time t;

C_0 – chloride concentration at the concrete surface;

m_e – an empirical coefficient which is strongly influenced by the *w/c* of concrete; and $m_e = 2.5(w/c) - 0.6$.

This chloride ponding test is time consuming and only suitable for laboratory investigations.

2.7.2 Bulk Diffusion Test (Immersing Test)

To overcome some of the deficiencies of AASHTO salt ponding test, a Nordic test method NTBuild 443 [1995] was developed as a bulk diffusion test. Firstly, it controls the specimen's initial moisture condition by saturating the specimens with limewater instead of drying the specimen for 28 days as in AASHTO T 259 test. This prevents any initial absorption effect when the chloride solution is introduced. Secondly, the specimens are immersed rather than ponded in a salt solution to ensure constant moisture condition during test duration. The other main difference between the tests NTBuild 443 and AASHTO T259 is the concentration of NaCl solutions used. NTBuild 443 uses a higher concentration of NaCl solution (2.8 M, about 14.2%), thus a greater concentration gradient of chloride ions between concrete pore solution and that in the exposure solution leads to a higher rate of chloride penetration. Because of the higher concentration of NaCl solution, the test duration of NTBuild 443 is 35 days.

For higher quality concretes, however, this period may be extended to 90 days or longer, similar to that of AASHTO salt ponding test [Stanish et al., 1997].

A Nordic round robin test on this method conducted on 3 different concrete mixtures (Portland cement concrete and concrete incorporating silica fume and slag) was reported by Tang and Sørensen [1998]. According to the results, the test yielded diffusion coefficients with repeatability coefficient of variation in the range of 8-14% and reproducibility coefficient of variation in the range of 16-23%. The other useful parameter C_0 (surface chloride concentration) had repeatability and reproducibility coefficient of variation in the range of 10-20%.

2.7.3 Determination of chloride content in concrete

Chloride can exist in three different forms in concrete, namely free chloride, physically adsorbed chloride, and chemically bound chloride. The sum of all these chlorides is known as total chlorides. However, the distribution of the chloride ions among the three forms is not permanent, since there exists equilibrium among them such that some free chloride ions are always present in pore water [Neville, 1995]. It is generally recognized that the free chlorides contribute to the corrosion of steel reinforcement. Practically, both total and free chlorides can be used for chloride thresholds based on available literature [Izquierdo et al., 2004; Neville, 1995].

Total chlorides are usually determined by acid extraction method and are commonly known as acid-soluble chlorides. Dhir *el al.* [1990] summarized various methods based on acid strength and contact time (Table. 2.6).

The chloride is firstly extracted from concrete and the solutions are then analyzed by various methods such as Volhard method (BS 1881-124), potentiometric titration method (AASHTO T260), and Ion Chromatography. Methods of X-ray

Fluorescence Spectrometry (XRF) can quantify chemical elements in the concrete samples without acid extraction. It was thus selected by Dhir *et al.* [1990] as a reference with which other tests were compared.

According to Dhir *et al.* [1990], Volhard method underestimates total chloride content by 0.1- 0.9% for a mean content of 12% with a coefficient of variation of 38%, particularly for low chloride content less than 100 ppm. However, RILEM Technical Committee TC 178-TMC [1999] considered Volhard method as the most suitable method for total chlorides determination.

Ion chromatography can also be used to determine the total chloride content. According to Oh [2003], however, this method may not be suitable as acid treatment may bring additional anions such as NO_3^-, NO_2^- and F^- into the filtrate and some of these anions have retention time close to that of Cl^- which will disturb Cl^- determination, especially at low Cl^- concentration.

Arya and Newman [1990] distinguished water soluble chloride content from the free chloride, and defined the latter as the chloride ions in the concrete pore solution.

Various methods have been proposed to determine the free chloride content by analyzing the pore solution expressed from concrete specimens [Barneyback and Diamond, 1981], and by analyzing decanted solutions from pulverized specimens such as AASHTO T 260 [1994] and ASTM C 1218 [2006] methods. Both ASTM C1218 and AASHTO T260 have some similarities in decantation methods which was summarized by Oh [2003] in Table 2.7. These two methods are functionally identical. Arya and Newman [1990] and Arya *et al.* [1990] reported that the pore solution expression method was very accurate for determining the free chlorides. Glass *et al.*

[1996] however, reported that the pore solution expression under pressure may result in an overestimation of the free chlorides.

2.8 Accelerated Test Methods with External Voltages

2.8.1 Rapid Chloride Penetrability Test

The rapid chloride penetrability test (RCPT) was originally developed in early 1980s by Whiting [1981]. It was shown that the charge passed through the plain cement concrete was well correlated with the chloride penetration data obtained from the 90-day salt ponding test. Based on the experimental results, guidelines were established to qualitatively classify concrete mixtures into different categories. Later, this method was adopted by the American Association of State Highway and Transportation Officials (AASHTO) as AASHTO T-277 and also by American Society for Testing and Materials (ASTM) as ASTM C 1202.

In such test, ionic transport is accelerated by an external voltage applied across a concrete specimen by using the set-up shown in Fig. 2.7. The upstream reservoir contains a 3.0 % NaCl solution and the downstream reservoir contains a 0.3 M NaOH solution. The electric current is measured and recorded over a 6-hour period. The total charge passed is determined and used to rate the concrete quality according to the criteria shown in Table 2.8.

Since the measurement of charge passed can be carried out in less time and with less complicated technique than the measurement of diffusion, this method has been used widely for quality control and to compare the resistance of different concretes to chloride penetration.

However, there are controversial opinions about this method as the results are affected by both the pore structure and the pore solution chemistry of concrete

[Detwiler and Fapohunda, 1993; Jiang et al., 2004]. On the one hand, this method is believed to provide reliable indications on the resistance of NWC and LWC to chloride penetration [Chia and Zhang, 2002; McGrath and Hooton, 1998; Thomas, 2006]. On the other hand, RCPT method is sensitive to differences in the chemistry of the pore solution, and therefore may exaggerate the effectiveness of supplementary cementitious materials on the reduction of penetrability [Jiang et al., 2004]. Also, the constantly applied voltage of 60 V may produce a varying amount of heat inside the specimen and thus affect the test results. Furthermore, direct current may cause a polarization of pore solution and alter the pore water composition [Elkey and Sellevold, 1995].

2.8.2 Non-steady state migration test

The rapid chloride penetration test ASTM 1202 does not determine the chloride diffusion coefficients, but provides a comparative measure of the resistance to chloride ion penetration. Though the improved AASHTO T259 test can determine the diffusion coefficients of concrete, it requires more than 90 days for the test. Tang and Nillson [1992] proposed a rapid migration test with an external voltage of 10 to 60 *V*. This method has been adopted as a Nordic Standard test NT BUILD 492 [1999].

A schematic test set-up is shown in Fig. 2.9 where a concrete specimen is exposed to a concentrated NaCl solution on one side and a NaOH solution on the other side. Immediately before testing, the test specimens are preconditioned according to a standard water-saturation procedure. An external potential from 10 to 60 V is applied across the specimen for varying periods of time from 6 to 96 hours. The strength of the external potential and the duration of the test time depend on the quality of concrete. After the test, the specimen is split into two pieces along its axis. The depth of chloride

ion penetration is determined by use of a colorimetric technique - spraying 0.1 N $AgNO_3$ solution. Based on the depth of chloride ion penetration and Nernst-Plank equation, the chloride migration coefficient can be calculated according to an established procedure [Tang, 1996; Tang and Nilsson, 1992].

The test duration of this method is relatively short. For ordinary concrete a test duration of 24 hours may be typical, whereas for dense concrete more time may be needed. Since this rapid migration test method requires only a short duration of time it can be used to control chloride diffusivity at any stage of hydration for a given concrete [Gjørv, 2009]. For severe environments, the early age resistance against chloride penetration may also be an important property of the concrete.

According to McGrath and Hooton [1998], the method generally produces good precision with a reproducibility coefficient of 12 - 24%, especially for concrete with Portland cement and silica fume with coefficients of variation within 5 - 9%. Although the migration coefficient is normally used as a general parameter for characterizing the resistance of the given concrete against chloride ion penetration, this parameter has been used as a durability parameter for characterizing the general durability properties of concrete. Therefore, the migration test method has also been applied as part of regular concrete quality control and documentation of achieved construction quality of several concrete structures produced for a new sewage and water treatment plant in Trondheim [Rindal et al., 2000].

However, the method also has some disadvantages. The chemically bound chloride ions may affect the penetration profile of the chlorides inside the specimen. In addition, the chloride ion concentration at source, at distance *x* away from the source, and at the penetration front represents different media, and the measurement of the penetration depth by $AgNO_3$ spray may introduce some errors [Jiang et al., 2004].

According to this method, chloride concentration at which the color changed was approximately 0.07 N for ordinary Portland cement concrete. According to Otsuki et al. [1992], this whitish color will only be visible when the chloride content is > 0.15% by weight of cement with the spray of the $AgNO_3$ solution.

2.8.3 Steady state migration test

Contrast to the rapid non-steady-state migration test mentioned above, a more general analysis of chloride diffusivity in concrete based on an accelerated steady-state migration test was carried out by Zhang T and Gjørv [1994]. The test set up was similar to that of ASTM C 1202 and the applied external potential was reduced from 60 V to approximately 10 to 15 V. During the test, the chloride-ion concentration in the chloride collecting cell was monitored until a steady state was reached, and the relationship between the chloride-ion concentration and time could be established. Based on the steady-state migration tests and the relevant theoretical basis such as Einstein relation, Nernst-Einstein equation, or simplified Nernst-Planck equation, the chloride diffusion coefficient could be calculated [Andrade, 1993; Andrade and Sanjuan, 1994; ZhangT and Gjorv, 1994].

The steady-state migration test method has certain advantages over non-steady-state migration test, since it measures the diffusion of the chloride ions directly; it is not sensitive to differences in pore solution chemistry [Detwiler and Fapohunda, 1993]. However, practical shortcomings also need to be considered. The duration of the test can not be predicted. For HPC, the test may take several months to achieve its steady state and the increase in the real age of the concrete makes relative comparison difficult. Another practical difficulty is the need to measure low concentrations of chlorides in the NaOH solution. Moreover, the concentration of the chloride-ions in the

source solution changes with time and maintaining a constant chloride source concentration during a test over several months is difficult [Detwiler and Fapohunda, 1993; Jiang et al., 2004].

The test methods used in present study are described in Section 3.4 of Chapter 3.

Table 2.1 Effect of age of cement paste on its permeability coefficient (*w/c*=0.51) [Mindess et al., 2003]

Age, days	K_p, m/s	
Fresh paste	10^{-5}	Independent of w/c
1	10^{-8}	Capillary pores interconnected
3	10^{-9}	
4	10^{-10}	
7	10^{-11}	
14	10^{-12}	
28	10^{-13}	
100	10^{-16}	Capillary pores discontinuous
240 (maximum hydration)	10^{-18}	

Table 2.2 Classification of pore sizes in hydrated cement pastes [Mindess et al., 2003]

Designation	Diameter	Description
Capillary pores	10,000 – 50 nm (10 – 0.05 μm)	large capillaries (macropores)
	50 – 10 nm	medium capillaries (large mesopores)
Gel pores	10 -2.5 nm	small isolated capillaries (small mesopores)
	2.5 – 0.5 nm	micropores
	≤ 0.5 nm	interlayer spaces

Table 2.3 Influence of pore sizes on properties of the hydrated paste [Mindess et al., 2003]

Category	Role of water	Properties affected
Macropores	Behaves as bulk water	Permeability; Diffusivity
Large mesopores	Samll surface tension forces generated	Permeability in the absence of macropores; Shrinkage above 80% RH
Small mesopores	Large surface tension forces generated	Shrinkage between 80% RH and 50% RH
Micropores	Strongly adsorbed water; no menisci form	Shrinkage at all RH; creep

Table 2.4 Comparison between permeabilities of rocks and cement pastes [Powers, 1958]

Types of rock	Coefficient of permeability, K_P, m/s	w/c ratio of mature paste of the same permeability
Dense trap	2.47×10^{-14}	0.38
Quartz diorite	8.24×10^{-14}	0.42
Marble1	2.39×10^{-13}	0.48
Marble2	5.77×10^{-12}	0.66
Granite1	5.35×10^{-11}	0.70
Porous sandstone	1.23×10^{-10}	0.71
Granite2	1.56×10^{-10}	0.71

Table 2.5 Diffusion coefficient for chloride penetration of LWA [Zhang, 1989]

Types of aggregate	Diffusion coefficient, m^2/s	
		Average ± Standard deviation
Liapor 8	1.8×10^{-11} 1.3×10^{-11} 7.8×10^{-11}	$(3.6\pm3.6)\times10^{-11}$
Liapor 7	8.2×10^{-11} 5.4×10^{-11} 2.4×10^{-11} 3.3×10^{-11}	$(4.8\pm2.6)\times10^{-11}$
Liapor 6	1.3×10^{-10} 3.7×10^{-11} 7.4×10^{-11} 3.3×10^{-11}	$(6.9\pm4.5)\times10^{-11}$
H.S.Leca	9.8 ×10 1.9 ×10 3.6 ×10 5.3 ×10 4.1 ×10	$(8.4\pm6.4)\times10^{-11}$
Lytag	2.5 ×10 2.6 ×10 8.1 ×10 2.8 ×10 9.0 ×10	$(5.0\pm3.3)\times10^{-11}$

Table 2.6 Comparison of methods for acid extraction of chloride-ions from concrete [Dhir et al., 1990]

Standard method	Extraction treatment						
	Initial			Final			Total test period, min
	HNO_3, M	Temp, ^oC	Contact time, min	HNO_3, M	Temp, ^oC	Contact time, min	
AASHTO T260	3.7	20	1	1.0	boiled	1	30
ASTM C114	2.0	20	2	2.0	boiled	1	30
BS 1881-124	2.67	20	1	1.45	boiled	4.5	40

Table 2.7 Comparison between ASTM C1218 and AASHTO T260 [Oh, 2003]

	ASTM C1218	AASHTO T260
Sample size	10 g ≤850μm	3g ≤300-850 μm
Reagent water	50 ml	60 – 70 ml
Boiling	5min, without mechanical stir	5 min, with magnetic stirrer
Standing period	24 h	24 h
Reboiling	1-2 min	1 min

Table 2.8 RCPT ratings according to ASTM C 1202

Charge passed, Coulombs	Chloride ion penetrability	Typical of
> 4,000	High	High w/c ratio
2,000-4,000	Moderate	0.4-0.5 w/c ratio
1,000-2,000	Low	w/c ratio < 0.4
100-1,000	Very Low	Latex Modified concrete
< 100	Negligible	Polymer concrete

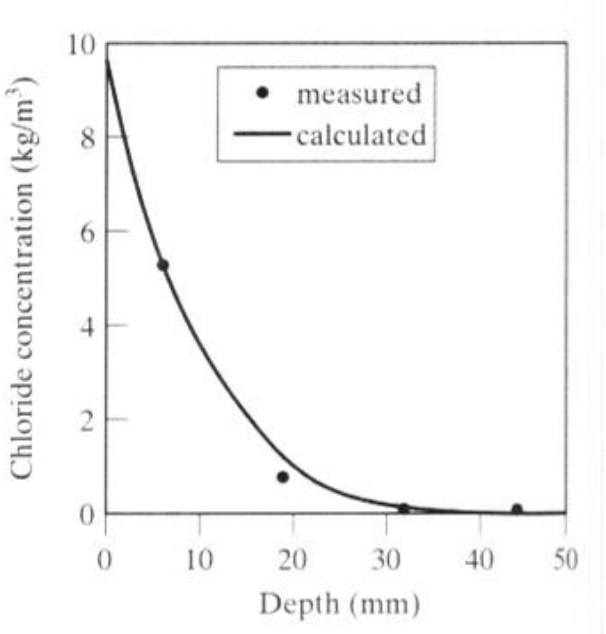

Fig. 2.1 Chloride concentration profile following Fick's Second Law for Parking garage in northern Midwest USA [Berke and Hicks, 1996].

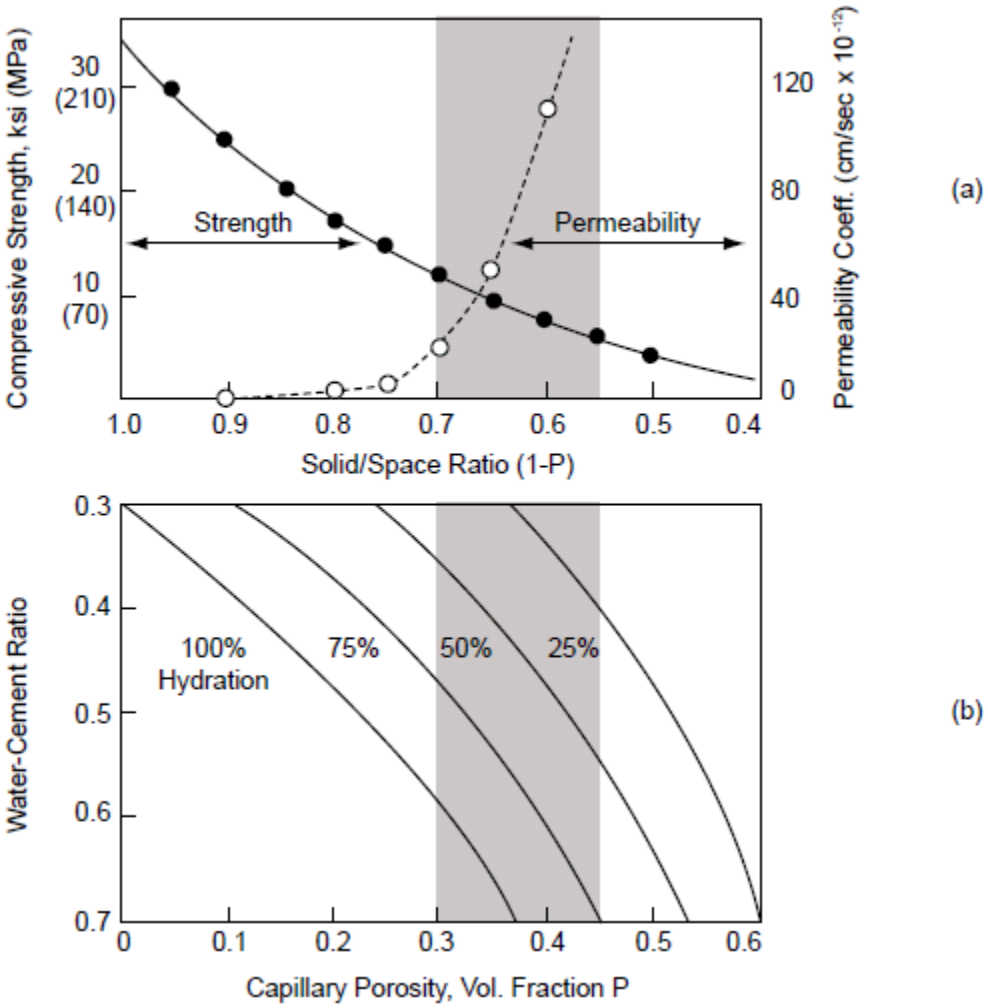

Fig. 2.2 Influence of w/c and degree of cement hydration on permeability of concrete [Mehta and Monteiro, 2005]

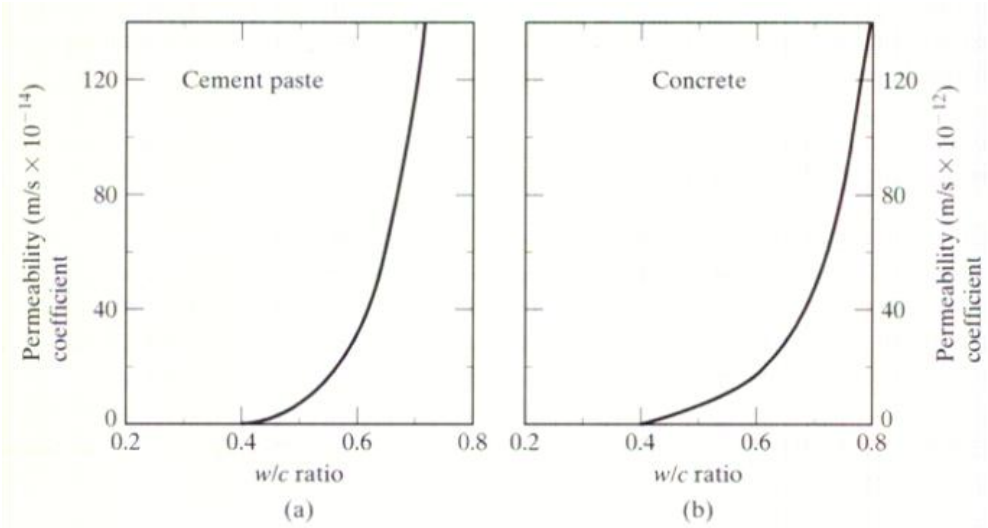

Fig. 2.3 Influence of w/c ratio on the permeability of (a) cement paste; (b) concrete [Mindess et al., 2003]

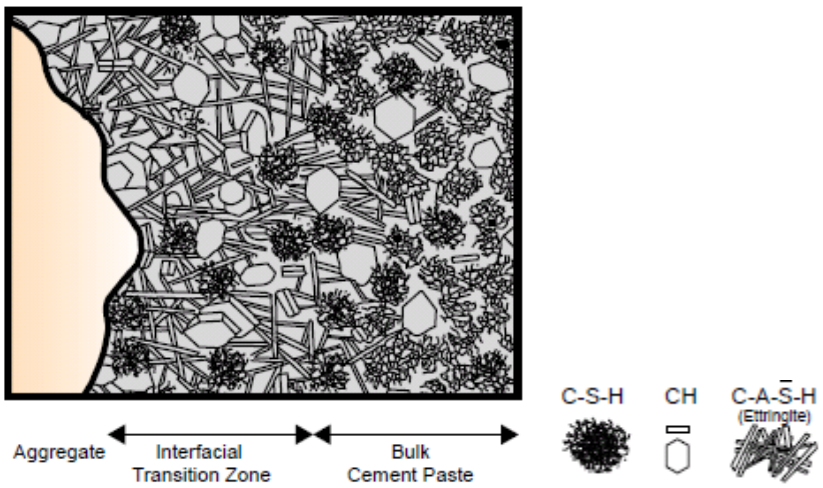

Fig. 2.4 Diagrammatic representation of interfacial transition zone near aggregate in NWC [Mehta and Monteiro, 2005]

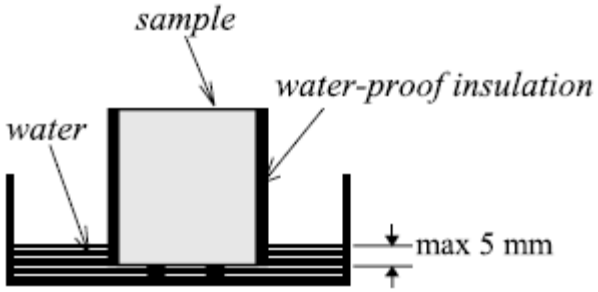

Fig. 2.5 Water absorption experimental set-up [Zaharieva et al., 2003]

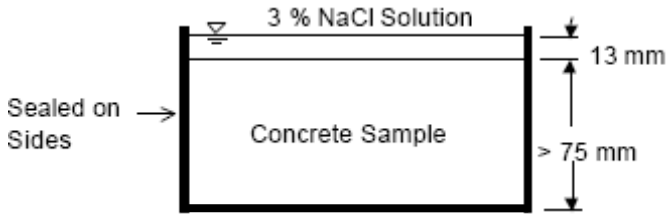

Fig. 2.6 Salt ponding test setup

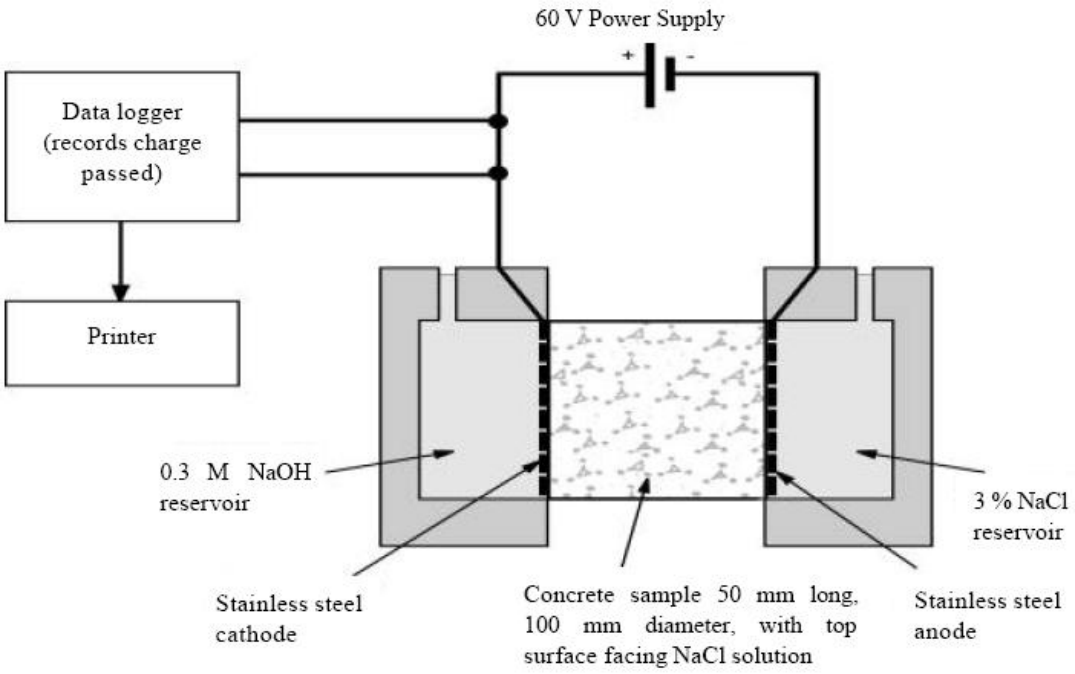

Fig. 2.7 ASTM C 1202 test set-up

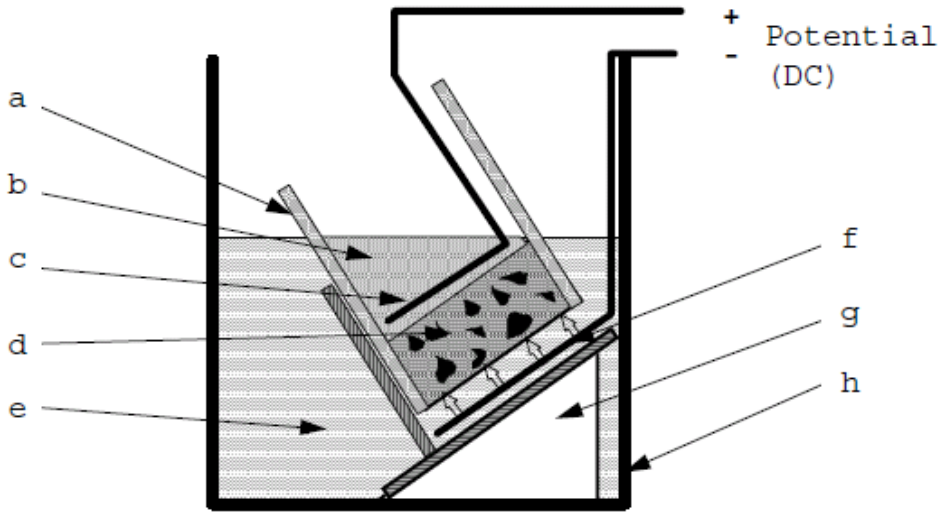

a. Rubber sleeve
b. Anolyte
c. Anode
d. Specimen
e. Catholyte
f. Cathode
g. Plastic support
h. Plastic box

Fig. 2.8 Rapid migration test set-up from NT Build 492.

CHAPTER 3 EXPERIMENTAL DETAILS

In the first part of this chapter, details on the constituent materials used, mixture proportions and preparation of cement and concretes are described. In the second part, test methods used in this study are introduced, including methods for determining basic physical and mechanical properties and transport properties of concretes such as sorptivity, water permeability, and chloride-ion resistance of concretes.

3.1 Materials

3.1.1 Aggregates

3.1.1.1 Normal weight aggregates

Granite aggregates with a maximum size of 9.5 mm was used in NWC. Natural sand was used in all the concretes except for all-LWC. Densities of the granite and natural sand were 2610 and 2560 kg/m^3, respectively. The absorption capacity of natural sand was about 0.6% (Table 3.1).

The aggregates were separated into four size fractions of <1.18 mm, 1.18-2.36 mm, 2.36-4.75 mm, and 4.75-9.5 mm, and then recombined to satisfy ASTM C 33-03 [2006a] grading requirements as presented in Fig. 3.1.

3.1.1.2 Lightweight aggregates

Lightweight aggregates used were commercially available expanded clay and expanded glass particles which were divided into the same four size fractions <1.18 mm, 1.18-2.36 mm, 2.36-4.75 mm, and 4.75-9.5 mm, and then recombined to have the same grading as NWA which also satisfies the grading requirements of ASTM C 330 (Fig. 3.2). The characteristics of the LWA including size, shape, porosity, particle density, and water absorption can be found in Table 3.1.

Lightweight aggregates F6.5 and F4.5 were made of expanded clay with round shape and relatively smooth surface (Fig. 3.3). Those expanded clay type aggregates are burned in a rotary kiln at approximately 1200 ^{o}C. They are produced from special types of clay suitable for bloating which expand during heating due to development of gases from organic material in the clay. This results in ceramic particles with a smooth dense skin and a honeycomb interior [FIP, 1983]. In addition, lower density expanded glass particles were also used in some concrete mixtures to reduce the unit weight of concrete. The expanded glass is produced from recycled glass and is commercially available. Recycled glass is crushed and mixed to obtain a glass mixture with restrictions to the mass percentage of alkalioxides. This mixture is pressed and next crushed into a coarse granulate. The granulate is foamed in an oven with temperatures from 700 to 850 ℃ for a period of 3 to 30 minutes. After a defined period of cooling, glass particles with low densities and surface layers in low permeabilities are produced [EuroLightCon, 1988].

The expanded clay in spherical particle have a bulk particle density within 750 – 1300 kg/m^3. The crushed LW sand has a much higher particle density of about 1600 kg/m^3. Compared with expanded clay, those spherical expanded glass particles have significantly lower particles densities in a range of 350 – 600 kg/m^3.

The total porosity of the LWA particles was calculated based on density of aggregate particles and density of solid material as follows:

$$f_a = 1 - \frac{\rho_b}{\rho_s} \quad (3.1)$$

where

f_a – total porosity of aggregate (%, by volume);

ρ_s – density of solid material (kg/m^3);

ρ_b – density of aggregate particles (kg/m^3).

The density (ρ_s) of the solid material was determined by helium pycnometer using a crushed LWA sample passing through a 150 μm sieve. The density of the aggregate (ρ_b) was determined according to ASTM C 128-04a [2006b]. The pores filled by water under vacuum condition were considered as open pores. The difference between the total and open pores was considered as closed pores.

The specific gravity of the solid material was measured on a powder sample passing through 150 μm sieve tested by helium pycnometer. The particle density can be determined by a pycnometer using vacuum saturated aggregates. For the test of aggregate particle density, the calculation is based on the following equation according to ASTM C 128-04a:

$$\rho_b = \frac{W_0}{B - W + W_m} \quad (3.2)$$

Where

ρ_b – bulk density of the aggregate (Oven Dry condition);

W – weight of pycnometer, water and "saturated" aggregate (g);

B – weight of pycnometer and water (g);

W_0 – weight of dry particle (g);

W_m – weight of "saturated" surface dry particle (g).

Those expanded clay aggregates have total porosities in a range of 50 -71%. Those lightweight sand < 1.18mm has a total porosity around 40%. The expanded glass aggregates have higher total porosities within 77 – 86% compared with the LWA made from expanded clay. For a given type of LWA, the total porosity is smaller for the smaller particles than for the larger ones, because the larger particles are more expanded. This occurs when the aggregates are manufactured by a heating process and the kiln is fed with ungraded raw material containing greatly varying particle sizes.

The 24-hr water absorption LWA F6.5 and F4.5 was ranging from 11.6 to 26.0 % by mass of aggregate particles, about 13.4% to 20.3% by volume of aggregate particles. About 50 - 70% of the aggregate volume was occupied by pores, but high percentages of the pores were closed ones. Lightweight sand with sizes <1.18mm was also expanded clay, but consisted of crushed particles with more open pores and high 1-hr water absorption. Its 1-hr water absorption was roughly the same as its 24-hr water absorption. Because of the nature of the crushed particles, it is difficult to accurately determine the absorption of the aggregate and to obtain saturated surface dry aggregate. The water absorption was estimated to be about 25 to 30% by oven-dry mass of the sand (Table 3.1).

One-hr water absorption of the expanded glass was from about 3 to 12% by mass of aggregate particles and about 1.7 to 4.2% by volume of aggregate particles (Table 3.1). However, there was a significant increase in water absorption from 1 to 24 hrs. Their 24-hr water absorption was about 28.4 to 52.0% by oven dry mass of aggregate particles. Compared with the expanded clay, the expanded glass had greater increase in the water absorption from 1 to 24 hrs. Because the expanded glass with size <1.18mm was very fine, it was also difficult to obtain saturated surface dry condition of the particles and to accurately determine its water absorption. Therefore, the

absorption value for the expanded glass <1.18mm given in Table 3.1 was also an approximation.

The water absorption of aggregates was tested on LWA according to ASTM 128-04a at 1 and 24 hrs and calculated based on the mass and volume of the aggregate particles respectively.

For LWA used for internal curing desorption of the aggregates was also determined. The oven dried LWA was firstly immersed in water for 24 hrs and then exposed the LWAs to different RH at 30^{o}C until constant mass is reached. The different RH can be achieved by saturated salt solutions. For example, the environment over saturated K_2SO_4 solution has a RH of 97%, that over saturated KNO_3 solution has a RH of 92%, that over saturated KCl solution has a RH of 85%, and that over saturated NaCl solution has a RH of 75%. The desorption of LWA under RH of 85% was presented in Table 3.1 and later on used for calculation for the content of LWA to provide enough water for internal curing of the cement paste around the aggregates.

3.1.2 Cementitious and pozzolanic materials

ASTM Type I Portland cement with a specific gravity of 3.15 and Blain surface area about 347.2 kg/m^{3}was used for all cement paste and concretes. Its chemical composition and physical properties are given in Table 3.2, together with the estimated cement compounds based on Bogue's equations given in ASTM C 150-05 [2008]. A commercially available dry undensified silica fume was used for a selected concrete to achieve high resistance to water and chloride-ion penetration. Specific gravity of the silica fume was approximately 2.2 and 95% of its composition was silicon dioxide.

3.1.3 Chemical admixtures

A naphthalene based superplasticizer [1] was used in all concretes with a water/cement (or cementitious material) ratio (w/cm) of 0.38, and a polycarboxylate-based superplasticizer[2] was used in LWC with a w/cm of 0.20 for workability purpose. The naphthalene based superplasticizer was a dark brown solution with a specific gravity of 1.2 and a solid content of about 40%. The polycarboxylate-based superplasticer had a specific gravity of 1.1 and a solid content of about 36%. Both superplasticizers conform to requirements of ASTM C494-05 - Type F high range water-reducing admixture.

In addition, a commercially available shrinkage reducing admixture[3] (SRA) (glycol derivative) was used in a concrete mixture RS4 to compare with those with LWA for internal curing. The SRA is a liquid admixture with a specific gravity of approximately 0.93. According to the manufacture's data sheet, this SRA significantly reduces concrete shrinkage at an early age. It was also recommended to reduce the amount of mix water by an equal volume of SRA used when incorporated into concrete.

3.2 Mixture Proportions

3.2.1 Mixtures to study the effect of incorporation of LWA used for internal curing on transport properties of concrete

Five concretes with assigned names of NC1 and RS1-RS4 with w/cm ratios of 0.39 ± 0.01 were included in this study, and their mixture proportions are summarized

[1] Super 20, W.R.Grace Pte. Ltd. Singapore
[2] Adva 181, W.R.Grace Pte. Ltd. Singapore
[3] Eclipse, W.R.Grace Pte. Ltd. Singapore

in Table 3.3. Mixture NC1 was a control concrete. Mixtures RS1 to RS3 incorporated LWA of different sizes for internal curing. Mixture RS4 incorporated SRA for comparison. For Mixtures RS1 to RS3, the amount of LWA required to provide sufficient water for internal curing was determined based on the equation (2.17).

The amount of the LWA incorporated was determined according to the equation proposed by Bentz et al. [2005] for internal curing as reviewed in Section 2.4. Tthe cement factor (C_f) in equation (2.17) was obtained from the mixture proportions. The chemical shrinkage (*CS*) of cement was calculated based on the cement composition of 0.066 g water/g of solid cement based on Tables 3.1 and 3.4. The expected degree of cement hydration was conservatively taken as 1 for a w/c ratio of 0.38 according to Bentz et al. [2005]. The 24-hr water absorption was used for $Ø_{LWA}$. About 94% to 98% of the water absorbed in 24 hours (Table 3.1) could be desorbed from the LWAs when exposed to a relative humidity of about 85% (over saturated potassium chloride solution). The desorbed water would be useful for internal curing, hence the degree of saturation of aggregate (*S*) was roughly taken as the percentage of the water which can be desorbed as given in Table 3.1.

In these three concrete mixtures, the LWAs replaced the corresponding fractions of normal weight aggregate (NWA) so that the volumes and grading of aggregates were kept the same for all the concrete mixtures. In the concrete with SRA (RS4), the same mass of water was reduced according to the manufacturer.

3.2.2 Mixtures to study the effect of cumulative LWA content on transport properties of concrete

Four LWC (LC1 – LC4) with a w/c 0.38 were prepared with different cumulative LWA contents. The mixture proportions are given in Table 3.5. All the concretes had the same volumes of coarse and fine aggregates. Different size fractions

of LWA were included in the concretes so that the cumulative volume of the LWA increased from 50% by volume of total aggregate in Mixture LC1 to 100% in LC4. Mixture LC1 contained coarse LWA with natural sand, whereas for Mixtures LC2, LC3 and LC4, the natural sand portion was gradually substituted by lightweight sand at decreasing size fractions such that Mixture LC4 was an all-LWC. The LC4 had crushed lightweight sand with size < 1.18 mm, and it was difficult to accurately determine water absorption for such fine crushed particles. An estimated range of 25-30% by oven-dry mass of the crushed lightweight sand was obtained instead. As such, two concrete mixtures were prepared with the estimated absorptions of 25 and 30%, denoted as LC4-25 and LC4-30, respectively. Control NWC with w/c of 0.38 (NC1) and 0.54 (NC2) were included for comparison. The NC1 had the same w/cm as that of the LWC, whereas NC2 had similar 28-day strength to that of LC1 and LC2. In addition, a cement paste with a w/c of 0.38 was also included for comparison.

3.2.3 Mixtures to study the effect of porosities and surface textures of LWA on transport properties of concrete

Lightweight concretes LC1 and LW1 used different coarse aggregates with particle densities of 1200 and 780 kg/m^3, respectively. They will be compared with each other and with NC1 in which granite coarse aggregate was used. Mixture LW4 was compared with LC1 and LC4 to evaluate the effect of fine aggregate. Concrete had the same type and amount of coarse aggregate (F6.5), but different fine aggregates. Mixture LC1 contained natural sand. Mixture LC4 contained lightweight sand with 0 - 1.18 mm fraction being crushed particles and their water absorption was taken as 25%. Mixture LW4 also contained lightweight sand but the fraction from 0 - 1.18 mm was spherical expanded glass particles.

3.2.4 Mixtures to study the effect of w/cm on transport properties of concrete

To develop lighter concrete with high resistance to water and chloride-ion penetration, All-LWC LW5 was designed by using low density coarse LWA (F4.5), expanded glass fine aggregate, and dense paste matrix with a w/cm of 0.20 inclusive of 10% silica fume. Mixture LW5 was compared with LW4 which had similar unit weight and 28-day compressive strength, but was designed with different w/cm and different coarse and fine aggregates.

3.3 Preparation of concretes

The concretes were mixed in a pan mixer with a mixing speed of 50 rounds per minute (rpm), whereas the cement paste was mixed in a Hobart mixer, both at ambient temperature of about 28^{o}C. Slump of the concrete was determined according to ASTM C143 [2006c] and is presented in Tables 3.3 and 3.5. The slump of the concretes was controlled to be 100 ± 30 mm except for NC2 which had a slump of 60 mm without using any superplasticizer.

The LWC was prepared with spherical LWA pre-soaked in water for 24 hrs before concrete mixing. For concrete with the crushed LW sand, water that would be absorbed by these particles in 24 hrs was added into mixing water. For concrete with expanded glass particles, water that would be absorbed by these particles in 1 hr was added into mixing water. Prior to soaking/mixing, all the LWA were oven dried and cooled down to room temperature.

For each mixture, specimens listed in Table 3.6 were cast for various tests. The molded specimens were covered with wet linen and plastic sheet to prevent water evaporation and left in the laboratory for about 24 hrs. The specimens were then transferred to a fog room after demolding and cured for another 6 days at a temperature

of about 28 ^{o}C. After that, the specimens were exposed to laboratory air with relative humidity of about 80-85 % at a similar temperature until the time of testing except those used for the water permeability test.

3.4 Test Methods

3.4.1 Unit weight, compressive strength and elastic modulus

The unit weight, compressive strength and elastic modulus of the concretes were determined according to British Standard BS EN 12390: Part 7 and Part 3[2000b; 2000a] and BS 1881-121 [1983].

3.4.2 Water absorption, permeability, and resistance of concrete to chloride-ion penetration

3.4.2.1 Water absorption test

Water absorption and sorptivity of the concrete will be tested according to ASTM C 1585 based on the direct gravimetric method by measuring increase in mass of the specimens resulting from absorption of water as a function of time when one surface of the specimen was exposed to water.

For each mixture, three ø100×50 mm specimens were obtained from a ø100×200 mm cylinder (Table 3.6) with approximately 10 mm from the top and bottom removed. The specimens were moist cured for 7 days followed by exposure in laboratory air for 21 days. The end surfaces of the specimens were ground before the test. The specimens were then placed in an environmental chamber at a temperature of 50^{o}C and relative humidity of 80% for 3 days before being stored in a sealable plastic bag at 23±2^{o}C for 15 days. Finally, the specimens were coated with epoxy on side surfaces before the absorption test to ensure one-dimensional absorption. The top

surface was covered to prevent evaporation during the test. Increase in mass of the specimens with time was monitored. After the test, two parameters were calculated according to Buyle-Bodin and Hadjieva-Zaharieva [2002] as follows:

- Initial water absorption (kg/m^2) – quantity of water absorbed by a unit surface area during the 1^{st} hour of the test, and
- Sorptivity ($kg/m^2\ h^{0.5}$) – slope of the regression curve of the quantity of water absorbed by a unit surface area versus square root of the elapsed time from 1 to 24 hours.

3.4.2.2 Water permeability test

The water permeability test can determine permeability value of the concrete which directly reflects the influence of LWAs on the permeability of concrete. Depth of water penetration in the concrete was determined on specimens with 7-day of moist curing according to BS EN 12390-8 [2000c] with some modifications. The specimens were subjected to a pressure about 0.75 MPa for 14 days for relative comparison of different concretes. The reason for testing at an early age of 7 days was due to relatively low maximum pressure that can be achieved by the equipment, thus it would be difficult to get water penetration if the concrete was cured longer. The schematic test set up was shown in Fig. 3.4.

Specimens with a diameter of 75 mm and a height of 150 mm were roughened on the circumferencial surface immediately after demolding, and cured in a fog room for 7 days. The circumferencial surface of the specimens was then coated with epoxy mortar of a thickness of 25mm as shown in Fig. 3.4 after surface drying to ensure one dimensional flow of water. Both end-surfaces of the cylinder specimens were then

ground level to prevent water leakage under pressure. The mass of the specimens coated with hardened epoxy mortar was determined before the permeability test.

After the test, the face of the specimen exposed to the water pressure was wiped dry and mass of the specimen was recorded. The specimen was then split into two halves to determine the average depth of water penetration. Water permeability coefficient can be calculated according to Valenta's equation in Eq. (2.15).

3.4.2.3 Resistance of concrete to chloride ion penetration

Rapid chloride penetrability test

The test was conducted according to ASTM C 1202 by using German instrument PROOVE IT. The specimens was cured under moist condition for 7 days and then exposed in lab air for 21 days before being conditioned for test. After 28 days, each cylinder was cut into three Ø100×50 mm specimens after approximately 10 mm from the top and bottom removed and ground. The specimens were subjected to conditioning specified by the standard before testing.

The test procedure followed for RCPT was in conformity with ASTM C 1202. The positive reservoir of the cell was filled with 0.30 N sodium hydroxide solution, while the negative reservoir was filled with 3.0% NaCl solution. A direct current (DC) of 60±0.1 volts was applied across the specimen faces, and the current across the specimen was recorded at every 5 min interval, covering a total period of 6 hrs. By knowing the current and time history, the total charges passed can be obtained from integration of current over the time duration. The total charge passed, in coulombs, is used to evaluate the resistance of concrete to the penetration of chloride ions by using standard rating given in Table 2.8.

Rapid migration test

Rapid migration test according to NT Build 492 was conducted to determine chloride diffusion coefficient more rapidly compared with AASHTO T 259 test. The principle of the test setup is similar to that of ASTM C 1202, but the external potential applied was 30 V instead of 60 V. The test set-up is given in Fig.3.5. After 28 days, each cylinder was cut into three Ø100×50 mm specimens after approximately 10 mm from the top and bottom removed and ground. The specimens were subjected to a standard water-saturation conditioning. The specimens are then mounted into PVC sleeves and placed in a container with a 10% NaCl solution, while the insides of the sleeves are filled with a 0.3 N NaOH solution. Through the use of the separate electrodes placed on each side of the specimens, an electrical voltage gradient of 30 V is applied.

Immediately after the above accelerated exposure to the chloride solution for 24 hours, the test specimens are split into two halves. The chloride penetration depth was determined by spraying $AgNO_3$ solution on the split open concrete specimens. This chloride penetration depth was then used to calculate the chloride migration coefficient according to Eq. (3.3).

$$D_m = \frac{RT}{zFE} \cdot \frac{x_d - \alpha\sqrt{x_d}}{t} \tag{3.3}$$

Where:

$$E = \frac{U - 2}{L} \tag{3.4}$$

$$\alpha = 2\sqrt{\frac{RT}{zFE}} \cdot \mathrm{erf}^{-1}\left(1 - \frac{2c_d}{c_0}\right) \tag{3.5}$$

D_m – migration coefficient, m^2/s;

z – absolute value of ion valence, for chloride z=-1;

F – Faraday constant, F = 9.648 $\times$ 10^4 J/(V mol);

U – absolute value of the applied voltage, V;

R – gas constant, R=8.314 J/(V mol) ;

T – average value of the initial and final temperatures in the anolyte solution (K);

L – thickness of the specimen (m);

x_d – average value of the penetration depths (m);

t – test duration (s),

erf $^{-1}$ – inverse of error function;

c_d – chloride concentration at which the color changes, $c_d \approx 0.07$ N for OPC concrete;

c_0 – chloride concentration in the catholyte solution, $c_0 \approx 2$ N.

Salt ponding test

Resistance of the selected concretes and the cement paste to chloride-ion penetration was also determined according to the AASHTO T259 [2002] method with some modifications. One of the modifications was 3-day water ponding of the specimens prior to salt ponding. The purpose was to create a condition to simulate a diffusion process for chloride ions rather than a combination of diffusion and capillary suction as the original AASHTO test. The other modification was curing age. AASHTO T259 specifies 14 days moist curing followed by 28 days drying before the test. In this study, the slabs were moist cured for 7 days followed by exposure in laboratory air for 21 days. In addition, concrete was sampled at about every 5 mm in depth after the ponding test, instead of 13 mm as specified by the standard for sampling concrete in AASHTO T 260.

At 28 days, the sides and bottom of the slabs were sealed by epoxy, and a dam was built around top edges of each specimen using foam plates. The epoxy was allowed to dry overnight. After that, the specimens were ponded by water for 3 days

before ponding with a 3% sodium chloride solution by mass for 90 days. The ponding depths for water and sodium chloride were 30 mm. The initial 3-day ponding with water might have caused some OH^- ions in the concrete to be leached out. However, due to low w/c of the concrete and small volume of water used for the ponding, effect of OH^--ion leaching within 3 days on results was probably not significant. The top of the ponding dams was covered with plastic sheet to minimize evaporation, and additional solution was added periodically to maintain approximately 13 mm depth of solution specified by AASHTO method.

After 90 days of exposure, the ponding solution was removed and the specimens were allowed to dry. The surfaces were brushed to remove salt crystal buildup. Concrete samples were taken at various depths of the slabs at about 5 mm intervals by drilling at four locations of each slab and then combining the samples. The combined samples were dried at 105 ^oC and ground to pass a 150 μm sieve. Acid soluble chloride content of the concrete was determined according to BS 1881-124 [1988]. Chloride content expressed as volume of the dry concrete samples was plotted versus the depth at mid-point of each interval.

Diffusion of chloride ions in concrete may be described by Fick's second law:

$$\frac{\partial C}{\partial t} = K_d \frac{\partial^2 C}{\partial x^2} \tag{3.6}$$

where

C – concentration (mol/m^3);

t – time (s);

K_d – diffusion coefficient (or diffusivity) (m^2/s);

x – depth (m).

Chloride concentration in a semi-finite slab is given by Equation (3.6) with boundary conditions $C_{(x = 0, t > 0)} = C_0$, $C_{(x = \infty, t > 0)} = 0$, and $C_{(x = 0, t = 0)} = 0$.

$$C(x,t) = C_0\left[1 - erf\left(\frac{x}{2\sqrt{K_d t}}\right)\right] \quad (3.7)$$

where

$C(x, t)$ – chloride concentration at depth x and time t;

C_0 – surface chloride concentration; and erf = error function.

Based on the chloride profile after the ponding test and Fick's second law, chloride diffusion coefficient K_d of the concretes was obtained from curving fitting. The first point in the chloride profile near the surface was not included in the regression analysis according to Reference [Frederiksen, 1996].

3.4.3 Pore structure of cement paste and concrete

3.4.3.1 Estimation of total porosity of both LWC and NWC

The total porosity of different concretes was calculated based on mixture proportion of concrete, porosity of cement paste determined by mercury intrusion porosimeters (MIP), and total porosity of LWA.

Mercury intrusion porosimetry gives an appreciation of the capillary pore system and is based on the premise that a non-wetting liquid will only intrude capillaries under pressure. The relationship between the pressure and capillary diameter is given by Washburn equation [Washburn, 1921]as:

$$d_{cap} = \frac{-4\gamma \cos \theta_m}{P} \quad (3.8)$$

where

P – injection pressure;

γ – surface tension of the liquid;

θ_m – contact angle of the mercury;

d_{cap} – diameter of the capillary.

This equation estimates the diameter of the entry pores through which the pores are accessible. In spite of the distortion arising from the neck effect, the information obtained is useful because the resistance offered by pore structure to various transport phenomena is controlled mainly by the size of the pore necks.

Approximately 2 to 3 pieces of samples with 5 mm diameter (roughly) at the age of 28 days were used for each test. The specimens were dried in a vacuum oven at 50 ^{o}until a constant weight was achieved. The test was performed on a "Micromeritics Autopore WIN9400 Series" mercury porosimeter. The maximum pressure applied to the samples was 412.5 MPa. The minimum pore diameter reached under the maximum pressure was about 3.8 nm assuming a contact angle of 141.3 ° and a mercury surface tension of 0.485 N/m.

The total porosity of LWA was calculated based on density of aggregate particles and density of solid materials and is presented in Table 3.1. Porosity of the granite coarse aggregate and natural sand was considered negligible. No ITZ was considered in the calculation of total porosity of concrete.

3.4.3.2 Water accessible porosity and oven dry unit weight of concrete

According to Mindess [2003], water can only move through capillary pores (0.01μm-10μm) and air voids but does not easily move into small gel pores. Hence, water accessible porosity is an important parameter that could influence the transport properties of cement-based materials. Water accessible porosity of the concretes was determined by a water saturation method, which is similar to the one described in RILEM CPC 11.3 [CPC11.3, 1984].

Three cylindrical concrete specimens of ø100×50 mm were used for this test. The specimens were cut from a ø100×200 mm cylinder with about 10 mm from the top

and bottom removed. From the mass of 'saturated surface dry' specimens determined in air and in water, and the mass of specimens oven dried at 105 ^{o}C, the water accessible porosity (in volume of the concrete) was calculated according to Eq. (3.9). Oven dry unit weight of the concretes was also calculated based on the information.

$$P_w = \frac{(m_s - m_o)/\rho}{(m_s - m_a)/\rho} \times 100\% \quad (3.9)$$

where

m_a – apparent weight of the saturated specimen immersed in water (kg);

m_o – oven dry mass of the specimen in air (kg);

m_s – 'saturated surface-dry mass' of the specimen in air (kg);

ρ – density of water, about 1000 kg/m^3.

The "SSD" condition of the concrete specimens was achieved by a vacuum process. The specimens underwent vacuum treatment for 3 hours and were then immersed in water under vacuum for 1 hour. After that, the specimens were soaked in water for another 18 hours.

3.4.3.3 Scanning electron microscope

Scanning electron microscope (SEM) examination of selected concrete was conducted to characterize the pore structure of ITZ. The examination and anlyses were conducted on polished surface using backscattered electron (BSE) images together with energy dispersive X-ray images. The samples were coated with platinum and examined by JEOL JSM-5600 LV SEM. Low viscosity epoxy impregnated polished samples of concrete are used for BSE imaging. The detailed sample preparation process can be found from references [Detwiler et al., 2001; Stutzman and Clifton, 1999]. The underlying principle is that the contrast of the BSE images depends on the mean atomic number of the concrete constituents. In the BSE images anhydrous phases

of the unreacted cement particles appear bright, the calcium hydroxide light grey, the other hydration products as various shades of darker grey with the epoxy impregnated pores appearing black [Scrivener, 1989].

3.4.4 Autogenous deformation of concrete

The autogeneous deformation of the concrete was measured by a pair of laser sensors during the first 24 hrs and by a digital Demec gauge after that. This test was conducted in a chamber with constant temperature of 30.5 ^{o}C and relative humidity of 75%.

Figure 3.6 illustrates the setup of the measurement with laser sensors for the first 24 hrs. Voltage changes as the specimens shrinks were detected by the sensors and the data captured were used to calculate the length change and the shrinkage of the specimens. The laser sensors were fixed on a steel plate, and the distance between the two sensors was about 400 mm. The size of the concrete prisms used was $75 \times 75 \times 300$ mm. The position of the sensors was approximately 50 mm from one end of the concrete prism. The measuring range of a laser sensor was ± 10 mm, and its resolution was about 5 micron. The resolution of the shrinkage measurement for the concrete prism was therefore about 10 micron (two sensors), which was approximately 0.003% of the length of the prisms. Screws with a length of approximately 55 mm and a diameter of 3 mm were embedded in the specimen at each end (Fig. 3.6), and the clear distance between the tips of the two screws was about 180 mm. This distance was used in the calculation of the shrinkage. A 3-mm thick Perspex plate was cast at each end of the specimen as a target surface to reduce measurement error due to the possibly uneven surface at the micro-scale level. The Perspex plates were covered with aluminum foil on the surface for reflection of laser. An 8-mm diameter hole was

drilled at the center of each end plate of the mold so that the laser beam can directly hit the target surface. To reduce friction between the concrete specimen and the walls of the mold, internal surfaces of the mold were lined with one-mm thick Teflon sheet except for the two end surfaces. Two layers of plastic sheets were fitted well inside the mold leaving two small holes for the screws. After casting the concrete was wrapped with the plastic sheets to prevent moisture loss. The initial concrete temperature was recorded as 29.1 ^{o}C.

The concrete was demoulded after one day and the specimen was wrapped with two layers of aluminum sheets to prevent moisture loss. Two Demec pins, 200 mm apart were glued using epoxy along the center line of each side-surface of the specimen. A digital Demec gauge was used to measure the length change between the two pins once a day for a week. The initial length was measured at about 8 hrs after the pins were glued and dried as a reference.

The initial setting time of the concretes was used as the starting point of the autogenous shrinkage measurement and was determined according to ASTM C 403.

During the first day, thermal expansion due to the heat of cement hydration may be generated simultaneously with the autogenous shrinkage. In this study, temperature change of the concrete specimen with time was monitored by a thermocouple embedded in the center of the concrete specimen. The temperature of the concrete measured with a thermometer right after the concrete mixing was used as a reference. Signals from the laser sensors and thermocouple were recorded by a data logger, thus the autogenous shrinkage and the temperature change of each concrete specimen can be determined at the same time. The autogenous shrinkage was calculated by subtracting the thermal expansion strain from the measured shrinkage

strain. The thermal expansion strain was calculated by multiplying the temperature rise of concrete by a thermal expansion coefficient of $10 \times 10^{-6} /^{o}C$ [Neville, 1995].

It should be noted that the thermal expansion coefficient used was an average value, and it may vary during the hydration process. Kada *et al.* [Kada et al., 2002] reported that the thermal expansion coefficient of concrete was higher at early age. This indicates that the thermal expansion strain might be higher than the values used in this research. On the other hand, the temperature monitored was at the center of the specimen which was the hottest part. As a result, the actual expansion caused by the temperature rise in the concrete might be less than the computed values.

Table 3.1 Characteristics of aggregates

Aggregate type		Particle size, mm	Dry particle density, kg/m^3	Porosity, %, by volume,			1 hr water absorption, % mass	24 hrs water absorption, % mass	1 hr water absorption, % vol.	24 hr water absorption, % vol.	Desorption (85% R.H.), % of water absorbed in 24hrs	Shape & surface texture
				Open	Closed	Total						
Granite		4.75-9.50	2610	-	-	-	-	-	-	-	-	Irregular
Natural sand		<4.75	2560	-	-	-	0.6	-	-	-	-	
Expanded clay	F6.5	4.75-9.50	1200	25.8	31.4	57.2	8.4	13.0	10.1	15.6	94.0	Spherical
	F6.5	2.36-4.75	1300	28.1	23.8	51.9	8.7	11.6	11.3	15.1	94.0	
	F4.5	1.18-2.36	1050	36.6	19.2	55.8	10.8	12.8	11.3	13.4	98.0	
	F4.5	4.75-9.50	780	29.8	41.1	70.9	12.4	26.0	9.7	20.3	-	
	LW sand	<1.18	1600	~40.0	~3.4	43.4	25.0-30.0	25.0-30.0	40.0-48.0	40.0-48.0	95.0	Irregular & crushed
Expanded Glass		2.36-4.75	350	30.2	55.5	85.7	12.0	46.0	4.2	16.1	-	Spherical and smooth
		1.18-2.36	420	36.4	46.4	82.8	6.0	52.0	2.5	21.8	-	
		<1.18	560	~42.1	~35.0	77.1	~3.0	~28.4	1.7	15.9	-	

Table 3.2 Chemical composition and physical properties of cement

		Type I Cement
Physical properties	Specific Gravity	3.15
	Blain surface area (kg/m^2)	347.2
Chemical Analyses, % Composition	CaO	66.8
	SiO_2	21.6
	Al_2O_3	5.3
	Fe_2O_3	3.1
	MgO	2.3
	SO_3	1.9
	K_2O	0.4
	Na_2O	0.1
	Equivalent alkali (Na_2O+0.658 K_2O)	0.4
Boque Potential Compound Composition, %	C_3S	63.0
	C_2S	14.5
	C_3A	8.7
	C_4AF	9.4

Table 3.3 Mixture proportions of concretes with LWA for internal curing in comparison to control concrete and concrete with SRA

Concrete	w/c	Cement, kg/m^3	Mixing Water*, kg/m^3	NWA† (SSD), kg/m^3				Dry LWA, kg/m^3				SP‡, l/m^3	SRA l/m^3	Slump, mm
				0-1.18 mm	1.18-2.36 mm	2.36-4.75 mm	4.75-9.5 mm	0-1.18 mm	1.18-2.36 mm	2.36-4.75 mm	4.75-9.5 mm			
NC1	0.38	500	188	517	172	76	850	-	-	-	-	2.5	-	105
RS1	0.38	500	194	514	171	76	271	-	-	-	269 [b]	1.4	-	75
RS2	0.39	500	195	411	-	-	850	64 [d]	83 [a]	40 [b]	-	1.6	-	70
RS3	0.40	500	200	327	171	76	850	117 [d]	-	-	-	1.9	-	65
RS4	0.39	500	188	514	171	76	850	-	-	-	-	1.7	8.0	75

* Including water in SP, but not including water absorbed by LWA.
† The absorption capacity of the dry sand (<4.75mm) was 0.6%.
‡ Superplasticizer - naphthalene-based.

Remarks on LWA:	
a	F4.5
b	F6.5
d	Crushed LW sand

Table 3.4 Calculated coefficients for chemical shrinkage due to cement hydration

Cement phase	Coefficient, g water/g solid cement phase
C_3S	0.0704
C_2S	0.0724
C_3A	0.171* (0.115†)
C_4AF	0.171* (0.086†)
Silica fume	0.20

* Assuming sufficient sulfate to convert all of the aluminate phases to ettringite.
† Assuming total conversion of the aluminate phases to monosulfate.

Table 3.5 Mixture proportions of the concretes to investigate the influence of cumulative LWA content, coarse aggregate, and fine aggregate etc.

Concrete	w/cm	Cement, kg/m^3	Silica fume, kg/m^3	Mixing Water*, kg/m^3	NWA† (SSD), kg/m^3				Dry LWA, kg/m^3				SP‡, l/m^3	Slump, mm
					0-1.18mm	1.18-2.36mm	2.36-4.75mm	4.75-9.5mm	0-1.18 mm	1.18-2.36mm	2.36-4.75mm	4.75-9.5mm		
CP	0.38	1442	-	542	-	-	-	-	-	-	-	-	-	-
NC1	0.38	500	-	188	517	172	76	850	-	-	-	-	2.5	105
NC2	0.54	400		215	517	172	76	850	-	-	-	-	-	60
LC1	0.38	500	-	190	517	172	76	-	-	-	-	395 [b]	2.7	125
LC2	0.38	500	-	191	517	172	-	-	-	-	40 [b]	395 [b]	2.3	70
LC3	0.38	500		190	517	-	-	-	-	83 [a]	40 [b]	395 [b]	2.3	100
LC4-25$^{\Delta}$	0.38	500	-	190	-	-	-	-	321 [d]	83 [a]	40 [b]	395 [b]	2.1	80
LC4-30$^{\Diamond}$	0.38	500	-	188	-	-	-	-	321 [d]	83 [a]	40 [b]	395 [b]	-	85
NC1	0.38	500	-	188	517	172	76	850	-	-	-	-	2.5	105
LC1	0.38	500	-	190	517	172	76	-	-	-	-	395[b]	2.7	125
LW1	0.38	500		188	517	172	76	-	-	-	-	255[a]	1.8	80
LC1	0.38	500	-	190	517	172	76	-	-	-	-	395 [b]	2.7	125
LC4-25$^{\Delta}$	0.38	500	-	190	-	-	-	-	321[d]	83 [a]	40 [b]	395 [b]	2.1	80
LW4	0.38	500	-	190	-	-	-	-	112 [c]	83 [a]	40 [b]	395 [b]	3.6	100
LW5	0.20	594	66	134	-	-	-	-	112 [c]	28 [c]	10 [c]	255 [a]	7.2^{+}	70

* Including water in SP, but not including water absorbed by LWA.
† The absorption capacity of the dry sand (<4.75mm) was 0.6%.
‡ Superplasticizer - naphthalene-based.
Δ Assume water absorption of the crushed LW sand is 25%.
◊ Assume water absorption of the crushed LW sand is 30%.
$^{+}$ Superplasticizer – polycarboxylate-based.

Remarks on LWA:	
a	F4.5
b	F6.5
c	Expanded glass
d	Crushed LW sand

Table 3.6 Specimens used for various tests and curing conditions

Properties to be determined	Size of specimen	Number of specimens	Curing age days	Curing conditions
Density & compressive strength	100x100x100 mm cubes	9	7, 28, 91	7-day moist curing, 21-day exposure in lab air afterwards
Elastic modulus	ø100×200 mm cylinders	3	28	
Water absorption	ø100×50 mm discs cut from ø100×200 mm cylinders with the top and bottom parts removed			
Chloride penetrability				
Migration coefficient				
Diffusion coefficient	300×300×90 mm slabs			
Water permeability	ø75×150 mm cylinders	3	7	7-day moist curing
Autogenous shrinkage	75×75×300 mm prism	1	refer to the section on test method	

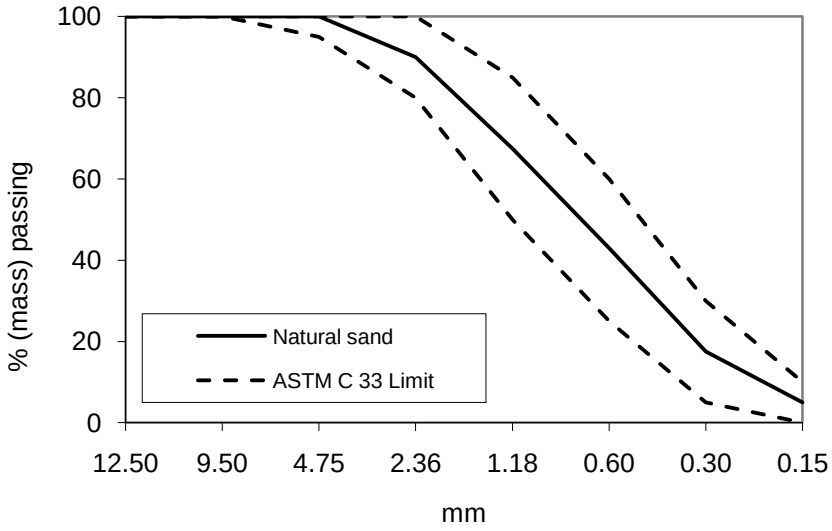

Fig. 3.1 Grading curve of natural sand in accordance to ASTM C 33

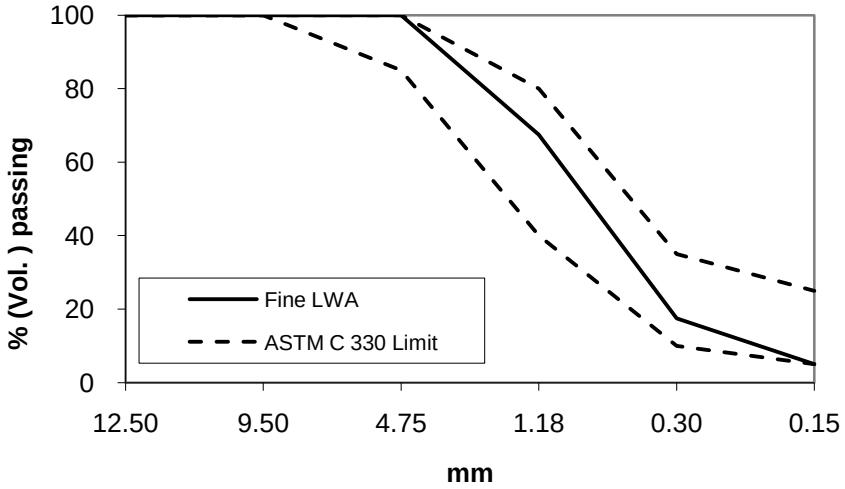

Fig. 3.2 Grading curve of fine lightweight aggregate in accordance to ASTM C 330

Fig. 3.3 The spherical expanded clay type lightweight aggregates.

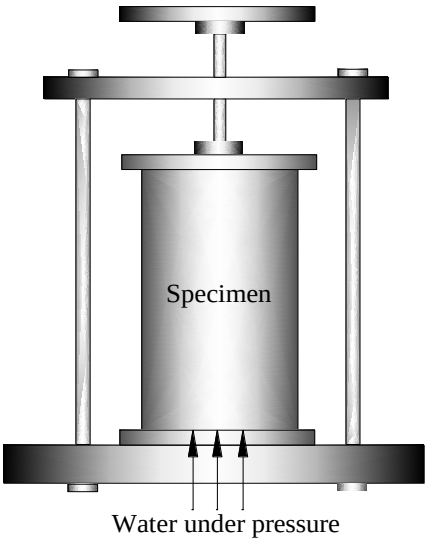

(a)

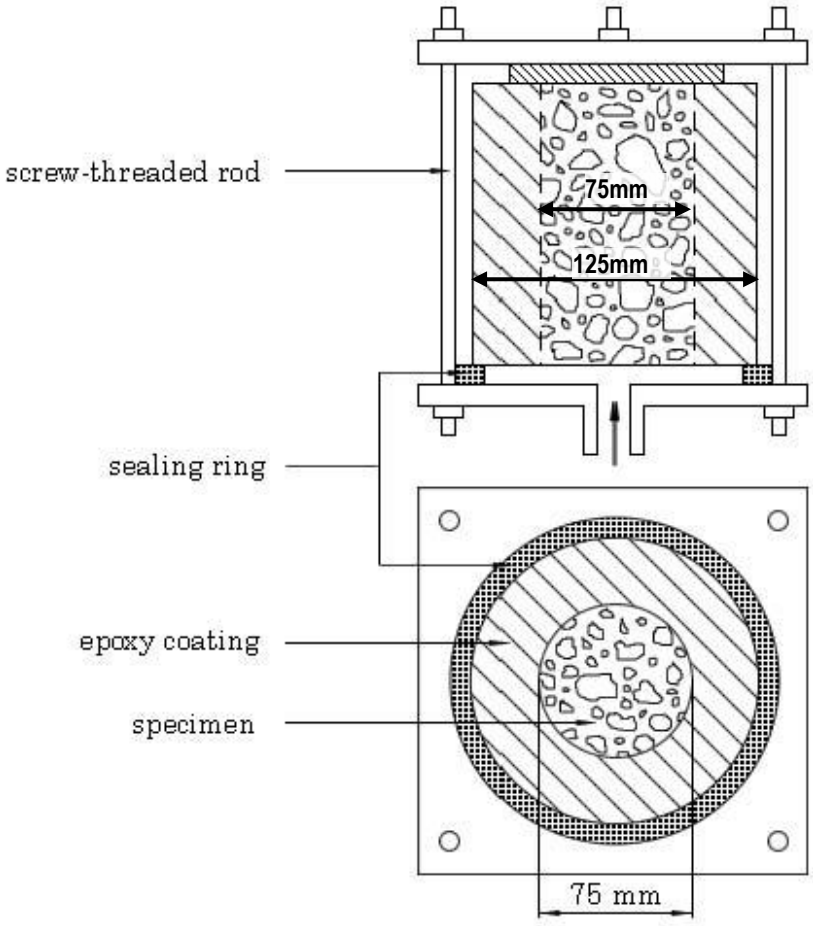

(b)

Fig. 3.4 Water permeability test set-up

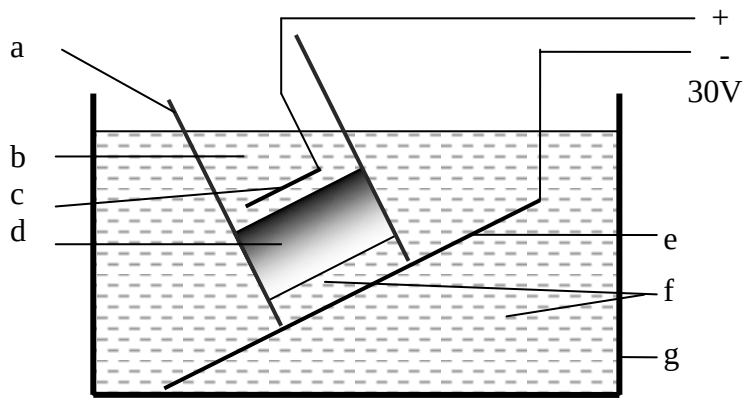

Fig. 3.5 Setup of NT Build 492 test.(a. Plastic tube; b. 0.3 N NaOH; c. Anodic stainless steel plate; d. Concrete specimen; e. Cathodic stainless steel plate; f. 10% NaCl; g: Glass container)

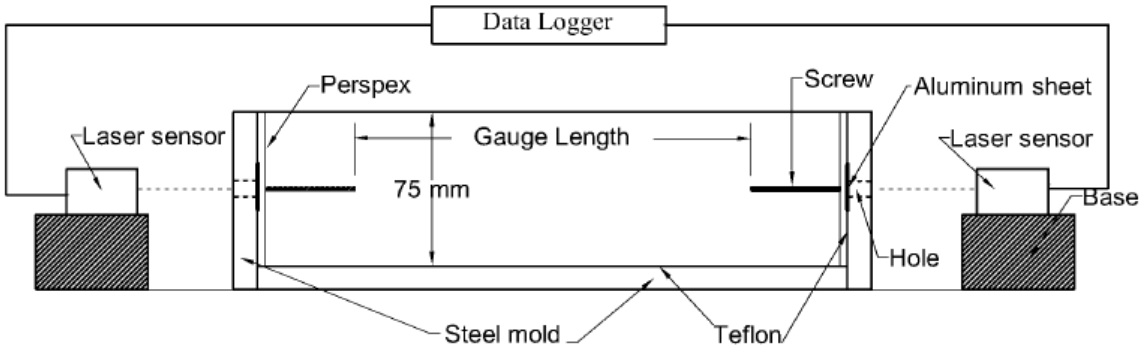

Fig. 3.6 Set-up for measuring the autogeneous shrinkage within the first 24 hrs after initial setting

CHAPTER 4 PERMEABILITY OF CONCRETE INCORPORATING PRESOAKED LIGHTWEIGHT AGGREGATES FOR INTERNAL CURING

4.1 Introduction

This section evaluated the effect of presoaked LWAs of different sizes in concrete on water permeability, water absorption, and resistance of the concrete to chloride-ion penetration. Mechanical properties and autogeneous shrinkage of the concretes were determined and presented. The results of those concretes with LWA for internal curing (RS1-RS3) were compared with those of the control concrete (NC1) and concrete with a shrinkage reducing admixture (SRA) (RS4) at a similar w/c ratio of about 0.39.

4.2 Basic Properties of Concrete

The basic properties of concrete including unit weight after being demoulded at 1 day, compressive strength at 7, 28, and 91 days, oven dry unit weight after 28 days, and elastic modulus of the concretes at 28 days are summarized in Table 4.1.

The concretes had slumps of 85 ± 20 mm. The concrete mixtures RS1 to RS3 had lower unit weight, compressive strength, and elastic modulus compared to those of the control concrete (NC1) as expected due to the incorporation of the LWAs in the

former mixtures. The reductions of these properties are more significant for the concrete with larger size LWA (RS1).

The addition of SRA did not affect the unit weight and elastic modulus, but reduced the compressive strength of the concrete somewhat. The observation of the slightly reduced strength was consistent with the findings by other researchers.

4.3 Water Absorption of concrete

The mass increase of specimens from each mixture due to water absorption up to 8 days was plotted against √time as shown in Figs. 4.1 - 4.5. The sorptivity of the concrete was obtained from the slope of the curves from these figures by regression. The regression coefficient for the sorptivity was > 0.99 for all the concrete specimens. Comparison of the average weight gain of different concretes from 1 to 24 hours is presented in Fig. 4.6. The average initial water absorption within 1 hour and sorptivity are presented in Fig. 4.7. The error bars in Fig. 4.7 represents the standard deviation of the initial water absorption and sorptivity for each mixture.

The concrete with LWAs for internal curing had initial water absorption and sorptivity comparable to those of the control concrete except for Mixture RS2 which had lower initial water absorption and sorptivity. The difference may be related to the pore structure of the LWA and the degree of cement hydration in concrete.

Comparing the concretes with LWA particles and the control concrete, they had similar w/c for the cement paste, and the differences were mainly the aggregate and degree of cement hydration. Although LWA particles are porous compared with the granite aggregate, many pores in LWAs are discrete and therefore are not accessible by water. Another factor that affects the sorptivity of the concrete is the size of the pores. In principle, water absorption is caused by capillary effect in pores. The

greater the pore sizes, the smaller the capillary stresses. Large pores may contribute little to water absorption even if they are continuous. In the concrete with LWA particles (RS1 to RS3), water inside the LWAs contributed to internal curing, thus the degree of cement hydration in these concretes would be higher compared with that in the control concrete (NC1). The increased cement hydration would reduce capillary porosity in the cement paste which may explain the reduced initial water absorption, sorptivity and mass increase in 8 days in some cases. In addition, improved interfacial transition zone between the LWA and cement paste may also contribute to the reduced water absorption of the concrete.

No clear correlation was observed between the particle size of the LWA incorporated and the sorptivity of the concrete. This might be due to the different porosities and surface textures of the LWAs used. In Mixture RS1, the LWA particles of 4.75 to 9.5 mm were spherical with smooth surface texture, whereas in Mixture RS3, the LWA particles < 1.18 mm were crushed with higher porosity and open pores. Mixture RS2 contained LWA with particle sizes ≤ 4.75 mm, and some of them were spherical with lower porosities than that of particles > 4.75 mm whereas a small amount of the particles < 1.18 mm was crushed. The sorptivity of these concretes were in the order of RS2 < RS1 < RS3.

The concrete with the SRA had initial water absorption, sorptivity, and mass increase in 8 days comparable to those of the control concrete. In principle, the sorptivity of a porous material is proportional to the square root of surface tension and inversely proportional to the square root of viscosity of pore solution in the porous material. The SRA decreased surface tension and increased viscosity, both of which reduce the sorptivity. However, the data indicate that the effect of these on the water absorption of the concrete due to the use of SRA was not significant.

4.4 Water Permeability of Concrete

The water permeability coefficients of the concretes are summarized in Table 4.2. The test results show that all the concretes had relatively low water permeability (10^{-13} m/s). The water permeability of the concrete with LWAs for internal curing and that with SRA had similar water permeability compared to the control concrete.

Although there is generally improved cement hydration and reduced capillary pores in concrete when LWAs are used for internal curing, the LWAs are porous and water can penetrate into the LWAs under high pressures. This means that under high pressure the increase in mass *m* of the concretes with the LWAs (RS1 to RS3) can be higher than that of the control concrete (NC1). Some discrete pores in the LWAs could also become continuous under the pressure. The higher *m* reflected greater porosity *v* of the concretes with LWAs. However, the water penetration depth of the concrete (RS1 and RS2) was lower than that of the control concrete under the pressure tested for the same duration. The water penetration depth of the mixture RS3 would also be lower compared with that of the control concrete if we assume that the penetration depth was proportional to the time duration under pressure. This is important from the durability point of view. For example, the initiation of corrosion of steel reinforcement embedded in concrete is affected by the concentration of chloride ions in the vicinity of the steel bars where the chloride ions can be brought into the concrete by hydraulic pressure.

4.5 Resistance to Chloride-Ion Penetration of Concrete

Table 4.3 summarizes the resistance of the concretes to chloride-ion penetration determined by the methods described. Each result was the average from three

specimens. The concrete with LWA (RS1 to RS3) showed higher charges passed compared with the control concrete (NC1), whereas the concrete with SRA (RS4) had lower charges passed compared with the control concrete. The charges passed through the concretes, however, were all within the range from 2000 to 4000 coulombs which was classified as "moderate" chloride penetrability according to ASTM C 1202. This method is affected by the pore structure and the chemistry of pore solution of the concrete specimens. The LWAs in the concrete RS1 to RS3 affected the pore structure of the concrete and SRA affected the pore solution which in turn affected the charges passed in the concrete. It should be mentioned that ASTM C 1202 may give a false estimate of the concrete diffusion when some supplementary cementing materials, chemical admixtures, or steel fibers are used.

The chloride penetration depths and migration coefficients of the concretes with the LWA particles and with SRA determined by the NT Build 492 method were in the same order as those of the control concrete. In this test, the chloride penetration depth was determined by the whitish color due to the precipitation of AgCl. According to the method, chloride concentration at which the color changes was approximately 0.07 N for ordinary Portland cement concrete. According to Otsuki *et al.* [1992], this whitish color will only be visible when the chloride content is > 0.15% by weight of cement with the spray of the $AgNO_3$ solution. This means that the actual chloride penetration depth in the specimens for the migration test might be greater than the values given in Table 4.3.

Figure 4.8 shows the profiles of chlorides in the concretes after the 90-day ponding test. The surface chloride content and chloride diffusion coefficient of the concretes obtained from curve fitting of the chloride profiles according to Fick's second law are summarized in Table 4.3.

The diffusion of chloride ions in the normal weight concrete is primarily dependent on the cement paste and the interfacial zone between the aggregate and cement paste matrix as the diffusion in the normal weight aggregate is negligibly small. For the concrete with LWA particles, however, the chloride ions may diffuse into the porous lightweight aggregate.

From the results, although the surface chloride content (*C*s) for the concrete with LWA particles (RS1 to RS3) was higher than that of the control concrete, the incorporation of presoaked LWAs for internal curing generally did not affect the chloride diffusion coefficient of the concrete significantly as their diffusion coefficients were in the same order as that of the control concrete and the concrete with SRA. The increase in the more porous crushed LWA particles in concrete seems to increase the chloride ion diffusion, and Mixture RS3 with crushed LWA particles of sizes < 1.18 mm appears to have somewhat higher chloride diffusion coefficient. However, it is noted that the w/c of the concrete RS3 was 0.40 which was slightly higher than that of the others.

Diffusion of chloride ions in the concrete is affected by the concentration difference of the ions in the concrete pore solution and external sources. The smaller the difference, the lower the driving force for the chloride ion diffusion in the concrete. It is also reported that the diffusion coefficient of chloride ions in concrete decreases with time. Further research is needed to determine the long-term diffusion of chloride ions in concrete with porous crushed LWA particles for internal curing.

The incorporation of the SRA in concrete did not affect the surface chloride content and the diffusion coefficient significantly compared with the control concrete.

It should be mentioned that in the salt ponding test the chloride contents were based on the weight of the dried concrete samples from the testing slabs. Due to the

small samples (5 grams) used for the determination of the chloride content in the concrete, relative proportion of cement paste and aggregate might vary from sample to sample. This may lead to some errors in the results.

In summary, the charges passed, chloride migration coefficient, and chloride diffusion coefficient of the concretes with LWA particles for internal curing were in the same order as those of the control concrete and the concrete with SRA.

4.6 Autogenous Shrinkage of Concrete

The autogenous deformation of the concrete mixtures is presented in Fig. 4.9. The "zero" point of the time was from the initial setting time of the control concrete (4 h 15 min) determined by penetration resistance method according to ASTM C 403 [2006]. The initial temperature of the concrete was 29.1 ^{o}C and the temperature rise was 4.1 ^{o}C. The benefit of internal curing by using presoaked LWAs in the concrete RS1 to RS3 for shrinkage reduction is clearly demonstrated in the figure. Furthermore, the smaller size of presoaked LWAs appears to be more effective in reducing the autogenous shrinkage. The results are consistent with other research.

As shown in Fig. 4.9, the use of SRA or presoaked LWA was efficient in reducing the autogeneous shrinkage. The principle of the former was due to the reduction in the surface tension of pore solution thus reducing the capillary stress and shrinkage, whereas the latter was due to the provision of water from internal sources which reduces the shrinkage of the cement paste.

4.7 Summary and conclusions

To produce high-quality durable concrete, the early-age cracking caused by autogenous shrinkage can be reduced by the incorporation of presoaked LWAs or SRA. When the presoaked LWAs or SRA are used in concrete for such purpose, their effects on water absorption, water permeability, and resistance to the chloride ion penetration of the concrete and the ease of use have significant impact on the applications. Based on the results presented and discussed, following conclusions appear to be warranted.

1. In general, the concretes with LWA particles had initial water absorption, sorptivity, and water permeability similar to or lower than those of the control concrete and the concrete with SRA. The charges passed, chloride migration coefficient, and chloride diffusion coefficient of such concretes were in the same order as those of the control concrete and the concrete with SRA. However, the incorporation of the LWAs for internal curing reduced unit weight, compressive strength, and elastic modulus of the concrete.

2. Comparing the LWAs of different sizes for internal curing, finer particles were more efficient in reducing the shrinkage and generally resulted in less reduction in the unit weight, compressive strength, and elastic modulus. However, the increase in the more porous crushed LW particles in concrete seems to increase the penetration of chloride ions in the concrete.

3. The concrete with SRA had initial water absorption, sorptivity, water permeability, and resistance to chloride ion penetration comparable to those of the control concrete. The use of SRA in concrete does not affect the elastic modulus of the concrete, except for a minor influence on the compressive strength of the concrete.

It should be mentioned that the results were obtained from laboratory tests where the specimens were not subjected to restraints. In practice where the concrete is restrained, the reduced shrinkage would reduce potential cracking, thus reduce the penetration of chloride ions through the cracks.

Table 4.1 Basic properties of the concretes

Concrete	w/c	Unit weight, kg/m^3					Compressive Strength†, MPa			Elastic Modulus†, GPa
		1 day	7 days	28 days	91 days	Oven dry	7 days	28 days	91 days	28 days
NC1	0.38	2360	2374	2365	2353	2267	54 (2)	71 (1)	75 (3)	33.5 (0.5)
RS1	0.38	2030	2037	2016	2011	1933	46 (1)	53 (2)	57 (3)	25.5 (0.5)
RS2	0.39	2160	2182	2162	2162	2189	50 (2)	57 (4)	63 (4)	27.6 (0.5)
RS3	0.40	2275	2292	2276	2270	2210	51 (3)	56 (3)	69 (4)	30.3 (0.4)
RS4	0.39	2350	2361	2348	2341	2287	51 (2)	63 (3)	70 (2)	31.9 (0.6)

† Number in bracket is the standard deviation for the average value from three specimens.

Table 4.2 Water permeability of the concretes

Concrete	Duration, days	1-day unit weight, kg/m^3	28-day unit weight, kg/m^3	Mass increase, *m*, g	Water penetration depth†, mm	Permeability coefficient†, $\times10^{-13}$m/s
NC1	14	2360	2365	4.1	20.6 (2.6)	0.9 (0.2)
RS1	14	2030	2016	8.0	12.2 (0.7)	1.0 (0.2)
RS2	14	2160	2162	8.7	15.4 (1.8)	1.1 (0.1)
RS3	17	2275	2276	5.7	21.5 (1.6)	1.4 (0.5)
RS4	14	2350	2348	6.3	19.5 (1.0)	1.2 (0.1)

† Number in bracket is the standard deviation for the average value from three specimens.

Table 4.3 Resistance of the concretes to chloride-ion penetration

Concrete	1-day unit weight, kg/m^3	28-day unit weight, kg/m^3	Total Charges Passed†, Coulombs	Rapid Migration Test		Salt Ponding Test	
				Penetration depth†, mm	Migration Coefficient†, $\times10^{-12}$m^2/s	Surface chloride content†, % of concrete mass	Diffusion Coefficient†, $\times10^{-12}$m^2/s
NC1	2360	2365	2528 (210)	18.4 (1.1)	8.8 (0.6)	0.46 (0.16)*	6.0 (0.7)*
RS1	2030	2016	2977 (257)	17.6 (0.6)	8.2 (0.2)	1.48 (0.03)	6.5 (0.2)
RS2	2160	2162	3112 (335)	17.8 (2.0)	9.2 (1.5)	1.84 (0.64)	5.8 (1.7)
RS3	2275	2276	2987 (616)	20.3 (1.2)	10.1 (0.6)	2.50 (0.30)	8.2 (0.5)
RS4	2350	2348	2012 (119)	19.1 (2.0)	9.7 (1.3)	0.50 (0.07)	5.0 (0.5)

† Number in bracket is the standard deviation for the average value from three specimens.

* The results were from a concrete with the same w/c and mix proportion but a slightly higher SP dosage of 2.9 L/m^3. The initial 3-day ponding for the concrete NC was by water instead of lime water. Because of this, some OH^- ion in the concrete might have leached out. However, due to the low w/c of the concrete and small volume of water on top of the concrete slabs for the ponding, the effect of leaching of OH^- ions on results was probably not significant.

Standard deviation is presented in the bracket after the average value from three specimens.

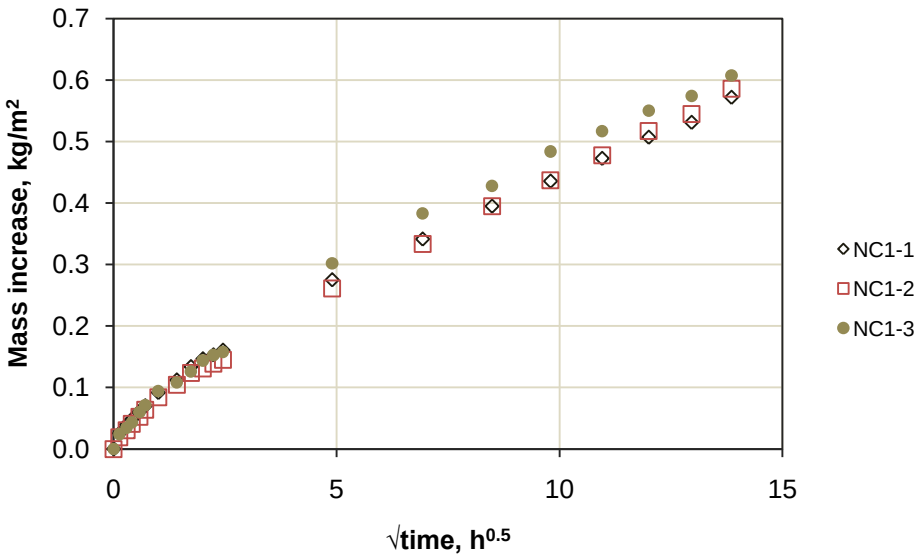

Fig. 4.1 Water absorption history of the NC1 up to 8 days

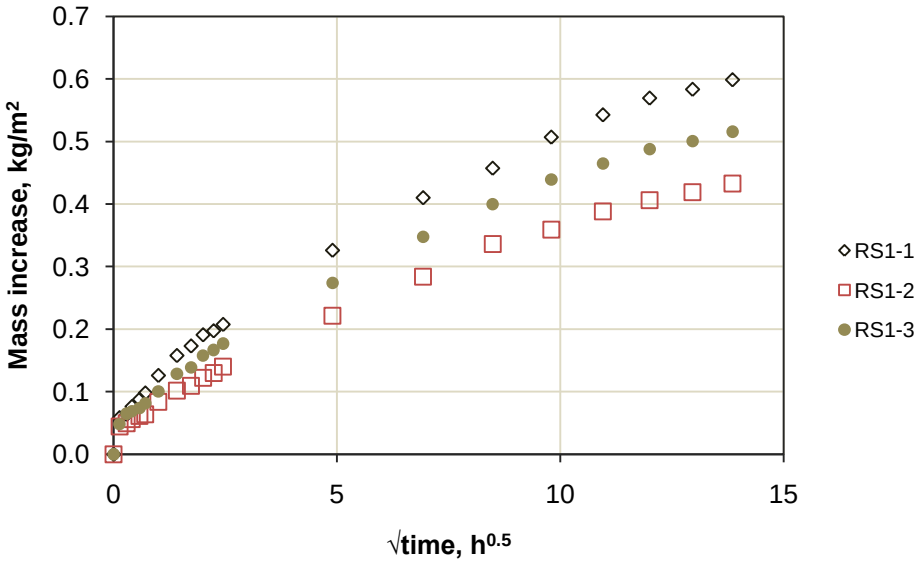

Fig. 4.2 Water absorption history of the RS1 up to 8 days

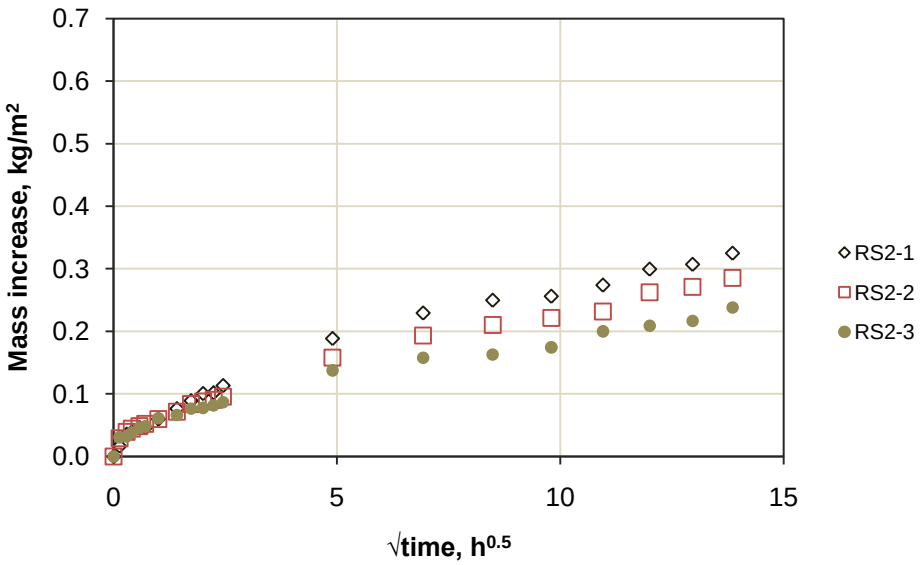

Fig. 4.3 Water absorption history of the RS2 up to 8 days

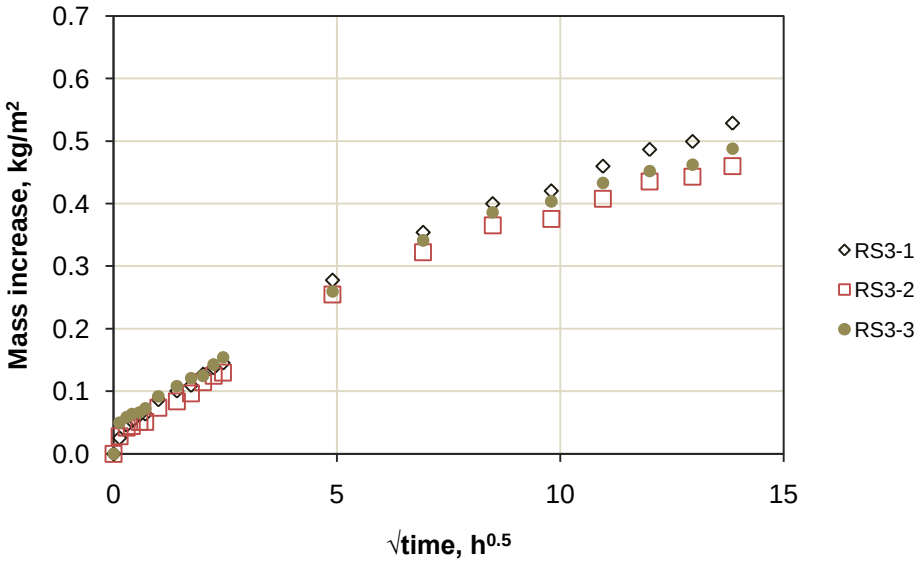

Fig. 4.4 Water absorption history of the RS3 up to 8 days

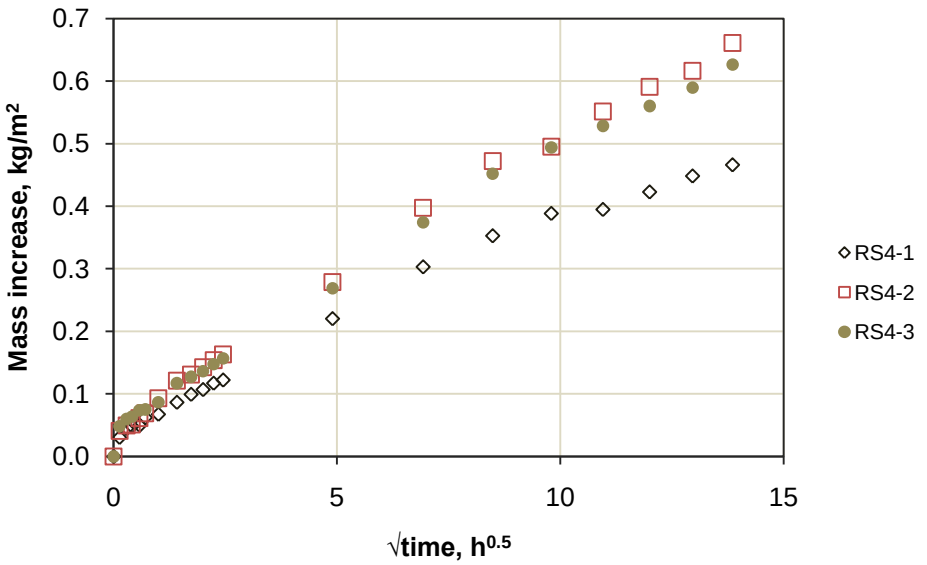

Fig. 4.5 Water absorption history of the RS4 up to 8 days

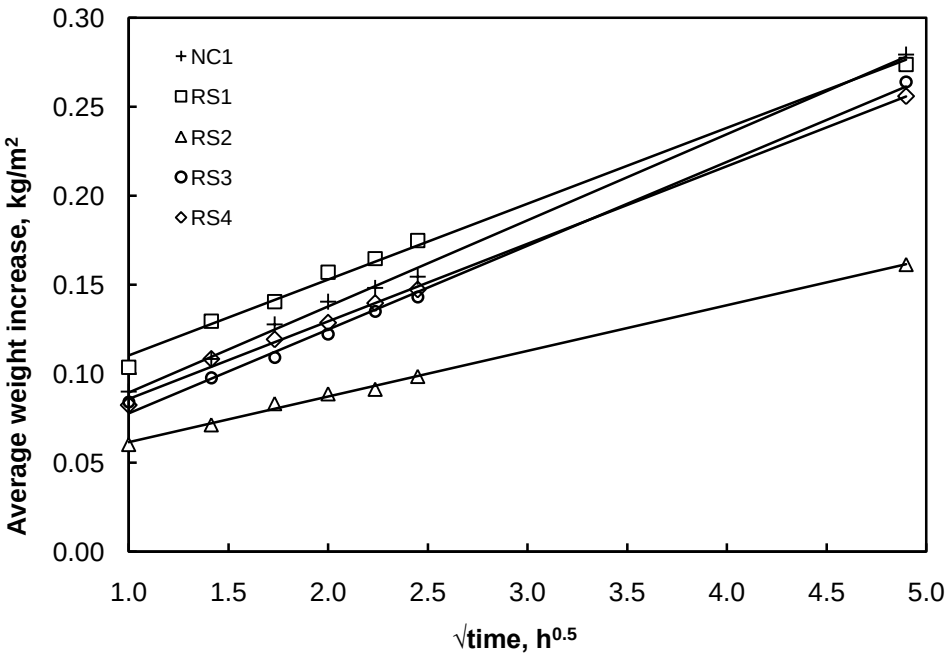

Fig. 4.6 Average weight increase of the concretes due to water absorption against √time

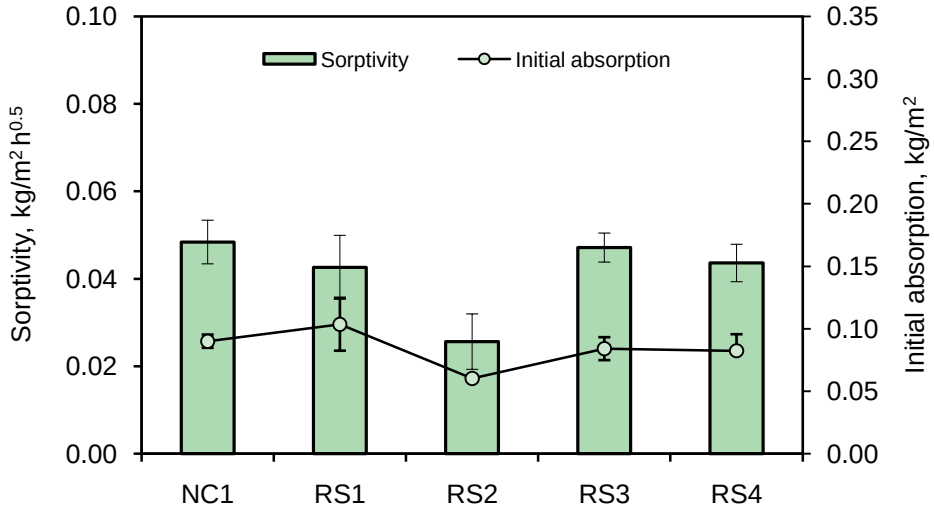

Fig. 4.7 Initial water absorption of the concretes

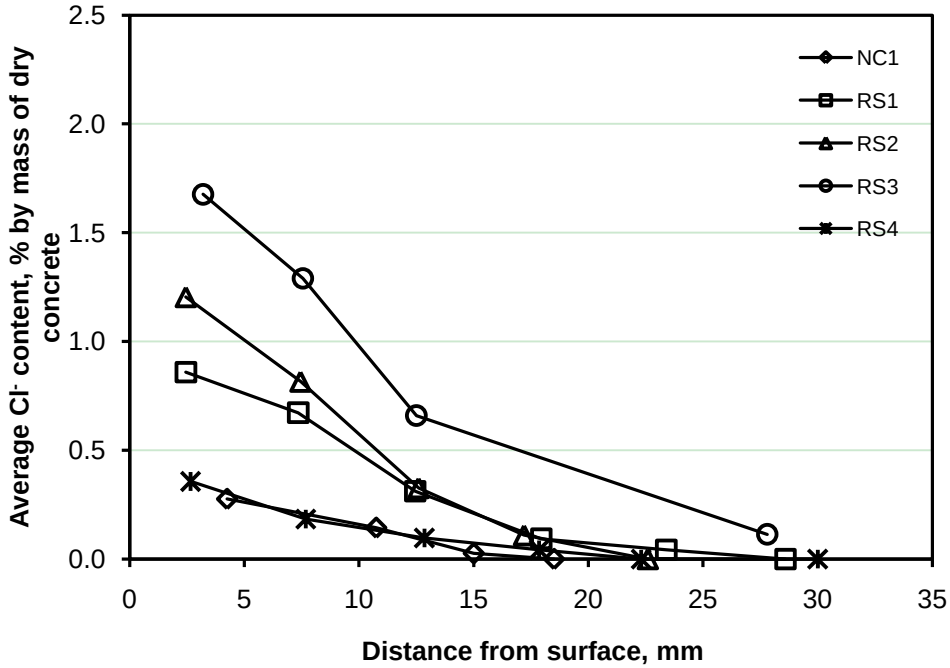

Fig. 4.8 Chloride profiles of the concretes after 90 days salt ponding test

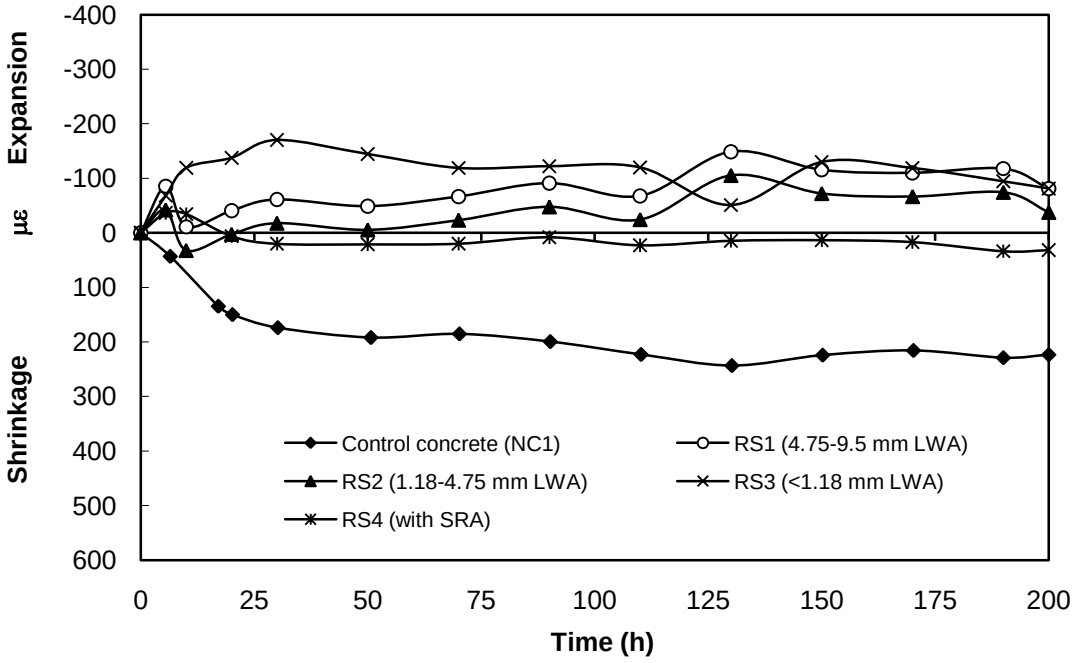

Fig. 4.9 Autogenous deformation of concrete with different sizes of LWAs or SRA.

CHAPTER 5 EFFECT OF CUMULATIVE CONTENT OF LIGHTWEIGHT AGGREGATE AND PROPERTIES OF AGGREGATES ON RESISTANCE TO WATER AND CHLORIDE-ION PENETRATION OF CONCRETE

5.1 Introduction

In many LWC, only coarse lightweight aggregates (LWA) are used. For structures with design requirement for much lower unit weight, both coarse and fine LWA may be used to further reduce the self weight of structures. However, contradicting opinions on the effect of LWA on the transport properties of concrete exist. By carefully analyzing the published information, it seems that the amount, size, and porosity of LWA and w/c of concrete all play important roles. Therefore, this chapter firstly presents experimental results and discussions on the effect of cumulative LWA content on the transport properties of concretes. Secondly, the effect of the porosities and surface textures of LWA on its water absorption, water permeability, and resistance to chloride-ion penetration was evaluated. Finally, LWC with low w/cm having lower unit weight of about 1300 kg/m^3 but relatively higher resistance to water and chloride-ion penetration was developed and discussed. Concrete mixtures used for comparison with different variables are given in Table 5.1.

5.2 Basic properties of concrete

Experimental results of the basic properties of concrete including unit weight after being demoulded at 1 day, compressive strength at 7, 28, and 91 days, oven-dry unit weight at 28 days, and elastic modulus of the concretes at 28 days are summarized in Table 5.2. The water accessible porosity and total porosity of different mixtures are also given in Table 5.2. Each result was the average from three specimens.

At w/c of 0.38, the density, compressive strength, and elastic modulus of the concrete decreased with increase in cumulative LWA content as expected. Lightweight concretes LC1 and LC2 had 28-day compressive strength similar to that of the control NWAC NC2, but had about 20% lower density. The oven dry unit weight of the concretes determined at 28 days ranged from 1216 kg/m^3 for LWC to 2287 kg/m^3 for NWC, and was correlated to the total porosity of the concretes (Fig. 5.1). The compressive strength of the concretes was strongly related to the oven dry unit weight of the concretes as shown in Fig. 5.2. The elastic modulus of concretes used here was strongly related to the total porosity of the concretes (Fig. 5.3). Those concretes with shrinkage reducing admixture and LWA for internal curing (RS1 – RS4) from Chapter 4 were also incorporated into these relationships. Comparing cement paste (CP) with NC1, cement paste CP has a lower unit weight and elastic modulus but comparable compressive strength at different ages as presented in Tabe 5.2. The lower unit weight and elastic modulus were due to the lack of natural aggregates which have higher density and elastic modus compared with the cement paste.

5.3 Effect of cumulative content of LWA

5.3.1 Water absorption of concrete

Mass increase of LWC LC1 – LC4 due to the water absorption versus √time can be found from Figs. 5.4 to 5.8 and that of NWC NC1 can be found in Fig. 4.1. The average weight increase due to water absorption of each mixture versus √time is given in Fig. 5.9. The initial water absorption and sorptivity of concretes together with their standard deviations are given in Fig. 5.10.

Comparing the LWC with different cumulative LWA content, it seems that with the increase in the cumulative content of porous LWA particles, the initial absorption of the concretes increased in general with the exception of LC2 (Fig. 5.10). And the sorptivity followed a similar trend except that LC4-25 had a sorptivity not significantly different from LC3. The increase in initial water absorption and sorptivity resulting from an increase in the cumulative LWA content indicates the contribution of LWA to the capillary porosity of concretes especially when the inner LWA pores exposed outside and the cut surface of concrete dominates the mechanism for the initial water absorption. The different contributions from the different cumulative LWA content to the porosity of concrete were presented in Table 5.2 where both water accessible porosity and the estimated total porosity of concrete generally increased due to the increase in cumulative LWA content.

The initial water absorption of all the LWC was higher than that of the control concrete NC1. This was probably related to the testing surface of the concrete which was cut from cylinder specimens. Exposed interior open pores in the LWA particles in these cut specimens probably contributed to the higher initial water absorption. As summarized in Fig. 5.10, the sorptivity of LC1 and LC2 is comparable to that of the control concrete NC1 with the same w/c of 0.38. However, with the increase in

cumulative lightweight aggregates in concrete, LC3 and LC4 show higher sorptivity compared with that of the control concrete NC1.

Comparing the LWC and the control concrete NC1, they had the same w/c for the cement paste, and the difference was mainly the aggregate and characteristics of ITZ between the aggregate and paste matrix. Although LWA particles were porous compared with the NWA, many pores in LWA were discrete and were inaccessible to water (Table 3.2), especially for those with a dense outer sintered shell. Another factor that affects the sorptivity of the concrete is the size of the pores. In principle, water absorption is caused by the capillary effect of pores. The greater the pore size, the smaller the capillary effect. Large pores in LWA may contribute little to water absorption even if they are continuous.

Figure 5.11 shows two images from scanning electron microscopy (SEM) performed on a polished sample of normal weight concrete NC1. From SEM imaging, it was observed that the typical ITZ around the NWA had more porous paste compared to surrounding bulk paste matrix (Fig. 5.11, bottom image) due to the wall effect [Ollivier et al., 1995]. The aggregate would act as obstacles and increase the path length of water migration around the aggregate, instead of going through the aggregate. Besides this, dense paste of similar quality as surrounding bulk paste matrix was also occasionally observed in certain regions at the ITZ around NWA (Fig. 5.11, top image). This would make aggregates effective barriers against water migration into the specimens, and reduce the continuity of capillary pores in the concrete.

In the LWC, denser ITZ between the LWA and cement paste might have reduced sorptivity of the concretes even though they contained porous aggregate particles. Figure 5.12 shows two images from SEM performed on a polished sample of LC1. The top image shows ITZ around a coarse LWA with undefined porous sintered

shell and undefined interface between the aggregate and paste matrix. The quality of the paste near the aggregate seems to be similar to that of bulk paste matrix. This observation is somewhat similar to what was observed at the ITZ of NC1 in the top image of Fig. 5.11. Therefore, this would reduce the continuity of capillary pores in the paste matrix. On the other hand, it has been observed occasionally that there is a different type of ITZ around LWA with denser sintered shell. For such region, the paste is seen to be more porous than the bulk paste matrix, as shown in Fig. 5.12 (bottom image). Nonetheless, the presence of the LWA with a dense shell would have an effect similar to that of dense NWA with a more porous ITZ in NC1 as discussed earlier based on Fig. 5.11 (bottom image). The dense shell would also act as barrier against water migration, and reduce the continuity of capillary pores in the concrete.

In the LWC, water inside the LWA contributed to internal curing, thus the degree of cement hydration in these concretes would probably be higher compared with that in the control concrete NC1. Examination of the polished concrete samples indicates that LC1 had less unhydrated particles (Fig. 5.12) than NC1 (Fig. 5.11). The increased cement hydration would reduce capillary porosity and increase the tortuosity of pores in the cement paste which might have also reduced sorptivity of the LWC even though the LWA was porous.

5.3.2 Water permeability of concrete

Measured penetration depth of water under pressure and calculated water permeability coefficient of the concretes NC1 and LC1 – LC4 are included in Table 5.3. The results show that the concretes with w/c of 0.38 had relatively low water permeability (10^{-13} m/s) regardless of aggregate type and amount of the porous LWA particles used in the concretes. With the increase in the cumulative content of LWA,

the water penetration depth and permeability coefficient of LWC is generally increased as shown in Table 5.3 which was similar to the sorptivity. The relatively low water permeability of LC4-25 will be discussed next. Comparing the concretes with the same w/c, the LWC showed higher water permeability than the control concrete NC1.

Although there is generally an improved ITZ between LWA and paste matrix and an improved cement hydration due to internal curing by water absorbed in the LWA leading to reduced capillary pores in LWC, the LWA is porous and water can penetrate through the aggregates under pressure. This means that under pressure the increase in mass "*m*" of the LWC can be higher than that of the control concrete NC1. The higher mass increase is related to higher porosity "*v*" in the LWC leading to the higher water permeability coefficient (Table 5.3).

On the other hand, the water penetration depth of the LWC was lower than that of the control concrete NC1 under pressure except for LC4-30 which will be discussed in next section. This is important from the durability point of view. For example, initiation of corrosion of steel reinforcement embedded in concrete is affected by concentration of chloride ions in the vicinity of the steel bars where the chloride ions can be brought into the concrete by hydraulic pressures. Rate of advancement of the critical chloride front toward the steel is of significant importance for consideration of service lifespan of reinforced concrete structures exposed to, e.g. marine environment.

5.3.3 Resistance to chloride-ion penetration of concrete

Experimental results on the resistance to chloride ion penetration of mixtures are given in Table 5.4. The LWC had similar charges passed compared with the control concrete NC1 of the same w/cm except for LC3 and LC4-30 which showed higher charges passed (LC4-30 will be discussed in next section). The charges passed

through the concretes, however, were all within the range from 2000 to 4000 coulombs which was classified as “moderate” chloride penetrability according to ASTM C 1202. In the LWC, LWA had higher porosity compared with the NWA. However, the porosity in cement paste in the LWC was probably lower due to the effect of internal curing compared with that in the NWC. In addition, the improvement in the ITZ between LWA and paste matrix in the LWC also affected pore structure of the concrete which in turn affected the charges passed.

The chloride penetration depth and migration coefficient of the LWC determined by the NT Build 492 method were similar to or lower than those of the control concrete NC1 of the same w/c. In this test, the chloride penetration depth was determined by a whitish color due to precipitation of AgCl. As mentioned before, according to Otsuki et al. [1992], this whitish color will only be visible when chloride content is > 0.15% by mass of cement using 0.1 N $AgNO_3$ solutions. This means that the actual chloride penetration depth in the specimens for the migration test might be greater than the values given in Table 5.4.

Figure 5.13 shows profiles of chlorides in the selected concretes after the 90-day ponding test based on the average value from 3 specimens. The available surface chloride content and chloride diffusion coefficient of the concretes obtained from curve fitting of the chloride profiles according to Fick’s second law are summarized in Table 5.4. Diffusion of chloride ions in NWC is dependent primarily on the pore structure of cement paste and ITZ between the aggregate and paste matrix as the diffusion in the NWA is negligibly small [Lu et al., 2002]. For concrete with LWA particles, however, chloride ions may diffuse through the porous lightweight aggregate. From the results, although the surface chloride content (C_0) of the LWC was higher than that of the control concrete, the increase in the cumulative LWA content generally

did not affect the chloride diffusion coefficient of the concrete significantly except for LC4-30 which will be discussed in next section. The higher surface chloride content of LWC might be attributed to the higher porosities of the LWA. Since diffusion process is related to concentration differentials of chloride in the exposure environment and in concrete pore solution, long-term tests are needed to evaluate diffusion in the LWC in comparison to NWC with the same w/c.

Comparing the 3 different tests used for evaluating concrete resistance to chloride-ion penetration, the chloride diffusion coefficient was calculated based on acid soluble chloride content in the concretes after the 90-day ponding test. Thus the trend established by the diffusion coefficient would be more accurate than that by the migration coefficient and charge passed. However, it should be mentioned that the chloride contents in the salt ponding test were determined from small sampling mass (5g) of the dried concrete slabs. Thus, relative proportion of cement paste and aggregate might vary from sample to sample, possibly leading to random errors in the results.

5.4 Comparison of control normal weight concrete (NC2) and lightweight concretes (LC1 – LC4) with similar or lower 28-day strength

The water absorption history up to 8 days of NC2 is presented in Fig. 5.14. The average weight increase of LC1- LC4 in comparison to NC2 due to the absorption of water against √time is presented in Fig. 5.15. The average initial water absorption and sorptivity of these concretes are compared in Fig. 5.16. The control concrete NC2 had 28-day compressive strength (49 MPa) similar to that of LC1 and LC2, but higher than that of LC3 and LC4. Results, however, show that the sorptivity of NC2 is higher than that of LC1 and LC2 (Fig. 5.16). It is also higher than LC3 and LC4-25. Mixture LC4-

30, however, has a slightly higher sorptivity than NC2 which was attributed to the higher moisture content of LWA before mixing which may result in some increase in w/cm of mixture LC4 compared with LC4-25.

As presented in Table 5.3, the permeability of normal concrete NC2 with a w/cm of 0.54 is in the order of 10^{-12}, however, those of LWC are in the order of 10^{-13}. Similarly, the migration coefficient of LWC was one order lower than that of NC2. The total charge passed through the LWC was classified as "medium chloride penetrability" which was lower than that for NC2 which was classified as "high chloride penetrability" (Table 5.4).

The significant difference of sorptivity, permeability and chloride ion resistance of NC2 and those LWC with comparable or slightly lower compressive strength can be attributed mainly to the lower w/cm of 0.38 of the LWC, and consequently lower porosity, in comparison to NC2 (w/cm=0.54).

5.5 Comparison of the concrete with cement paste of the same w/cm

The water absorption history up to 8 days of the cement paste is presented in Fig. 5.17. The average weight increase of LC1 and NC1 in comparison to CP due to the absorption of water against √time is presented in Fig. 5.18. The average initial water absorption and sorptivity of these mixtures are compared in Fig. 5.19. Comparing cement paste CP with the concretes LC1 and NC1, it seems that CP had higher sorptivity (Fig. 5.19) and lower resistance to chloride-ion penetration reflected by the higher charge passed (ASTM C 1202) and chloride diffusion coefficient and surface chloride content (salt ponding test) (Table 5.4).

The high resistance to water and chloride penetration of the concretes was mainly attributed to the increased tortuosity of the pores in concrete due to the

presence of aggregates (both LWA and NWA) compared to cement paste. Scanning electron microscopy images of NC1 and LC1 revealed both good and poor quality of the paste at ITZ as compared with the surrounding bulk paste (Figs. 5.11 and 5.12). For the LWC, ITZ with relatively denser paste typically occurred around LWA with undefined porous sintered shell from the effect of water absorption and internal curing (Fig. 5.12, top). Therefore, even if this type of LWA is more susceptible to ion penetration, the presence of a well-bonded dense layer of interface paste would serve as an effective barrier.

On the other hand, ITZ in LWC with relatively more porous paste of lower quality typically occurred around LWA with a well-defined dense sintered shell. The shell of this type of LWA could serve as an effective barrier to ion penetration on its own. In addition, despite having a more porous paste layer around the aggregates at these interface zones, the presence of the aggregates (both LWA and NWA) would act as obstacles and increase the path length of ion migration and diffusion around the aggregate, instead of going through the aggregate as mentioned before.

For the cement paste CP, it was likely that the degree of pore tortuosity is low without any aggregate inclusion as compared to the concretes NC1 and LC1. This explains why the NWC and LWC had lower sorptivity and higher resistance to chloride-ion penetration than the cement paste with similar w/c. The higher resistance of concrete to chloride-ion penetration in comparison to cement paste of the same w/c is consistent with the results by Delegrave et al. [1997].

Measured penetration depth of water under a pressure about 0.75 MPa and calculated water permeability coefficient of the concretes are summarized in Table 5.3 The results show that the concretes with w/cm of 0.38 had relatively low water

permeability (10^{-13} m/s) regardless of the type and amount of the porous LWA used in the concretes. Specific effects of coarse and fine aggregates will be discussed next.

5.6 Effect of porosities of coarse aggregates

To compare the effect of coarse aggregate type on the transport properties, three concretes, NC1 with granite, LC1 with F6.5 coarse LWA, and LW1 with F4.5 coarse LWA with same w/cm of 0.38 were discussed here.

5.6.1 Water absorption

The water absorption history up to 8 days of LW1 is presented in Fig. 5.20. The average weight increase of NC1, LC1, and LW1 in comparison due to the water absorption against √time can be found from Fig. 5.21 and their initial water absorption and sorptivity in average together with their standard deviations are shown in Fig. 5.22. Comparing sand-LWC LC1 and LW1 with NWC NC1, they had the same cement paste/mortar, and the difference was mainly the coarse aggregate type and quality of ITZ between the coarse aggregate and paste matrix. The incorporation of coarse LWA in LC1 and LW1 increased the sorptivity by about 19% and 21%, respectively, compared to NC1 (Fig. 5.22). The comparable sorptivity of LC1 and LW1 indicates that different porosities of the coarse LWA did not affect sorptivity of the concrete significantly as long as the aggregate were embedded in the same dense matrix.

In addition to the factors discussed in Section 3.3, another factor that influences sorptivity of the concrete is size of pores. In principle, water absorption is caused by capillary effect of pores. The greater the pore size, the smaller the capillary effect. Large pores in LWA may contribute little to water absorption even if they are continuous.

5.6.2 Water permeability

As shown in Table 5.3, LC1 and LW1 have slightly higher permeability coefficient than that of the NWC NC1. However, the water penetration depths of the LWC (LC1 and LW1) were lower than that of NC1 under the pressure as pores in the porous LWA became reservoirs to contain water during penetration. This is important from the durability point of view. For example, initiation of corrosion of steel reinforcement embedded in concrete is affected by the concentration of chloride ions in the vicinity of steel bars where the chloride ions can be brought into the concrete by hydraulic pressures. Advancement of the critical chloride front toward the steel is of significant importance for consideration of service life of reinforced concrete structures exposed to, e.g. marine environment.

5.6.3 Resistance to chloride-ion penetration

From Table 5.4, charge passed through LC1 with coarse LWA F6.5 was slightly lower than that of the NC1. The charge passed through LW1 with coarse LWA F4.5 of higher porosity was higher than those passed through LC1 and NC1 although they were all within the range from 2000 to 4000 coulombs which was classified as "moderate" chloride penetrability according to ASTM C 1202. The trend for chloride penetration depth and migration coefficient of the concretes determined by NT Build 492 method appeared to be consistent with those obtained from ASTM C 1202 test.

Lightweight aggregate is generally more porous than cement paste. It was found that diffusion coefficient of LWA, similar to F6.5 used in the present study, was in the order of 10^{-11} m^2/s [Zhang, 1989] which was similar to that of a pure cement paste with a w/cm of 0.9 cured in a sealed condition for at least half a year [Gautefall et al., 1986]. It was also found that the diffusion coefficient of expanded clay LWA

increased with the increase in porosity [Zhang, 1989]. Thus the resistance to chloride-ion penetration of the coarse LWA F4.5 in LW1 was probably lower than that of the coarse LWA F6.5 in LC1. In consideration of the results obtained, porosity of the coarse LWA could influence the concrete resistance to chloride-ion penetration. Nevertheless, it should be noted that the samples used for the diffusion test in reference [Zhang, 1989] were sliced from the middle of LWA particles. Therefore the outer shell of the aggregate was removed and its influence on diffusion was not considered.

5.7 Effect of porosities and surface textures of fine aggregates

5.7.1 Water absorption

The water absorption history up to 8 days of LW4 is presented in Fig. 5.23. The average weight increase of LC1, LC4, and LW4 in comparison due to the water absorption against √time can be found from Fig. 5.24 and their initial water absorption and sorptivity in average are also shown in Fig. 5.22. Mixture LC1 contained natural sand. Mixture LC4 contained lightweight sand with 0-1.18 mm fraction being crushed particles. Mixture LW4 also contained lightweight sand but the fraction from 0-1.18 mm was spherical expanded glass particles. From Fig. 5.22, the sorptivity of LC4 was higher than that of LC1. In LC1, porous coarse LWA particles were embedded in dense mortar matrix. In LC4, however, porosity of the mortar matrix was increased due to the use of LW sand, in particular the crushed fraction <1.18mm. As shown schematically in Fig. 1.2 (b), the porous lightweight sand particles reduced thickness of dense matrix among coarse LWA particles and possibly increased interconnectivity of pores compared with the concrete shown in Fig. 1.2 (a) thus resulting in higher sorptivity of LC4.

From Fig. 5.22, the sorptivity of LW4 containing spherical expanded glass was lower than that of LC4 containing crushed lightweight sand and also that of LC1 with natural sand. The lower sorptivity of LW4 might be related to its effective w/cm. As mentioned in Section 3.3, to take into consideration the water absorption of the expanded glass, its 1-hr water absorption was added to the mixing water. However, due to the great increase in the water absorption from 1 to 24 hrs (Table 3.2), the expanded glass might have absorbed more water than the 1-hr water absorption before concrete setting occurred. Thus, the actual w/cm of LW4 might be lower than that of LC1 and LC4.

5.7.2 Water permeability

The water penetration depth and permeability coefficient of LC4-25 are slightly higher than those of LC1 (Table 5.3). This indicates that the fine LWA may increase permeability of the LWC with the same coarse LWA. As mentioned earlier, absorption of the crushed LWA was estimated to be about 25% to 30% and the lower bound was used for LC4-25 in this study. Thus, the actual w/cm of LC4-25 may be <0.38. Another mixture (LC4-30) with the higher bound water absorption of 30% had much higher permeability coefficient than that of LC1, as discussed in Chapter 5. Therefore, with the same w/cm, the fine LWA would probably increase the permeability of the LWC compared with that containing only coarse LWA.

The penetration depth and permeability coefficient of LC1 and LC4-25 were higher than that of LW4. The lower water penetration depth and permeability coefficient of LW4 may be attributed to its lower effective w/cm due to the absorption of the expanded glass aggregates discussed before.

5.7.3 Resistance to chloride-ion penetration

As shown in Table 5.4, all-LWC LC4-25 had charge passed, chloride penetration depth, and migration coefficient similar to those of sand-LWC LC1. It was found that the increase in fine aggregate fractions may increase chloride-ion penetration in concrete. The comparable resistance to chloride-ion penetration of LC4-25 and LC1 observed was probably due to the lower w/cm of LC4-25 discussed earlier.

Mixture LW4 had high resistance to chloride-ion penetration compared with LC1 and LC4-25 based on the charge passed and migration coefficient. The high resistance of LW4 to chloride-ion penetration was attributed to its dense paste matrix due to the absorption of the expanded glass aggregate as discussed before.

5.8 Development of low unit weight concrete with high resistance to water and chloride ion penetration

5.8.1 Water absorption

The water absorption history up to 8 days of LW5 is presented in Fig. 5.25. The average weight increase of LW5 in comparison to NC2 and LW4 due to the water absorption against √time can be found from Fig. 5.26 and their initial water absorption and sorptivity on average are also given in Fig. 5.22. Comparing LW4 and LW5, the latter had lower sorptivity than the former due to its lower w/cm and incorporation of silica fume (Fig. 5.22). Comparing NC2 and LW5, the initial water absorption and sorptivity of LW5 was significantly lower than that of NC2. The above results indicate that LWC with unit weight as low as about 1300kg/m^3 can be produced with low sorptivity as long as the LWA particles are embedded in dense cement paste matrix.

5.8.2 Water permeability

The low unit weight concrete LW5 had a lower water penetration depth and permeability coefficient compared with LW4 (Table 5.3). The permeability coefficient of LW5 was one order lower than that of NC2. In LW5, low w/cm and silica fume played dominant roles for its low water permeability. The results indicate that low water permeability can be achieved even for LWC with very low unit weight and high total porosity.

5.8.3 Resistance to chloride-ion penetration

Low unit weight LWC LW5 has very low charge passed, chloride penetration depth, and migration coefficient compared with NC2 and LW4 as shown in Table 5.4. Similar to water absorption and water permeability, the high resistance of LW5 to chloride-ion penetration was mainly attributed to its low w/cm and use of silica fume. The results indicate that the quality of paste matrix exerted a significant influence on resistance to chloride-ion penetration and would affect durability of the concrete, regardless of whether both fine and coarse aggregates are used.

5.9 Discussion

The results presented and discussed above indicate that the quality of cement paste matrix plays an important role in controlling the penetration of water and chloride-ions in concrete. For various LWC and the control NWC, although there were some discrepancies due to different mechanisms of water and chloride-ion penetration, the results on water absorption, permeability, chloride-ion penetrability were generally consistent. Capillary pores and pore structure influence both water absorption and water permeability. However, in the water permeability test, some isolated pores

within the concrete may be penetrated through under pressure. The rapid chloride ion penetrability test and migration test were accelerated methods with application of external voltages. The results, therefore, are affected by pore solution chemistry in addition to the porosity and pore structure of the concretes.

From the results, it seems that the transport properties of the concretes were more closely related to the water accessible porosity than the total porosity of concretes presented in Table 5.2. Water sorptivity, permeability coefficient, and migration coefficient of the concretes may increase with an increase in the water accessible porosity of the concretes. However, unit weight of the concrete, which is related to the total porosity of the concrete, does appear to influence the transport properties of the concrete as well to certain extent. The correlations between transport properties and water accessible porosity and unit weight of the LWC and NWC will be discussed in a next chapter.

It should be noted that the w/cm of Mixtures LC4, LW4, and LW5 were only estimates. Mixture LC4 contained crushed LW sand which had open pore structure as mentioned before. Because of the open pore structure, it is difficult to obtain saturated surface dry aggregate, thus the w/cm of the concrete was only an approximation. Mixtures LW4 and LW5 contained expanded glass particles. Due to the uncertainty in determining water absorption of the fine expanded glass particles and the greater increase in water absorption from 1 to 24 hrs of the expanded glass aggregate, the actual w/cm of the concretes LW4 and LW5 was probably lower than originally designed.

In LW4 and LW5, expanded glass particles were used as fine aggregate to achieve lower unit weight of concrete. According to the manufacturer, the expanded glass consists of about 72% SiO_2, 13% Na_2O, and 8% CaO. X-ray diffraction analysis

indicated that the structure is mostly amorphous (Fig. 5.27). The aggregate contain alkalis and the alkalis from the aggregate may be released to the pore solution. Due to this, the fine expanded glass aggregates may react with alkalis [Mladenovič et al., 2004] and cause potential damage. Therefore, further research is needed.

5.10 Summary and Conclusions

Lightweight aggregate concrete differs from NWC in a number of aspects such as increased porosity, improved interface transition zone, improved cement hydration due to internal curing, and reduced microcracking that may affect the transport of water and chloride-ions in the concrete. The actual transport properties of the LWC in comparison to those of the NWC depend on which of these factors are dominant. Based on the experimental results and discussion, following conclusions can be drawn:

1. Although the total charge passed, migration coefficient, and diffusion coefficient of the LWC were not significantly different from those of NWC with the same w/c of 0.38, the resistance of the LWC to chloride-ion penetration decreased with an increase in the cumulative LWA content in the concrete. The water penetration depth under pressure and water sorptivity showed, in general, similar trends. The LWC with only coarse LWA had similar water sorptivity, water permeability coefficient and resistance to chloride-ion penetration compared to NWC.
2. The LWC had lower water sorptivity, water permeability and higher resistance to chloride-ion penetration than the NWC with similar 28-day strength.
3. Both NWC and LWC had lower sorptivity and higher resistance to chloride-ion penetration than the cement paste with similar w/cm.
4. The concrete containing coarse LWA had slightly higher water sorptivity and permeability when compared with NWC having a similar w/cm. This is related to

the increased porosity of the concrete due to pores in coarse LWA. The resistance of sand-LWC to chloride-ion penetration depends on the porosity of the coarse LWA. The performance of the LWC with less porous coarse LWA (F6.5) was similar to that of NWC, whereas the porous coarse LWA (F4.5) tends to reduce the resistance of the LWC to chloride-ion penetration.

5. Fine LWA has more influence on the transport properties of concrete than coarse LWA. Use of lightweight crushed sand of <1.18 mm tends to reduce the resistance of the LWC to water and chloride-ion penetration to some extent.
6. Quality of the paste matrix was important in controlling the transport properties of the concrete regardless of the porosity of aggregates used. With low w/cm and silica fume, low unit weight (about 1310 kg/m^3) was produced with higher resistance to water and chloride-ion penetration compared with NWC and LWC of higher unit weights.
7. It seems that the transport properties of concretes such as water sorptivity, permeability coefficient, and resistance to chloride-ion penetration were more closely related to the water accessible porosity than the total porosity of the concrete.

Effective w/c of LWC is affected by the water absorption of LWA, which in turn directly influences the resistance to water and chloride-ion penetration in concrete. Thus, the water absorption of LWA, especially those with fine crushed particles, needs to be carefully determined, and trial mixes are recommended for structures exposed to severe environments.

Table 5.1 Variables of the concretes for comparison

Concrete	w/cm	Silica fume	Variables	
CP	0.38	-		
NC1	0.38	-	Control concrete	Similar w/cm with
NC2	0.54	-		Similar compressive strength with some
LC1	0.38	-		
LC2	0.38	-		
LC3	0.38	-	Effect of cumulative LWA content	
LC4-25	0.38	-		
LC4-30	0.38	-		
NC1	0.38	-		Granite
LC1	0.38	-	Coarse aggregate	F6.5
LW1	0.38	-		F4.5
LC1	0.38	-		Natural
LC4-25	0.38	-	Fine aggregate	LWA with crushed 0 -1.18 mm particles [d]
LW4	0.38	-		LWA with spherical 0 – 1.18 mm expanded glass [c]
LW5	0.20	10%	To achieve low unit weight concrete with high resistance to water and chloride-ion penetration (low w/cm)	

Table 5.2 Basic properties of the concretes

Concrete	w/c	Silica fume	Water accessible porosity*, % by Volume	Estimated total porosity+, % by Volume	Unit weight, kg/m^3					Compressive strength†, MPa			Elastic modulus#, GPa
					1 day	7 days	28 days	91 days	Oven dry	7 days	28 days	91 days	28 days
CP	0.38		28.4	25.2	2010	2046	2022	2013	-	51 (7)	70 (3)	74 (5)	16
NC1	0.38		10.6	8.8	2360	2374	2365	2353	2267	54 (2)	71 (1)	75 (3)	34
NC2	0.54		16.1	12.7	2290	2314	2273	2269	2188	40 (1)	49 (1)	50 (1)	27
LC1	0.38		11.0	28.2	1900	1912	1877	1881	1780	47 (1)	50 (1)	58 (3)	23
LC2	0.38		10.9	29.8	1860	1872	1841	1830	1762	42 (6)	47 (6)	49 (1)	22
LC3	0.38		12.6	33.5	1740	1748	1708	1693	1624	32 (2)	42 (4)	41 (4)	19
LC4-25	0.38		21.5	42.2	1610	1623	1556	1536	1402	31 (7)	38 (2)	45 (1)	15
LC4-30	0.38		20.7	42.2	1620	1641	1595	1584	1413	31 (2)	34 (8)	42 (4)	15
NC1	0.38	-	10.6	8.8	2360	2374	2365	2353	2267	54 (2)	71 (1)	75 (3)	34
LC1	0.38	-	11.0	28.2	1900	1912	1877	1881	1780	47 (1)	50 (1)	58 (3)	23
LW1	0.38	-	13.0	32.7	1790	1798	1759	1731	1682	26 (2)	30 (1)	31 (1)	17
LC1	0.38	-	11.0	28.2	1900	1912	1877	1881	1780	47 (1)	50 (1)	58 (3)	23
LC4-25	0.38	-	21.5	~42.2	1610	1623	1556	1536	1402	31 (7)	38 (2)	45 (1)	15
LW4	0.38	-	17.1	49.0	1390	1407	1364	1336	1225	24 (3)	24 (3)	24 (1)	11
LW5	0.20	10%	13.6	49.9	1310	1313	1317	1310	1216	19 (0)	21 (1)	23 (1)	12

* (Mass of saturated surface dry concrete - mass of oven dry concrete) / (volume of the concrete), 28-day.
+ Calculated based on mix proportion of concrete, total porosity of LWA in Table 2, and MIP test of CP.
† Number in bracket is the standard deviation.
# Average results from 3 specimens (standard deviation < 1 GPa).

Table 5.3 Water permeability of the concretes

Concrete	w/cm	Silica fume	1-day unit weight, kg/m^3	28-day strength, MPa	Water penetration depth†, mm	Permeability coefficient†, $\times 10^{-13}$ m/s
NC1	0.38	-	2360	71	20.6 (2.6)	0.9 (0.2)
NC2	0.54	-	2290	49	77.1 (0.9)	14.7
LC1	0.38	-	1900	50	12.4 (0.2)	1.1 (0.2)
LC2	0.38	-	1860	47	13.4 (1.8)	1.9 (1.1)
LC3	0.38	-	1740	42	14.2 (2.3)	1.6 (0.4)
LC4-25	0.38	-	1610	38	12.8 (0.1)	1.2 (0.2)
LC4-30	0.38	-	1620	34	24.2 (2.6)	4.0 (0.8)
NC1	0.38	-	2360	71	20.6 (2.6)	0.9 (0.2)
LC1	0.38	-	1900	50	12.4 (0.2)	1.1 (0.2)
LW1	0.38	-	1790	30	15.7	1.2 (0.3)
LC1	0.38	-	1900	50	12.4 (0.2)	1.1 (0.2)
LC4	0.38	-	1610	38	12.8	1.2 (0.2)
LW4	0.38	-	1390	24	9.9	0.4 (0.1)
LW5	0.20	10%	1310	21	3.1	0.1 (0.1)

Note: Cement paste was also tested, however, the wetting front due to the water penetration was almost invisible and the penetration depth, thus, could not be determined.
† Number in bracket is the standard deviation for the average value from three specimens.

Table 5.4 Resistance to chloride-ion penetration of the concretes cured for 28 days

Concrete	w/c	1-day unit weight, kg/m^3	28-day strength, MPa	Total Charge Passed† (ASTM C 1202), Coulombs	Rapid Migration Test†		Salt Ponding Test†	
					Penetration depth, mm	Migration Coefficient, $\times 10^{-12}\ m^2/s$	Surface chloride content, kg/m^3	Diffusion Coefficient, $\times 10^{-12}\ m^2/s$
CP	0.38	2010	70	8610 (117)	18.1 (7.2)	8.9 (4.1)	20.8 (0.4)	6.7 (1.5)
NC1	0.38	2360	71	2528 (210)	18.4 (1.4)	8.8 (0.6)	10.4 (3.6)+	6.0 (0.7) +
NC2	0.54	2290	49	6199 (765)	32.8 (2.8)	19.1 (2.5)	N.A.	N. A.
LC1	0.38	1900	50	2385 (141)	14.3 (3.7)	6.5 (1.8)	13.0 (4.3)	5.3 (1.1)
LC2	0.38	1860	47	2496 (175)	17.9 (0.3)	7.6 (0.1)	22.6 (3.1)	5.9 (1.5)
LC3	0.38	1740	42	3278 (273)	17.8 (1.8)	8.8 (0.8)	17.7 (8.3)	6.4 (1.9)
LC4-25	0.38	1610	38	2559 (200)	14.3 (1.2)	6.6 (1.2)	N.A.	N. A.
LC4-30	0.38	1620	34	3620 (529)	12.3 (1.0)	8.9 (0.6)	24.68	9.0 (0.7)
NC1	0.38	2360	71	2528 (210)	18.4 (1.4)	8.8 (0.6)	10.4 (3.6)+	6.0 (0.7) +
LC1	0.38	1900	50	2385 (141)	13.0 (4.3)	6.5 (1.8)	13.0 (4.3)	5.3 (1.1)
LW1	0.38	1790	30	3676 (900)	21.6 (1.8)	10.4 (0.8)	N.A.	N. A.
LC1	0.38	1900	50	2385 (141)	13.0 (4.3)	6.5 (1.8)	13.0 (4.3)	5.3 (1.1)
LC4-25	0.38	1610	38	2245 (562)	14.3 (1.2)	6.4 (1.3)	N.A.	N. A.
LW4	0.38	1390	24	1581 (60)	11.8 (1.3)	5.2 (0.5)	N.A.	N. A.
LW5	0.20	1310	21	110 (35)	11.3 (2.0)	2.4 (0.6)	N.A.	N. A.

N.A.- not available

† Number in bracket is the standard deviation.

+ Results were from a concrete with the same w/c and mix proportion but a slightly higher SP dosage of 2.9 L/m^3.

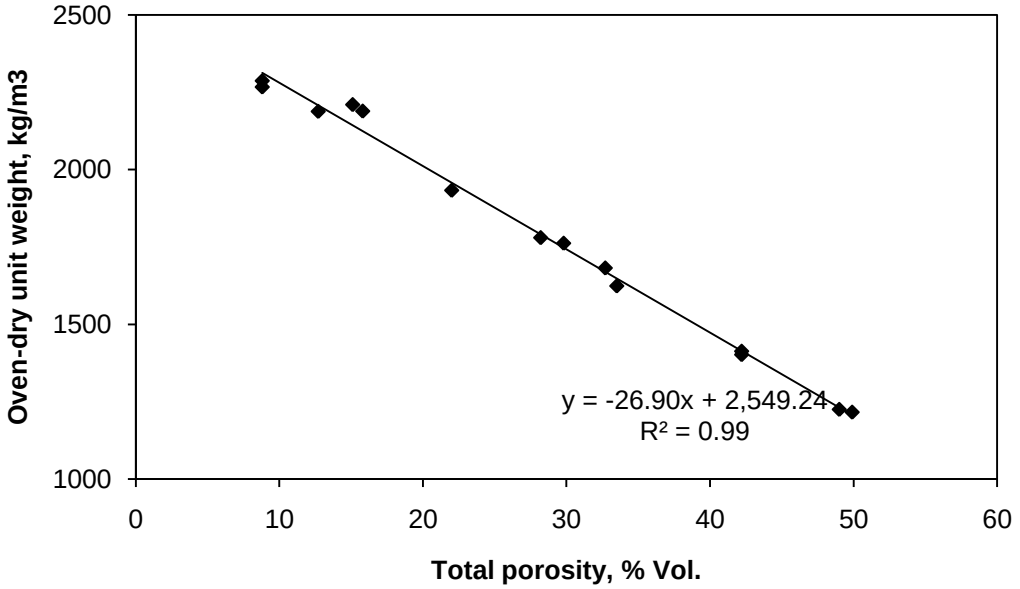

Fig. 5.1 Correlation between oven-dry unit weight and total porosity of concrete (including concretes with shrinkage reducing admixture and LWA for internal curing)

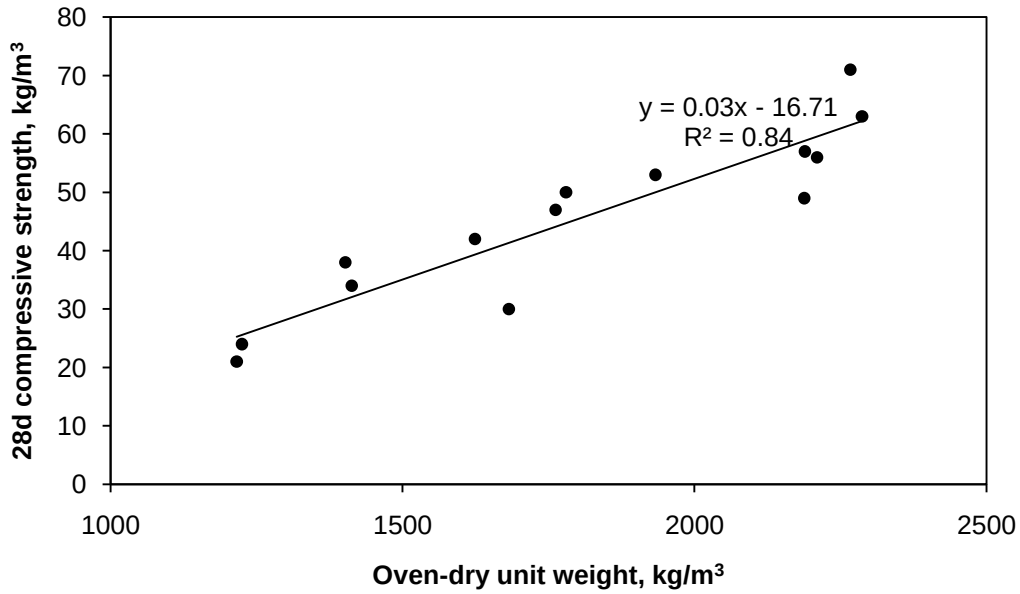

Fig. 5.2 Correlation between 28-day compressive strength and oven-dry unit weight of concrete (including concretes with shrinkage reducing admixture and LWA for internal curing)

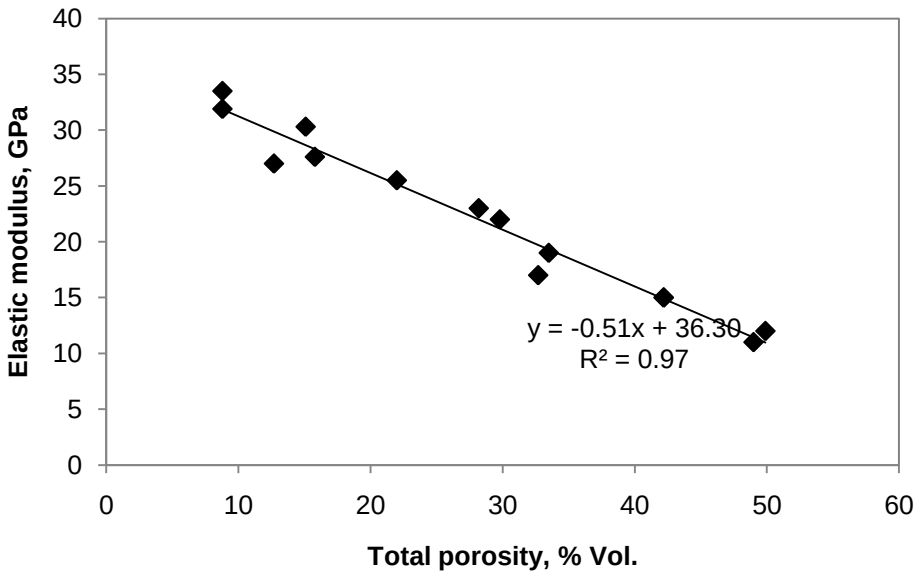

Fig. 5.3 Correlation between elastic modulus of and total porosity of concrete (including concretes with shrinkage reducing admixture and LWA for internal curing)

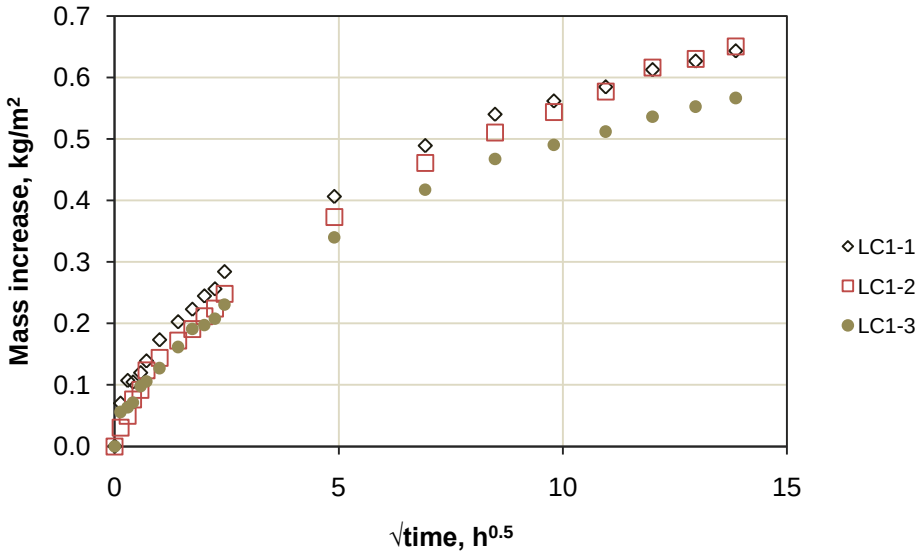

Fig. 5.4 Water absorption history up to 8 days of LC1 (w/c=0.38)

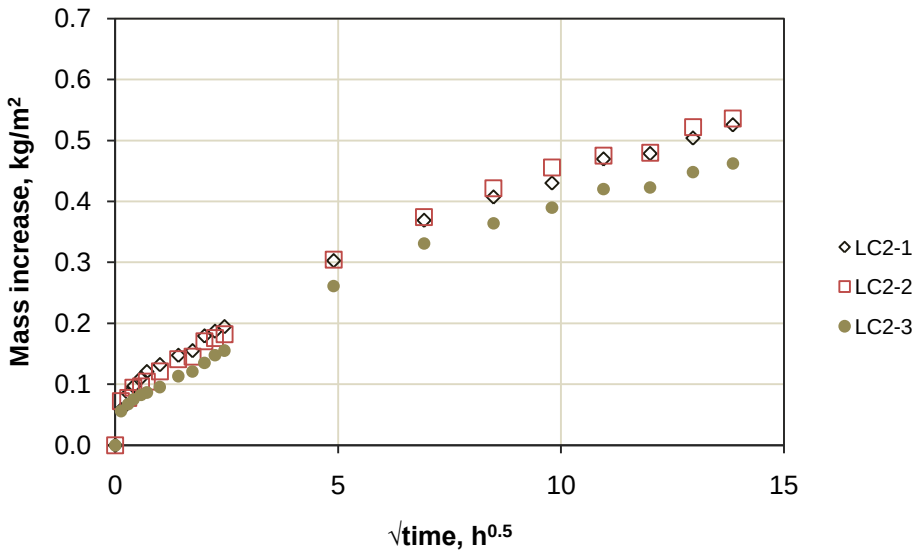

Fig. 5.5 Water absorption history up to 8 days of LC2 (w/c=0.38)

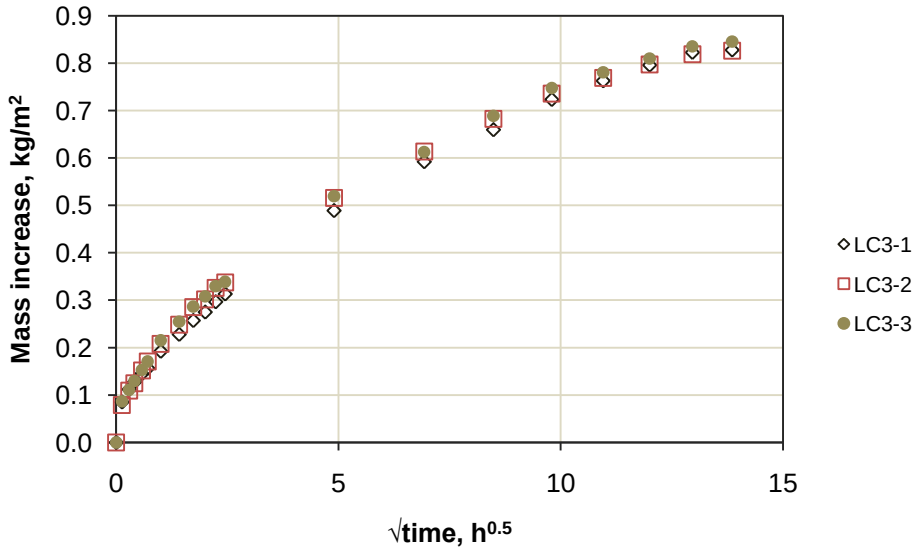

Fig. 5.6 Water absorption history up to 8 days of LC3 (w/c=0.38)

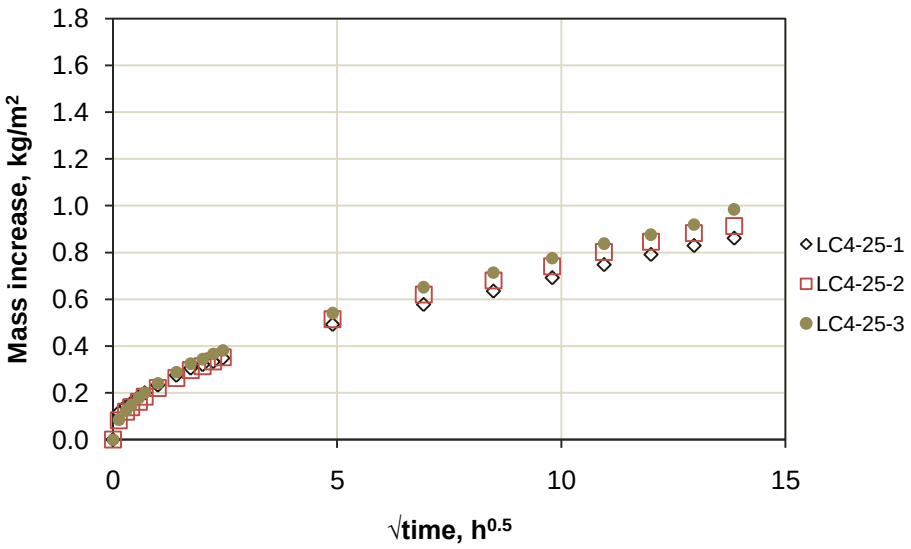

Fig. 5.7 Water absorption history up to 8 days of LC4-25 (w/c≈0.38)

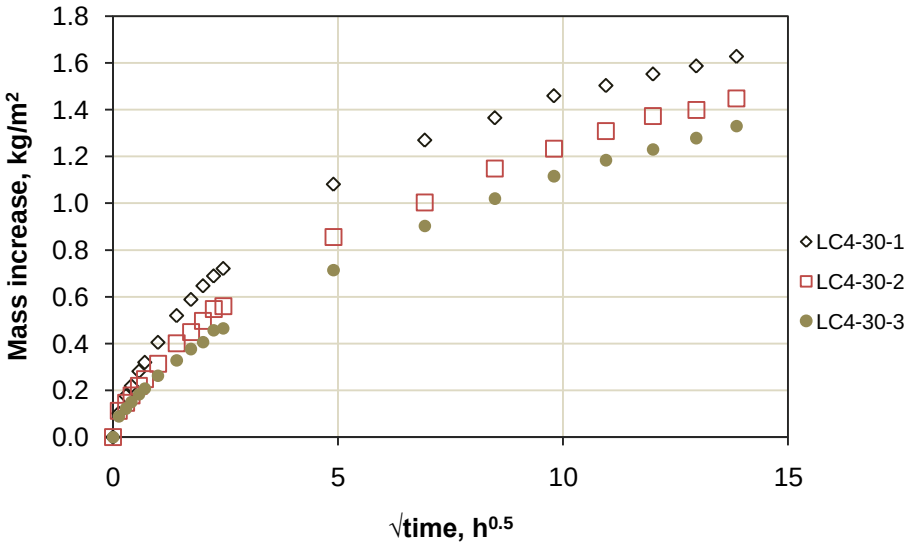

Fig. 5.8 Water absorption history up to 8 days of LC4-30 (w/c≈0.38)

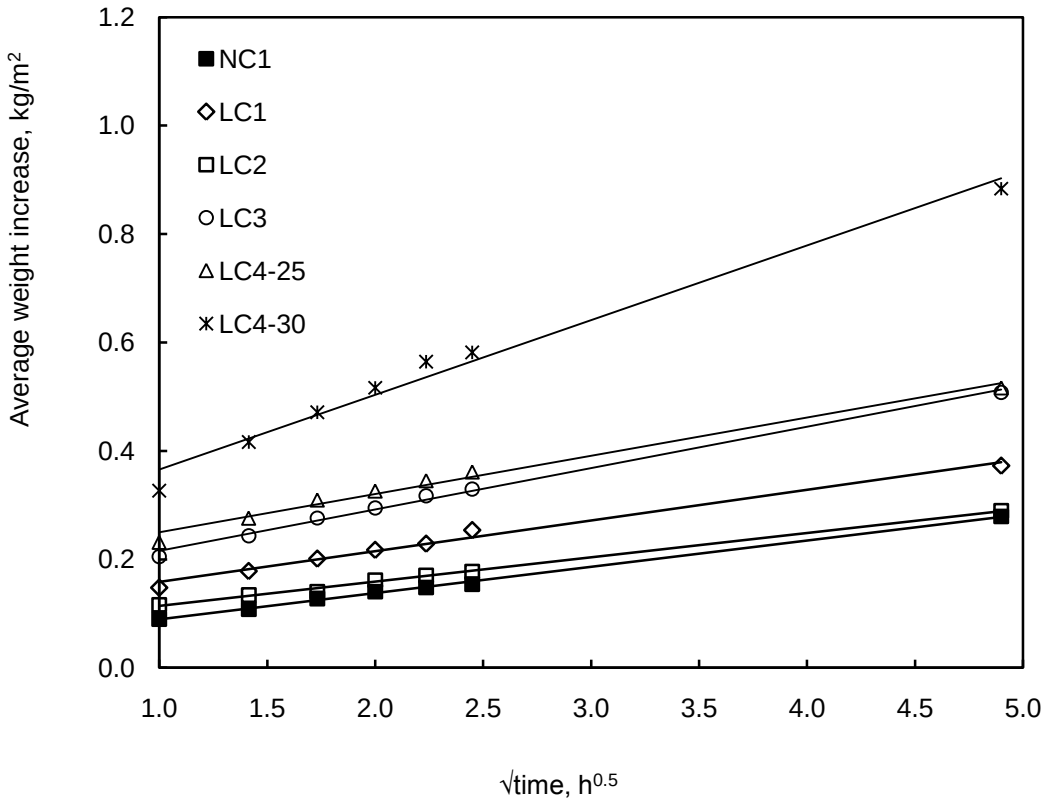

Fig. 5.9 Average weight increase of mixtures due to the absorption of water against √time.

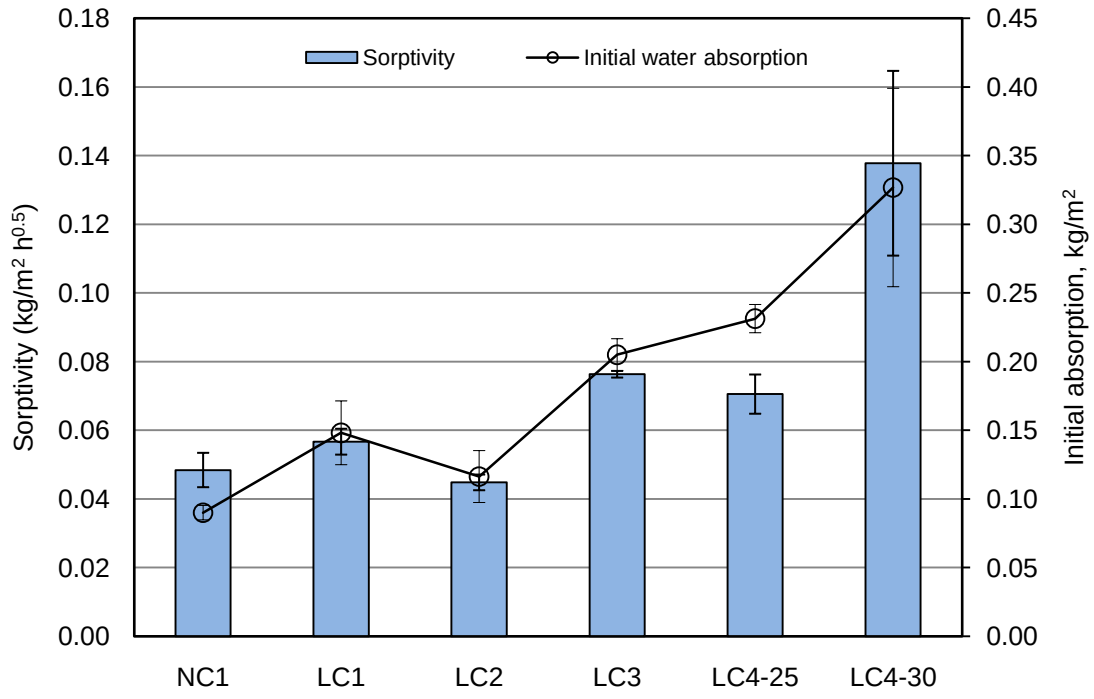

Fig. 5.10 Initial water absorption and sorptivity of LWC in comparison to NC1.

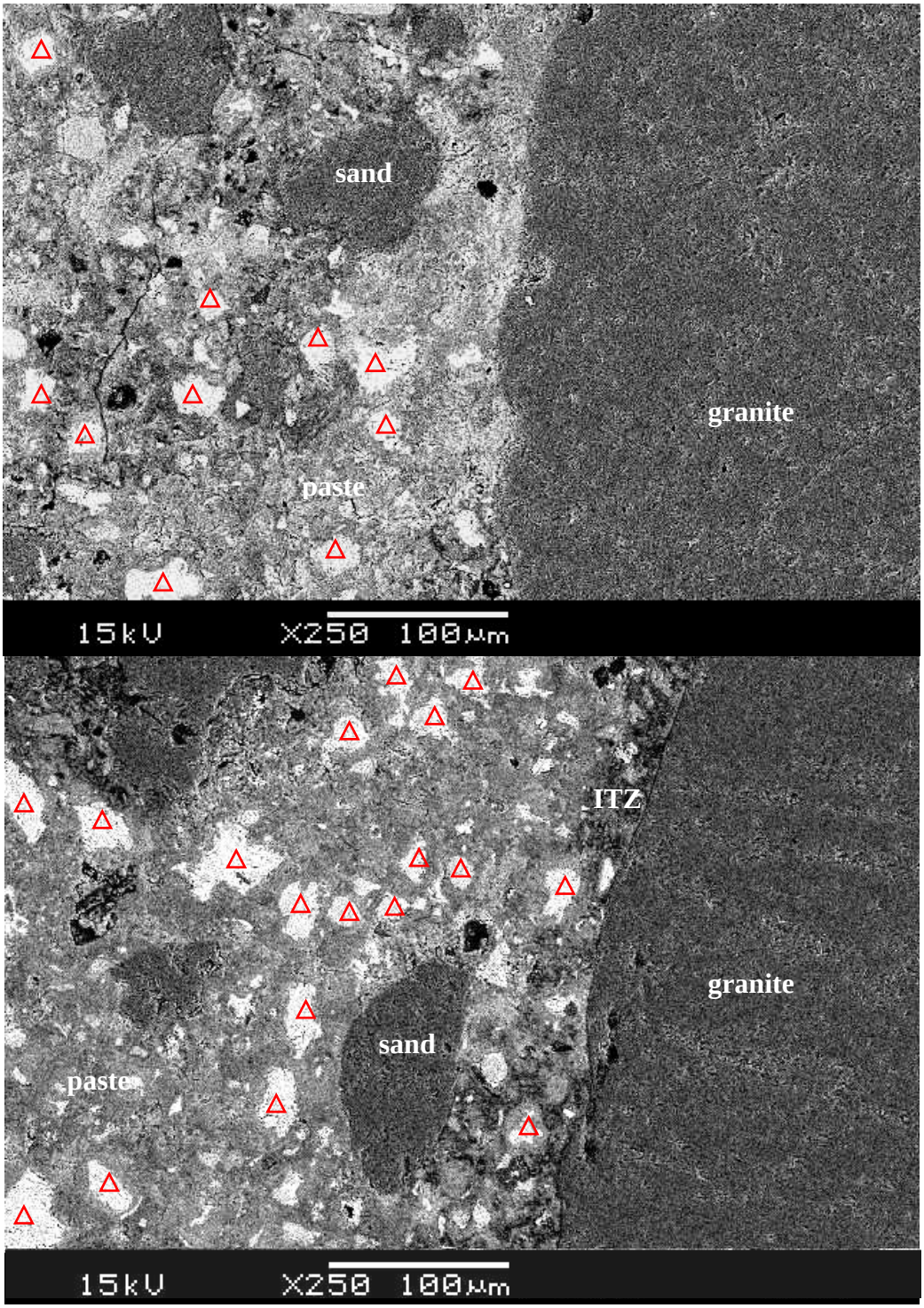

Fig. 5.11 SEM images on interface transition zone around a coarse NWA well-bonded to dense paste of similar quality compared to surrounding bulk paste matrix (top), verses another with a more porous interface (bottom), in NC1(*Note*: Δ - unhydrated cement particles).

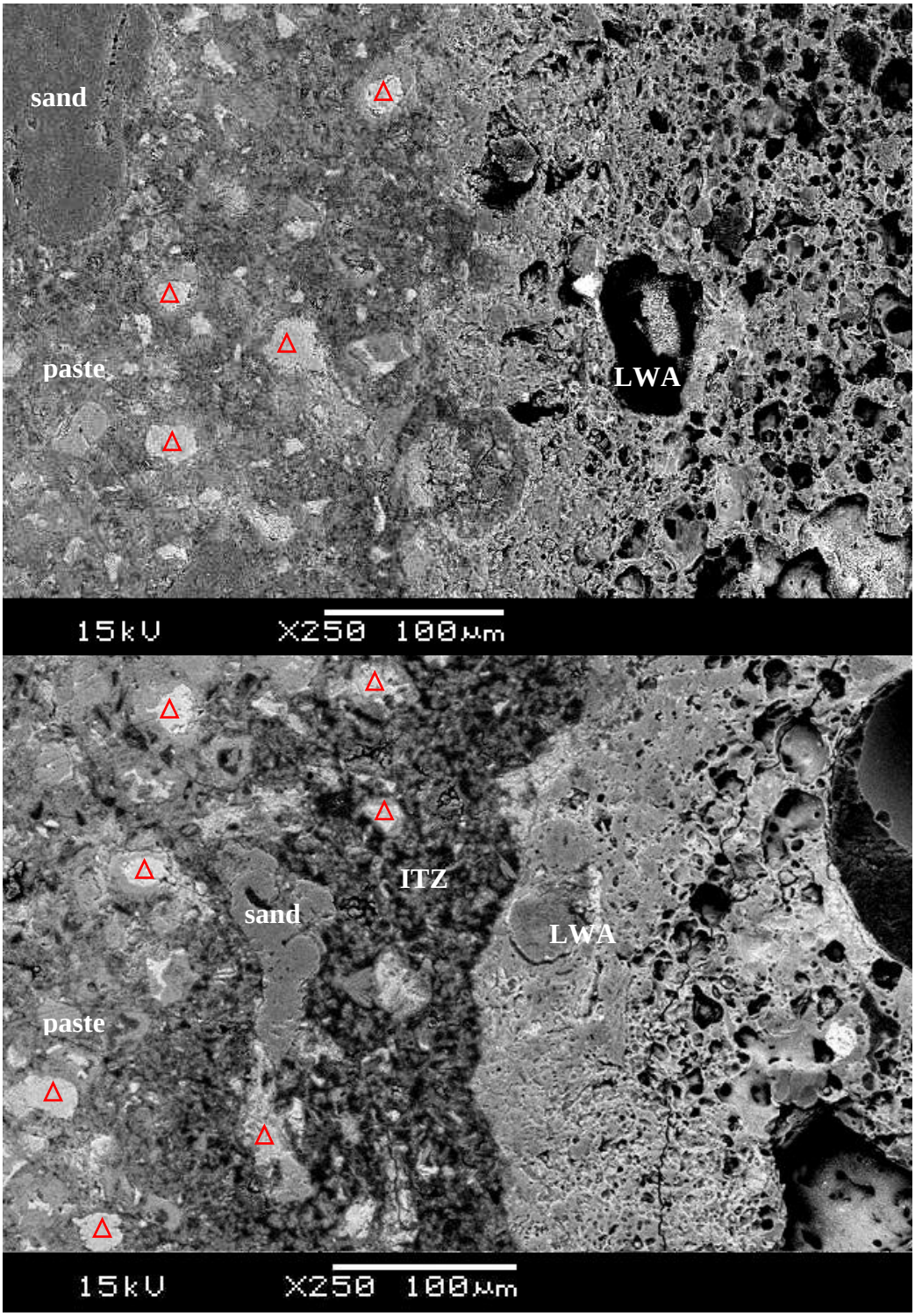

Fig. 5.12 SEM images on interface transition zone around a coarse LWA with an undefined porous sintered shell having dense paste of similar quality compared to surrounding bulk paste matrix (top), verses another LWA with a well-defined dense sintered shell having a more porous paste of lower quality at interface zone (bottom), in LC1 (*Note*: Δ - unhydrated cement particles).

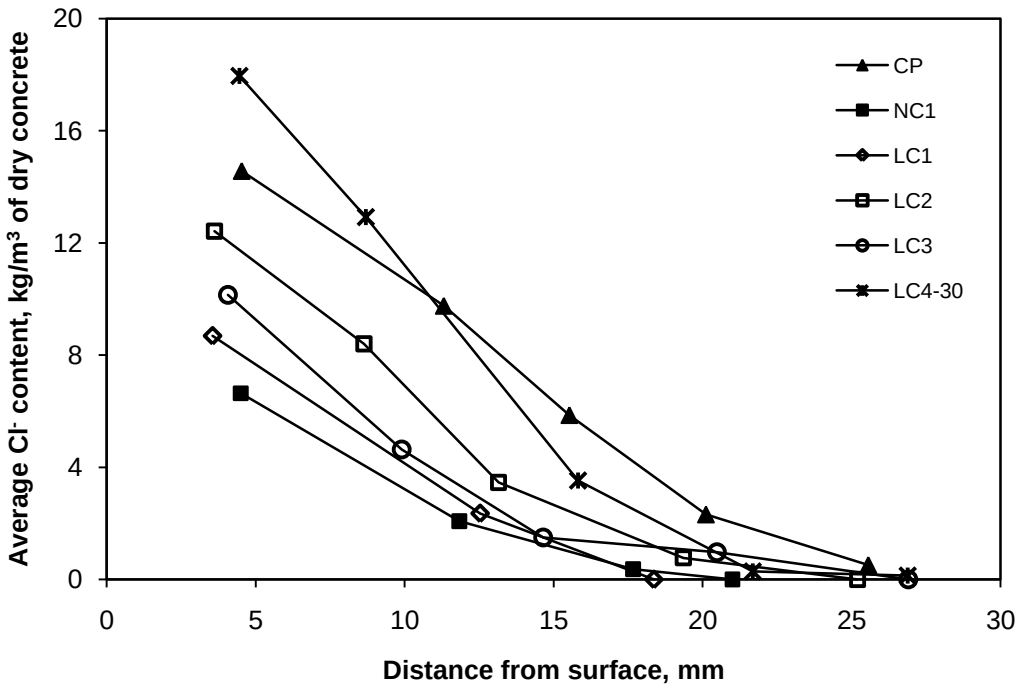

Fig. 5.13 Average chloride profile of different mixtures (w/c =0.38) after 90 days salt ponding.

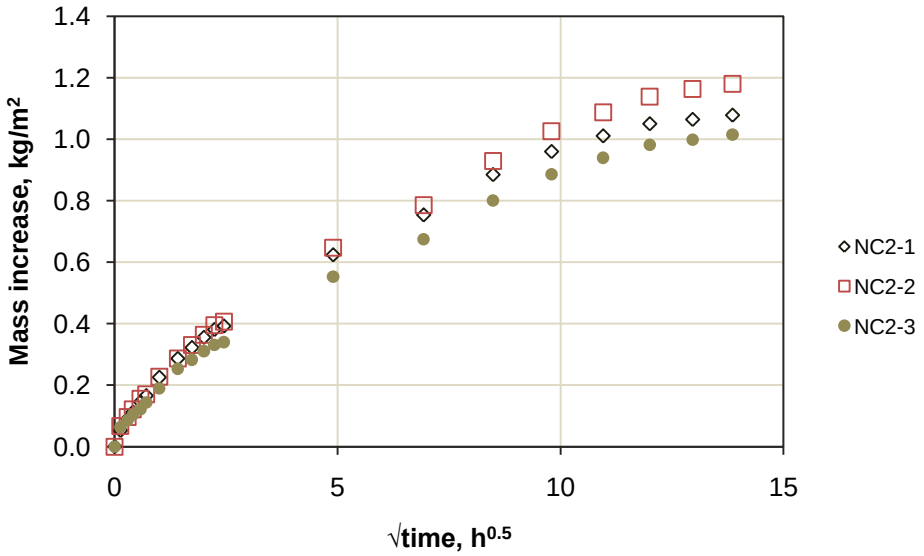

Fig. 5.14 Water absorption history up to 8 days of NC2 (w/c=0.54)

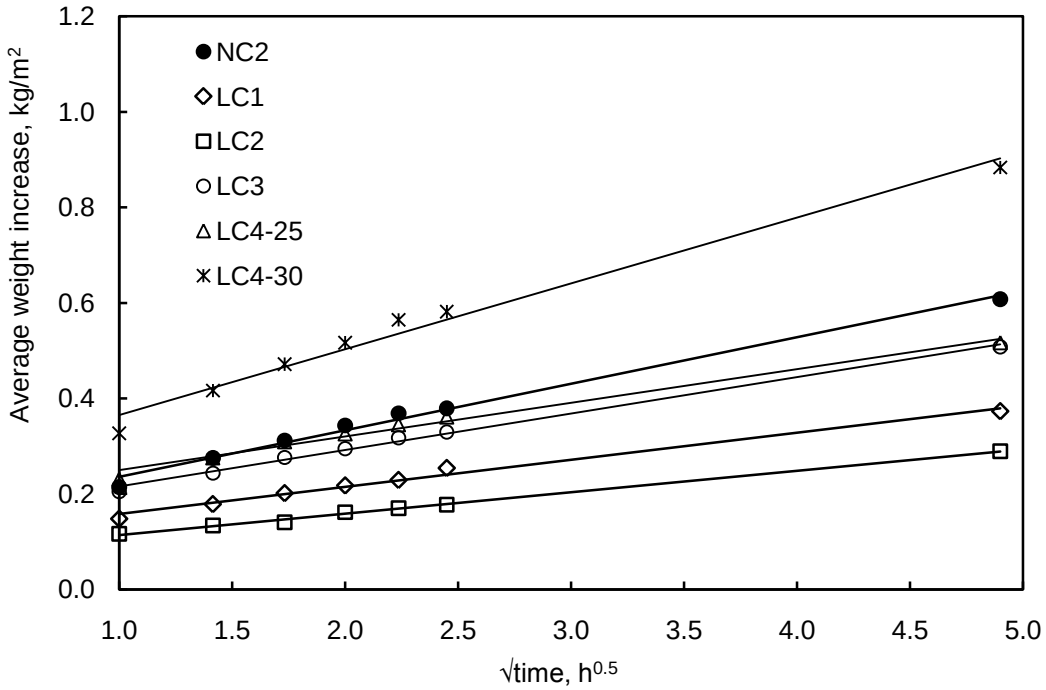

Fig. 5.15 Average weight increase of LWC in comparison to NC2 due to the absorption of water against √time.

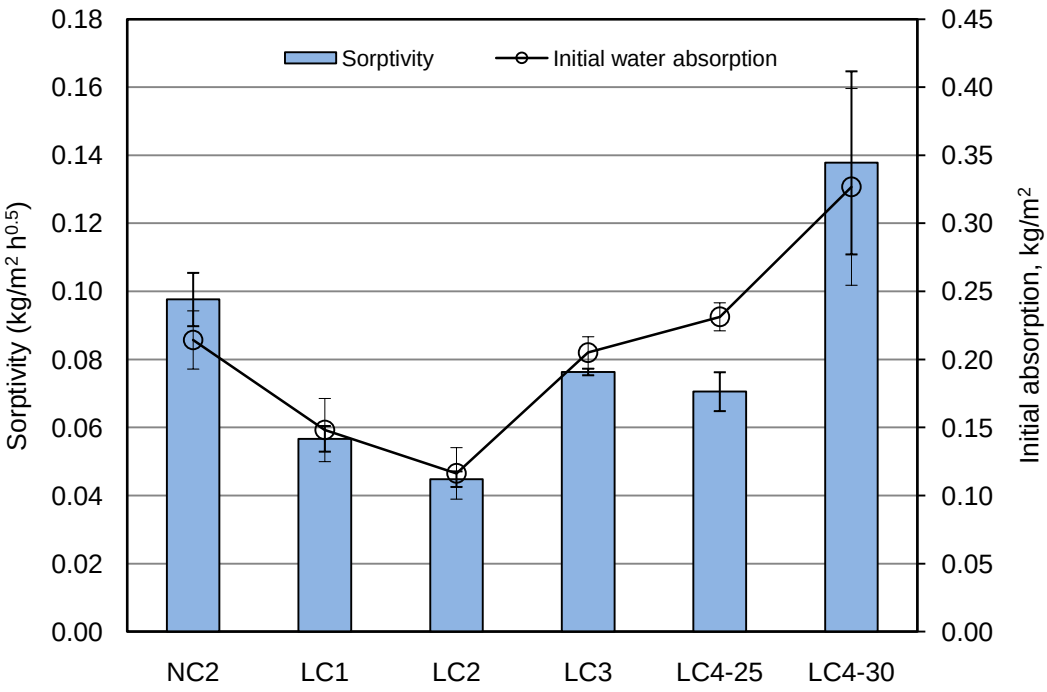

Fig. 5.16 Initial water absorption and sorptivity of LWC in comparison to NC2.

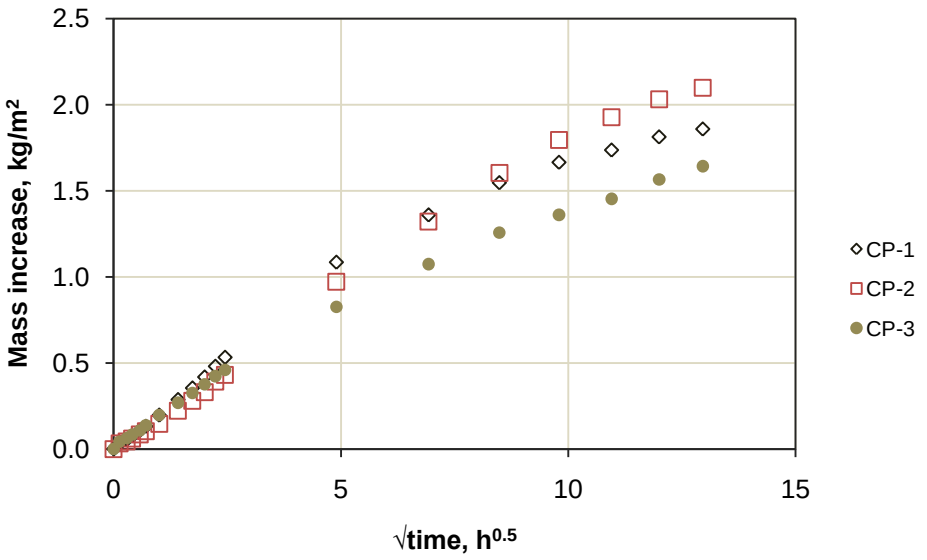

Fig. 5.17 Water absorption history up to 8 days of cement paste (w/c=0.38)

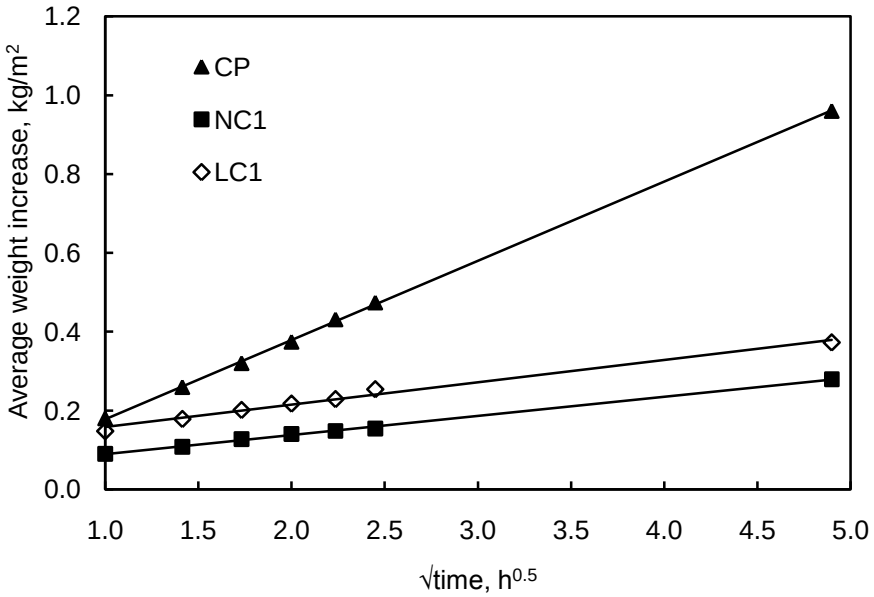

Fig. 5.18 Average weight increase of concrete and cement paste due to the absorption of water against √time.

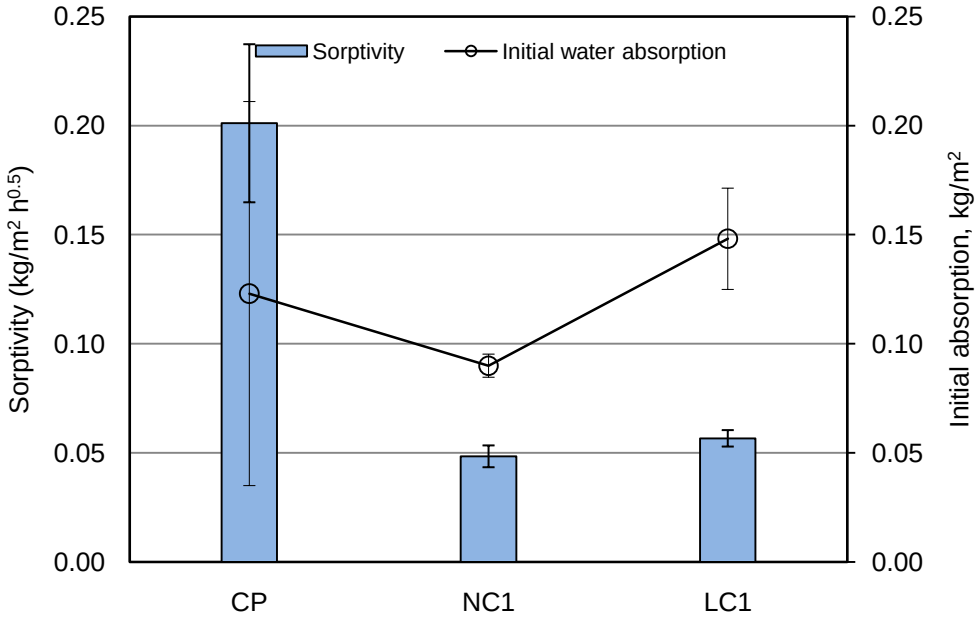

Fig. 5.19 Initial water absorption and sorptivity of concrete and cement paste.

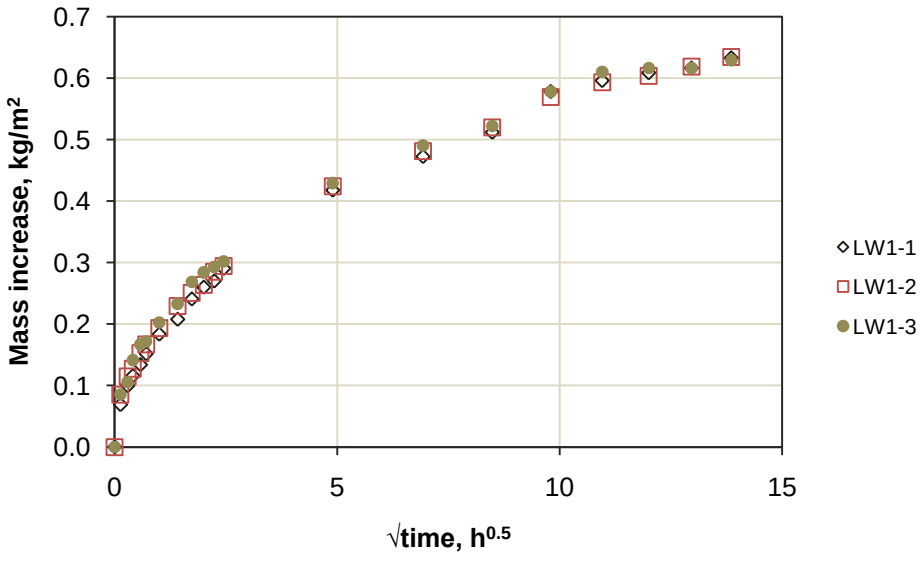

Fig. 5.20 Water absorption history up to 8 days of LW1 (w/cm=0.38)

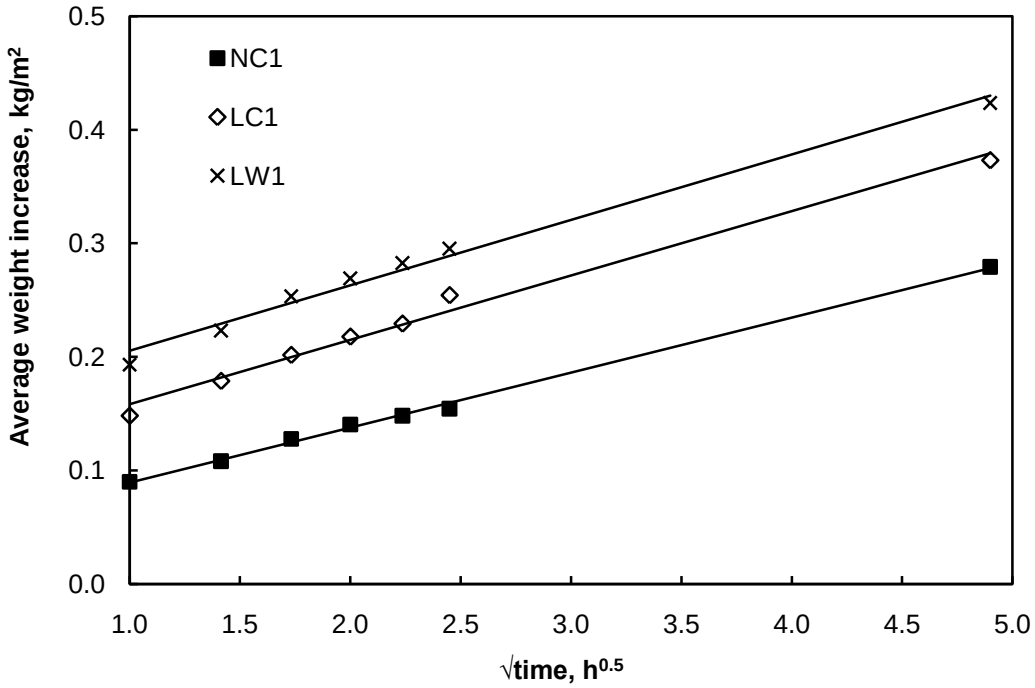

Fig. 5.21 Average weight increase of different concretes due to the water absorption against √time.

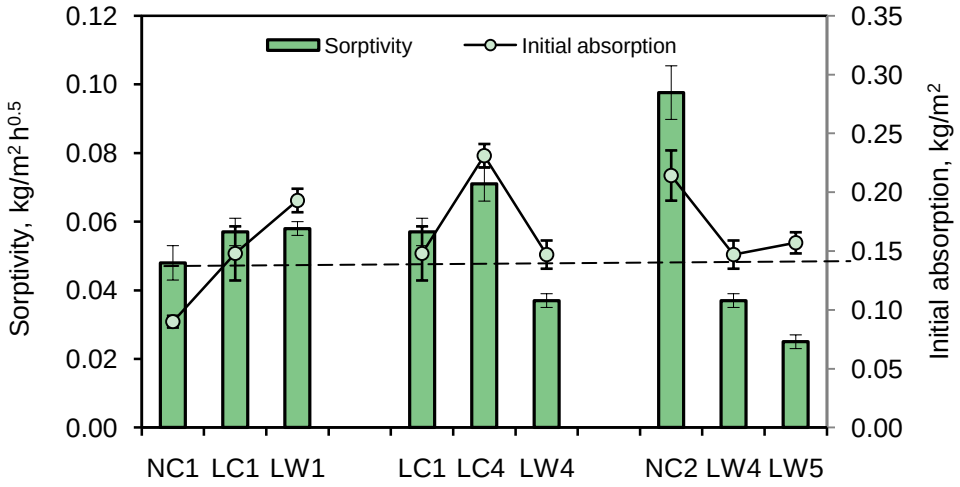

Fig. 5.22 Initial water absorption and sorptivity of concretes.

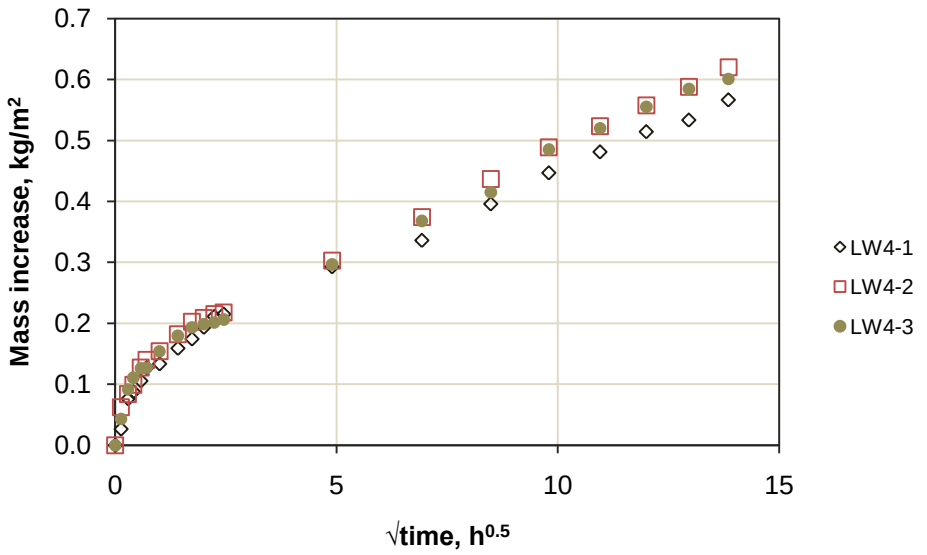

Fig. 5.23 Water absorption history up to 8 days of LW4 (w/cm=0.38)

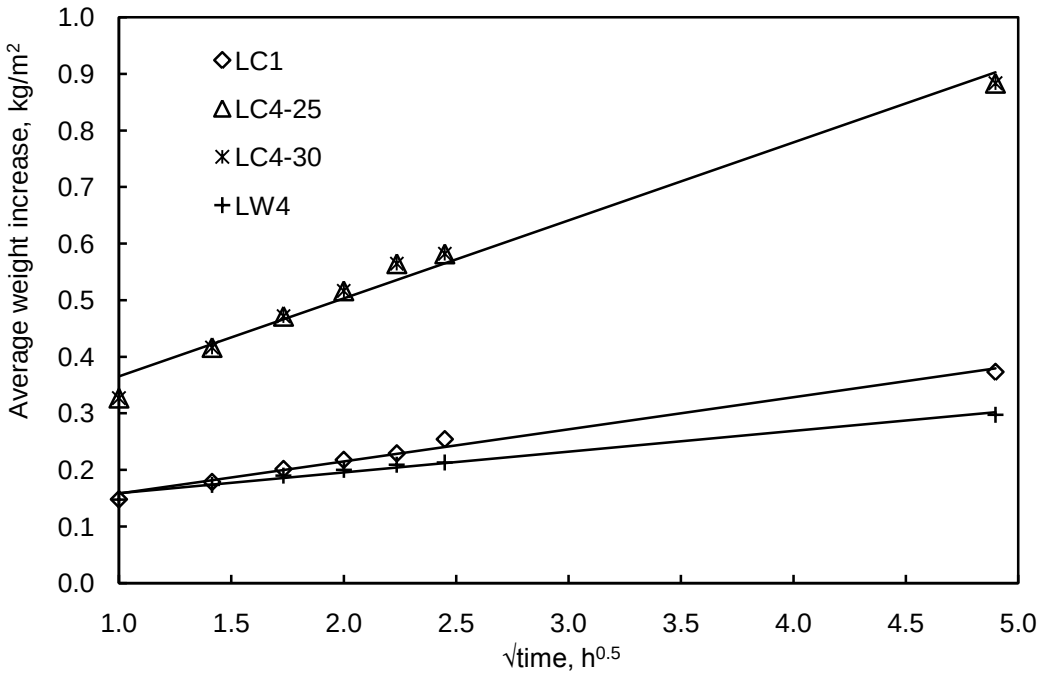

Fig. 5.24 Average weight increase of different concretes due to the water absorption against √time.

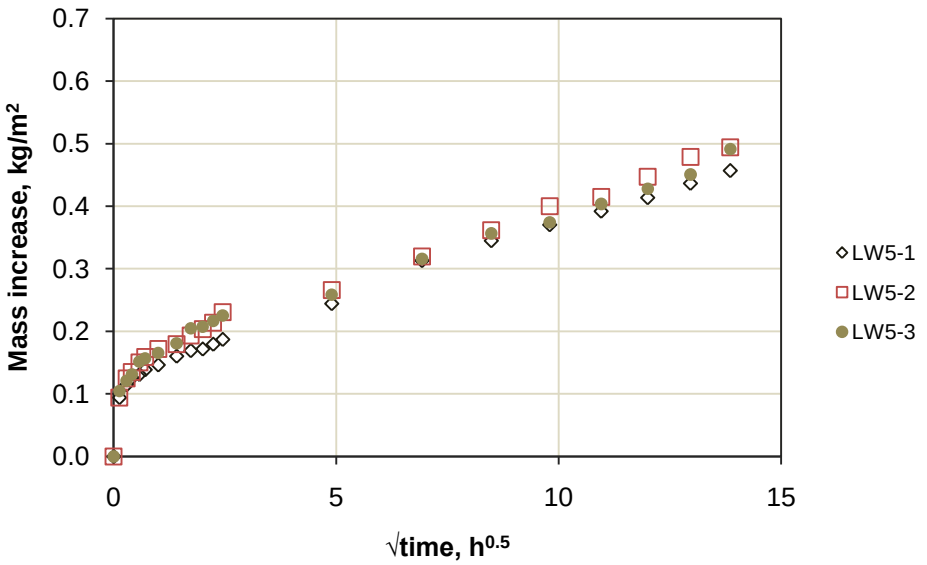

Fig. 5.25 Water absorption history up to 8 days of LW5 (w/cm=0.20)

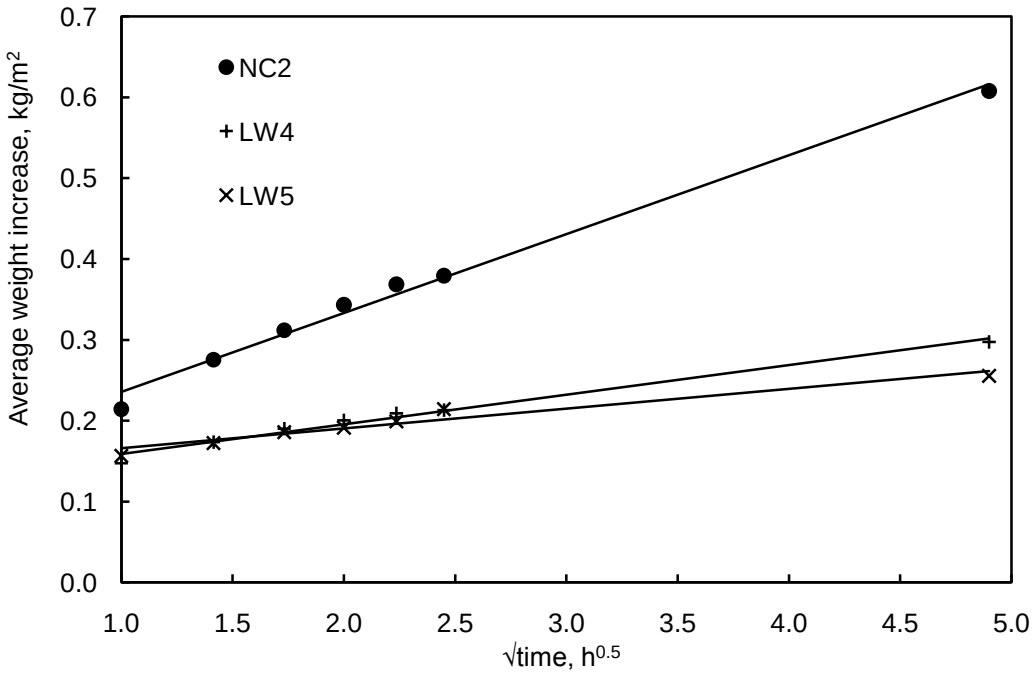

Fig. 5.26 Average weight increase of concretes with different w/cm due to the water absorption against √time.

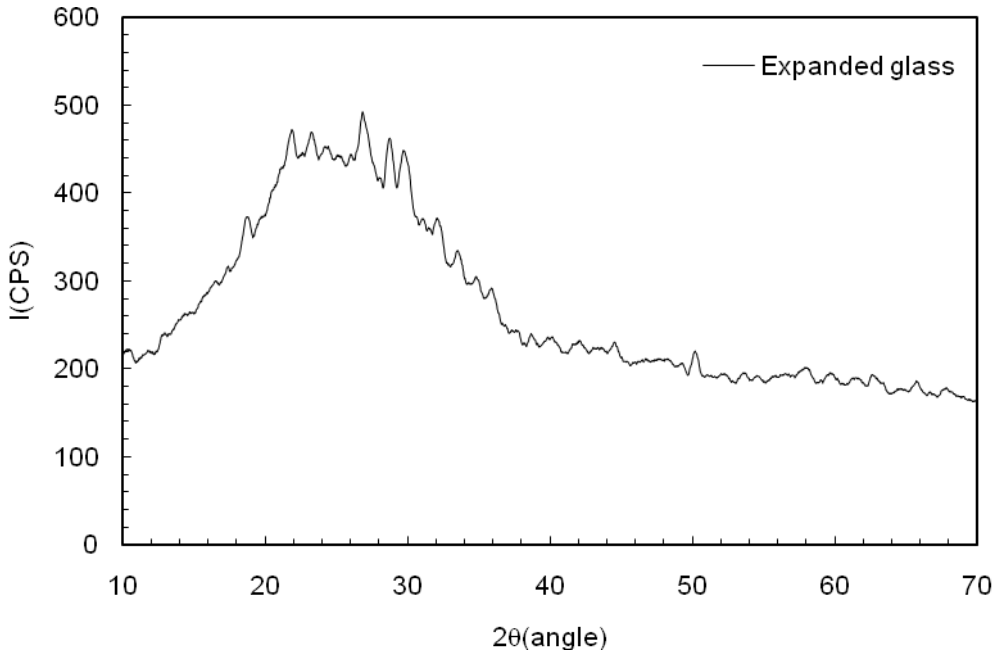

Fig. 5.27 X-ray diffraction spectrum of ground expanded glass particles.

CHAPTER 6 EMPIRICAL RELATIONSHIPS OF TRANSPORT PROPERTIES OF LIGHTWEIGHT CONCRETE VS WATER ACCESSIBLE POROSITY AND UNIT WEIGHT

6.1 Introduction

Effects of LWA for internal curing, cumulative LWA content, porosity and surface texture of LWA, w/cm of cement paste binder on the water absorption and resistance to chloride ion penetration of concrete were studied and discussed in chapters 4 and 5, and experimental results have been discussed and reported in comparison to those of NWC [Liu et al., 2009a; Liu et al., 2009b; Liu and Zhang, 2009]. The results indicate that the water absorption and resistance to chloride ion penetration are related to water accessible porosity of concrete. There has been considerable interest in establishing correlations between basic physical properties of concrete that can be easily determined and the transport properties of concrete. The empirical relationships may then be used to estimate the transport properties of the concretes and durability of concrete exposed to severe environments.

Therefore, this chapter firstly evaluates the influence of water accessible porosity on the resistance to water and chloride ion penetration. Secondly, empirical relationships between the water absorption and resistance to chloride ion penetration of concrete and water accessible porosity and oven dry unit weight was established based on experimental results.

6.2 Water accessible porosity in comparison to total porosity of the concrete

Although concrete with lightweight particles had higher total porosity than NWC, many pores in the LWA particles are closed ones (Table 3.2) which in principle do not affect transport of water and ions in concrete. A material can be porous but still has low permeability as long as the pores are not interconnected. On the other hand, a material can have lower total porosity but higher permeability if the pores are interconnected. Figure 2.5 shows schematic differences between the porosity and permeability [EuroLightCon, 1998]. Total porosity including both connected and discrete pores may not be a suitable parameter to correlate to permeability and chloride-ion penetration in LWC. For concrete exposed to severe environments, water accessible porosity is more important and more appropriate than total porosity of the concretes to correlate to their transport properties such as water absorption and resistance to chloride ion penetration.

As shown in Table 6.1, the water accessible porosities of the concrete with LWA particles were significantly lower than the total porosity, particularly for the LWC. For the NWC, however, their water accessible porosity was comparable to or higher than the total porosity. This may be attributed to the higher porosity in the ITZ between aggregate and cement paste in the NWC which was not considered in the estimation of the total porosity.

Comparing the concrete with a given w/cm of about 0.38, it seems that the water accessible porosity of the concretes with LWA particles (concrete with LWA for internal curing, sand-LWC, and all-LWC) increased with an increase in content and porosity of LWA. However, the extent of the increase was much less significant

compared with the total porosity. This confirmed that many pores in the concrete with LWA particles were discrete and did not contribute to water penetration.

The results in Table 6.1 also show that the incorporation of LWA particles < 1.18 mm in all-LWC had more significant influence on their water accessible porosity. This might be attributed to increased porosity due to a higher amount of LWA in the concretes and possibly increased pore connectivity.

The use of fine LWA particles in concrete (RS2 and RS3) for internal curing reduced the water accessible porosity slightly even though their w/cm was slightly higher than the control NWC (NC1). This may be attributed to increased cement hydration due to the internal curing from the pre-soaked LWA which reduced the capillary porosity and pore connectivity in the cement paste.

Comparing the control NWC with w/cm of 0.54 (NC2) and all-LWC with w/cm of 0.20 and 10% silica fume (LW5), the former had higher water accessible porosity than the latter although the latter had much higher total porosity and much lower unit weight. This indicated that the w/cm and density of the cement paste binder in concrete had significant influence on the water accessible porosity of concrete, thus concrete resistance to the penetration of harmful substances.

6.3 Influence of water accessible porosity on sorptivity, total charge passed, and migration coefficient of concrete

Figures 6.1, 6.2, and 6.3 show effects of water accessible porosity on the sorptivity, total charge passed, and migration coefficient of different concrete mixtures, respectively. It is clear that the water absorption and resistance to chloride ion penetration of the concretes are strongly correlated to their water accessible porosity. The sorptivity, total charge passed, and migration coefficient of the concrete were all

increased with the increase in the water accessible porosity. In addition to the water accessible porosity, unit weight of the concrete seems to have influences on the sorptivity, total charge passed, and migration coefficient as well.

6.4 Correlations between water accessible porosity and water absorption and resistance to chloride ion penetration of concrete with different unit weights

To test the significance of the water accessible porosity (P_w) (in percentage) and oven dry unit weight of concrete (D) (in kg/m^3) on the influence of the sorptivity, charge passed, and chloride migration coefficient, best subset regression method [Montgomery and Runger, 2002] and Minitab software package were used to find significant predictors for estimating the transport properties. Multiple regression analyses were then carried out to find out relationships between the transport properties of the concretes and the significant predictors.

Using best subset regression method it was found that P_w^2 and P_w^2/D were significant predictors for the transport properties of the concretes. Least squares regression analyses were carried out and empirical relationships between the transport properties and the water accessible porosity and oven dry unit weight of concrete were established as shown in Equation (6.1).

$$\mu = a_0 + a_1 P_w^2 + a_2 \frac{P_w^2}{D} \quad (6.1)$$

where μ represents different transport properties of the concretes including sorptivity, total charge passed, and migration coefficient. Least squares estimates a_0, a_1, and a_2 were obtained from the regression analyses of the experimental results, and are presented in Table 6.2 together with corresponding regression coefficients R^2. The p-values in the statistic significance tests for the constants and estimated coefficients of

P_w^2 and P_w^2/D at a level of significance of 0.05 are also given in Table 6.2. The small p-values indicate that the constants and the terms of P_w^2 and P_w^2/D are significant in estimating the sorptivity, charge passed, and migration coefficient. The regression coefficient of R^2 for sorptivity (S), total charge passed (C_T), and migration coefficient (D_m) was about 0.75, 0.84, and 0.84, respectively. It shows the empirical relationships fit the experimental data well. And the transport properties including sorptivity, total charge passed, and migration coefficient can be predicted by these models reasonably. From the practical point of view, such regression equations would give reasonable estimations for the transport properties of the concretes.

Tables 6.3 - 6.5 compared the results obtained from the experiments and those from the empirical equations. The estimated results from the empirical equations generally agreed well with the experimental results with a few exceptions. There is a great difference between the charge passed estimated from the empirical equation and that determined by the experiment for mixture LW5 with 10% silica fume. The use of supplementary cementing materials such as ground blast furnace slag, silica fume, metakaoline, coal fly ash and natural pozzolan can have very significant effect on pore solution chemistry of concrete, depending on the dosage and composition of these supplementary cementing materials [Diamond, 1983; Duchesene and Berube, 1994; Glasser et al., 1988; Page and Vennesland, 1983; Rasheeduzzafar and Ehtesham Hussain, 1991; Shehata et al., 1999; Wiens et al., 1995]. ASTM C 1202 test method is based on the electrical resistivity of concrete which depends on both pore structure and pore solution chemistry of the concrete. The incorporated silica fume could influence the pore solution chemistry of LW5 and therefore influence the total charge passed when subjected to the ASTM C 1202 test. However, the empirical equation considered the water accessible porosity and unit weight without consideration of the pore

solution chemistry of the concrete. This could be the main reason contributing to the significant difference between the experimental result and the predicted value using equation 6.1 for this concrete. Further research is needed to verify these empirical equations with more data.

In the regression analyses, the water accessible porosity P_w ranged from about 9 to 21%, and oven-dry unit weight of the concretes D ranged from 1216 to 2287 kg/m^3. The regression equations are valid within the ranges. Due to limited experimental results available, further research is need to validate the equations for concrete with various w/cm, curing conditions, LWA, and mineral admixtures.

It should be noted that the size of the concrete specimens used for determining the water accessible porosity is important, particularly for LWC. In this study, the specimens had a diameter of 100 mm and a thickness of 50 mm cut from a 100×200 mm cylinder with approximately 10 mm from the top and bottom removed. For the LWC, cut surface exposes closed pores within LWA. The area of the cut surface relative to the thickness and volume of the specimen thus influences the water accessible porosity of the concrete. For a thin specimen, for example, the cut surface with exposed internal pores of the LWA would have more significant influence on the water accessible porosity than a thicker specimen. In addition, thickness and volume of the specimens are critical as it is more difficult to achieve saturation for thick specimens. This will affect the accuracy of the water accessible porosity of the concrete determined.

Based on Equation (6.1) and values of a_0, a_1, and a_2 in Table 6.2, a reduction of the unit weight of concrete will result in a decrease in the transport properties if the water accessible porosity is kept constant. To reduce the unit weight of concrete with given LWA, the volume content of LWA in concrete needs to be increased. As the

increased LWA volume may lead to increased water accessible porosity, w/cm of concrete needs to be reduced to keep the water accessible porosity constant. The reduced w/cm results in a decrease in transport properties of concrete.

Since the water accessible porosity and oven dry unit weight of concrete can be easily determined, the water absorption, total charge passed, and migration coefficient of the concretes can be estimated for quality control and for estimating durability of concrete.

No relationship was found between water absorption, water permeability, and chloride ion penetration because they all have different mechanisms.

6.5 Conclusions

Based on the experimental results and regression analyses, the following conclusions may be drawn:

Water accessible porosity is an important parameter that is strongly correlated to the water sorptivity, charge passed, and chloride migration coefficient of the LWC and NWC. Based on the experimental results and regression analyses, empirical relationships of the water sorptivity, charge passed, and chloride migration coefficient versus the water accessible porosity and oven dry unit weight of the concrete are established. Using basic physical properties of water accessible porosity and oven dry unit weight which can be easily determined, the transport properties such as sorptivity, total charge passed, and migration coefficient of the concrete can be estimated for quality control and for estimating durability of concrete.

Table 6.1 Summary of experimental results

Type of concrete	Mixtures	w/cm	28-day unit weight, kg/m^3	Oven dry unit weight, D, kg/m^3	fc,28, MPa	Water accessible porosity, P_w, %	Estimated total porosity#, P_T, %	Sorptivity, S, kg/m^{2}h$^{0.5}$	Total charge, C_T, Coulombs	Migration coefficient D_m, $\times 10^{-12}$ m^2/s
NWC	NC1	0.38	2365	2267	71	10.0	8.8	0.048	2528	8.8
	NC2	0.54	2273	2188	49	16.1	12.7	0.098	6199	19.1
	RS4	0.39	2348	2287	63	8.5	8.8	0.044	2012	9.7
Concrete with LWA for Internal curing	RS1	0.38	2016	1933	53	10.6	22.0	0.043	2977	8.2
	RS2	0.39	2162	2189	57	9.8	15.8	0.026	3111	9.2
	RS3	0.40	2276	2210	56	9.4	15.1	0.047	2987	10.1
Sand-LWC	LW1	0.38	1759	1682	30	13.0	32.7	0.058	3676	10.4
	LC1	0.38	1877	1780	50	11.0	28.2	0.057	2385	6.5
	LC2	0.38	1841	1762	47	10.9	29.8	0.045	2496	7.6
	LC3	0.38	1708	1624	42	12.6	33.5	0.076	3278	8.8
All-LWC	LC4-25	0.38	1556	1402	38	21.5	~42.2	0.071	2559	6.6
	LC4-30	0.38	1572	1413	34	20.7	~42.2	0.083	3620	8.9
	LW4	0.38	1364	1225	24	17.1	49.0	0.037	1581	5.2
	LW5	0.20	1317	1216	21	13.6	49.9	0.025	110	2.4

Calculated based on mixture proportion of concrete, total porosity of LWA, and porosity of cement paste determined by mercury intrusion porosimeter.

Table 6.2 Results from regression analysis

μ	unit	a_o	p-value	Significant (α-level: 0.05)	a_1	p-value	Significant (α-level: 0.05)	a_2	p-value	Significant (α-level: 0.05)	R^2
S	kg/m^{2}h$^{0.5}$	0.02	0.02	Yes	6.16	0.00	Yes	-6795	0.00	Yes	0.75
C_T	Coulombs	1040	0.01	Yes	4.5×10^5	0.00	Yes	-5.6×10^8	0.00	Yes	0.84
D_m	$\times10^{-12}$m^2/s	4.73	0.00	Yes	1200	0.00	Yes	-1.6×10^6	0.00	Yes	0.84

Table 6.3 Comparison of the sorptivity estimated from the empirical equation and that determined from the experiment

Type of concrete	Mixtures	w/cm	Oven dry unit weight, D, kg/m^3	Water accessible porosity, P_w, %	Experimental sorptivity, S, $kg/m^2h^{0.5}$	Estimated sorptivity, $kg/m^2h^{0.5}$	Differences	% in difference
NWC	NC1	0.38	2267	10	0.048	0.052	0.004	8%
	NC2	0.54	2188	16.1	0.098	0.099	0.001	1%
	RS4	0.39	2287	8.5	0.044	0.043	-0.001	-2%
Concrete with LWA for Internal curing	RS1	0.38	1933	10.6	0.043	0.050	0.007	16%
	RS2	0.39	2189	9.8	0.026	0.049	0.023	90%
	RS3	0.4	2210	9.4	0.047	0.047	0.000	1%
Sand-LWC	LW1	0.38	1682	13	0.058	0.056	-0.002	-4%
	LC1	0.38	1780	11	0.057	0.048	-0.009	-15%
	LC2	0.38	1762	10.9	0.045	0.047	0.002	5%
	LC3	0.38	1624	12.6	0.076	0.051	-0.025	-32%
All-LWC	LC4-25	0.38	1402	21.5	0.071	0.081	0.010	14%
	LC4-30	0.38	1413	20.7	0.083	0.078	-0.005	-6%
	LW4	0.38	1225	17.1	0.037	0.038	0.001	3%
	LW5	0.2	1216	13.6	0.025	0.031	0.006	22%

Table 6.4 Comparison of the total charge passed estimated from the empirical equation and that determined from the experiment

Type of concrete	Mixtures	w/cm	Oven dry unit weight, D, kg/m^3	Water accessible porosity, P_w, %	Experimental charge passed, C_T, Coulombs	Estimated charge passed, Coulombs	Differences	% in difference
NWC	NC1	0.38	2267	10	2528	3070	542	21%
	NC2	0.54	2188	16.1	6199	6070	-129	-2%
	RS4	0.39	2287	8.5	2012	2522	510	25%
Concrete with LWA for Internal curing	RS1	0.38	1933	10.6	2977	2841	-136	-5%
	RS2	0.39	2189	9.8	3111	2905	-206	-7%
	RS3	0.4	2210	9.4	2987	2777	-210	-7%
Sand-LWC	LW1	0.38	1682	13	3676	3018	-658	-18%
	LC1	0.38	1780	11	2385	2678	293	12%
	LC2	0.38	1762	10.9	2496	2610	114	5%
	LC3	0.38	1624	12.6	3278	2710	-568	-17%
All-LWC	LC4-25	0.38	1402	21.5	2559	3378	819	32%
	LC4-30	0.38	1413	20.7	3620	3340	-280	-8%
	LW4	0.38	1225	17.1	1581	831	-750	-47%
	LW5	0.2	1216	13.6	110	845	735	668%

Table 6.5 Comparison of the migration coefficient estimated from the empirical equation and that determined from the experiment

Type of concrete	Mixtures	w/cm	Oven dry unit weight, D, kg/m^3	Water accessible porosity, P_w, %	Experimental migration coefficient, D_m, $\times 10^{-12}$ m^2/s	Estimated migration coefficient, $\times 10^{-12}$ m^2/s	Differences	% in difference
NWC	NC1	0.38	2267	10	8.8	9.7	0.9	10%
	NC2	0.54	2188	16.1	19.1	16.9	-2.2	-12%
	RS4	0.39	2287	8.5	9.7	8.3	-1.4	-14%
Concrete with LWA for Internal curing	RS1	0.38	1933	10.6	8.2	8.9	0.7	9%
	RS2	0.39	2189	9.8	9.2	9.2	0.0	0%
	RS3	0.4	2210	9.4	10.1	8.9	-1.2	-12%
Sand-LWC	LW1	0.38	1682	13	10.4	8.9	-1.5	-14%
	LC1	0.38	1780	11	6.5	8.4	1.9	29%
	LC2	0.38	1762	10.9	7.6	8.2	0.6	8%
	LC3	0.38	1624	12.6	8.8	8.1	-0.7	-8%
All-LWC	LC4-25	0.38	1402	21.5	6.6	7.4	0.8	13%
	LC4-30	0.38	1413	20.7	8.9	7.6	-1.3	-14%
	LW4	0.38	1225	17.1	5.2	1.6	-3.6	-69%
	LW5	0.2	1216	13.6	2.4	2.6	0.2	8%

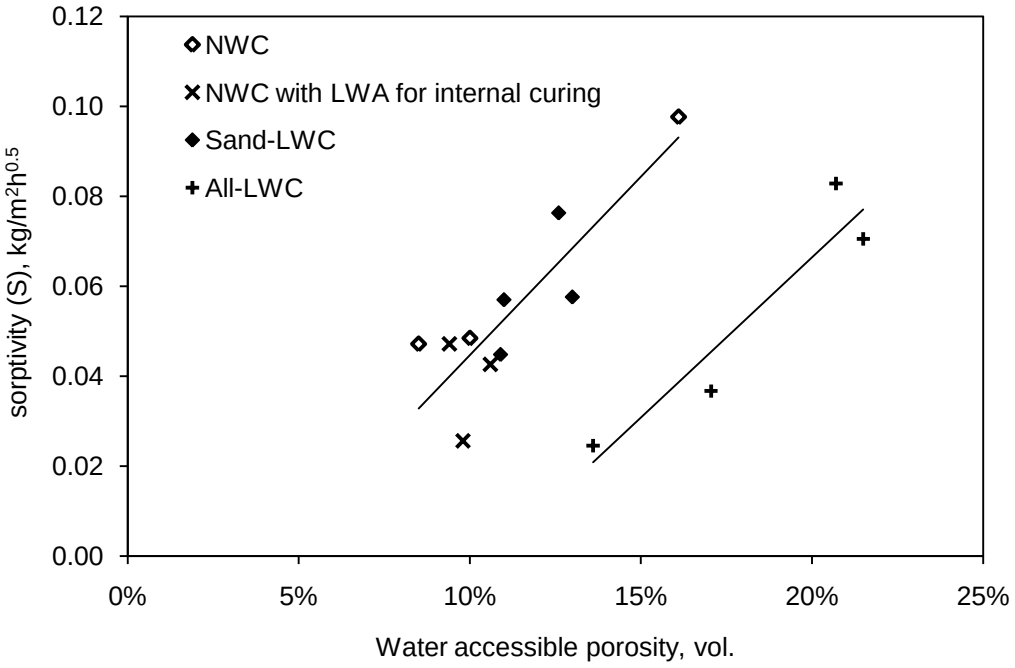

Fig. 6.1 Influence of water accessible porosity on sorptivity of concrete.

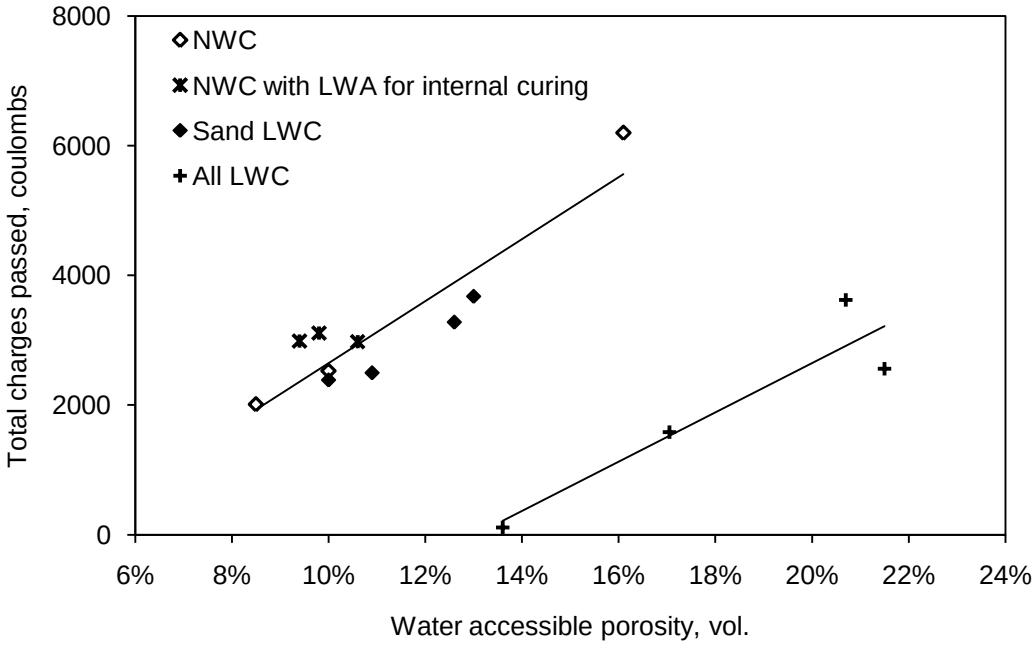

Fig. 6.2 Influence of water accessible porosity on total charges passed through concrete based on rapid chloride penetrability test.

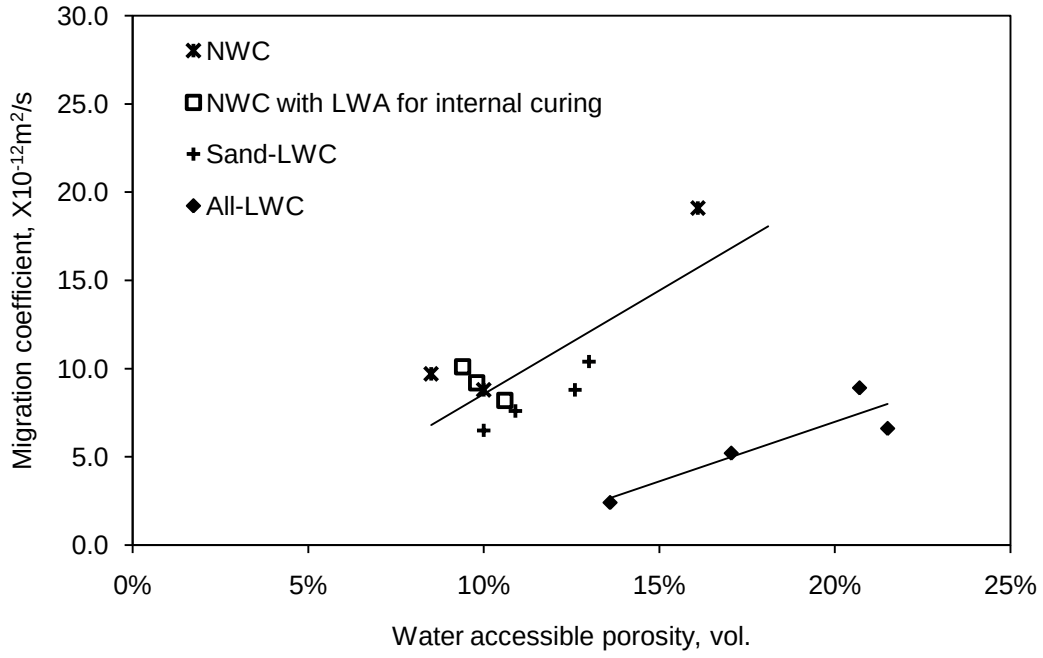

Fig. 6.3 Influence of water accessible porosity on migration coefficient of concrete.

CHAPTER 7 CONCLUSIONS AND RECOMMENDATIONS

7.1 Conclusions

This research investigates the effect of LWA on transport properties of concrete including water absorption, water permeability, and resistance to chloride ion penetration. It covers normal weight concretes in which LWA is used for internal curing, lightweight concrete where only coarse LWA is used, and lightweight concrete where all aggregate are lightweight. Effects of the cumulative LWA content, porosities and surface textures of LWA, and w/c of concrete on the transport properties of concrete are also investigated. Control normal weight concretes and concrete with a shrinkage reducing admixture are also included for relative comparisons.

All concrete mixtures were cured in moisture condition for the first 7 days at a temperature around 28 ^{o}C followed by exposure in laboratory air with a relative humidity of about 80-85 % at a similar temperature until testing or conditioning at 28 days except for those used for water permeability test. Specimens used for the water permeability test were cured for 7 days in moist condition.

The initial water absorption and the sorptivity of the concrete were tested according to ASTM C 1585, but were calculated according to Buyle-Bodin and Hadjieva-Zaharieva [2002]. Water penetration depth in the concrete subjected to a pressure of 0.75 MPa was determined according to BS EN 12390-8, and water

permeability coefficient was calculated according to Valenta's equation [1970]. The chloride penetrability and rapid chloride migration tests of concretes were conducted according to ASTM C 1202 and NT Build 492. AASHTO T 259 salt ponding test was conducted on selected concretes.

Based on the experimental results and analyses presented, the following conclusions can be drawn:

1. For normal weight concrete (*w/c* ≈ 0.38) where LWA was used for internal curing
    a. In general, the concretes with LWA particles for internal curing had initial water absorption, sorptivity, and water permeability similar to or lower than those of the control concrete and the concrete with shrinkage reducing admixture. The charges passed, chloride migration coefficient, and chloride diffusion coefficient of such concretes were in the same order as those of the control concrete and the concrete with shrinkage reducing admixture. However, the incorporation of the LWAs for internal curing reduced unit weight, compressive strength, and elastic modulus of the concrete of similar w/c.
    b. Comparing the LWAs of different sizes for internal curing, finer particles were more efficient in reducing the shrinkage and generally resulted in less reduction in the unit weight, compressive strength, and elastic modulus. However, the increase in the more porous crushed LW particles in concrete seems to increase the penetration of chloride ions in the concrete. This is very important as most structures are designed based on 28-day strength. To use pre-soaked

LWA in concrete for internal curing, the accurate determination of the water absorption of LWA is important.

c. The concrete with shrinkage reducing admixture had initial water absorption, sorptivity, water permeability, and resistance to chloride ion penetration comparable to those of the control concrete. The use of shrinkage reducing admixture in concrete does not affect the elastic modulus of the concrete, except for a minor influence on the compressive strength of the concrete.

When design high-performance lightweight concrete, shrinkage reducing admixture or pre-soaked LWA can be used to reduce/eliminate autogenous shrinkage of concrete. Fine LWA with smaller size and spherical shape would be a better choice for internal curing purpose compared with LWA with bigger size. Therefore, the 1st objective is achieved.

2. For lightweight aggregate concretes, comprehensive investigations were carried out to investigate the influence of cumulative LWA contents, porosity, and surface textures of LWA on the transport properties of LWC and the second objective set out in Chapter 1 was achieved.

    a. Although the total charge passed, migration coefficient, and diffusion coefficient of the LWC were not significantly different from those of NWC with the same w/c of 0.38, the resistance of the LWC to chloride-ion penetration decreased with an increase in the cumulative LWA content in the concrete. The water penetration depth under pressure and water sorptivity showed, in general, similar trends. The LWC with only coarse LWA had similar water sorptivity, water

permeability coefficient and resistance to chloride-ion penetration compared to NWC of similar w/c.

b. The LWC had lower water sorptivity, water permeability and higher resistance to chloride-ion penetration than the NWC with similar 28-day strength. This is very important as most structures are designed based on 28-day strength.

c. Both NWC and LWC had lower sorptivity and higher resistance to chloride-ion penetration than the cement paste with similar w/c. The high resistance to water and chloride penetration of the concretes were mainly attributed to the increased tortuosity of the pores in concrete due to the presence of aggregates (both LWA and NWA) compared to cement paste.

d. The increase in porosity of coarse LWA in concrete increased the water sorptivity and permeability slightly compared to NWC of similar w/c. This is related to the increased porosity of the concrete due to the pores in coarse LWA. The performance of the LWC with less porous coarse LWA (F6.5) was similar to that of the NWC, whereas more porous coarse LWA (F4.5) tends to reduce the resistance of the concrete to chloride-ion penetration.

e. Fine LWA has more influence on the transport properties of concrete than coarse LWA. Use of lightweight crushed sand of <1.18 mm tends to reduce the resistance of the LWC to water and chloride-ion penetration to some extent.

f. To obtain concrete with very low unit weight and high resistance to water and chloride ion penetration, low w/cm of 0.20 and 10% of

silica fume was used. Lightweight concrete with low unit weight about 1300 kg/m^3 had very low water absorption and water permeability and high resistance to chloride ion penetration compared with other concretes with higher w/c and unit weight. Quality of the paste matrix plays a significant role in controlling the transport properties of the concrete regardless of the porosity of aggregates used. The concrete with low unit weight but high resistance to water and chloride ion penetration as mentioned in the 3rd objective in Chapter 1 was developed and evaluated.

g. It should be pointed out that the effective w/cm of LWC is affected by the water absorption of LWA, which in turn influences the concrete resistance to water and chloride-ion penetration. Thus, the water absorption of LWA, especially those fine particles, needs to be carefully determined, and trial mixes are highly recommended for structures exposed to severe environments.

For a given type of LWA, coarse LWA did not influence the water sorptivity and permeability significantly compared to NWC of similar w/c and mix proportion. Fine LWA has more influence on the transport properties than coarse LWA.

For given size and content of coarse LWA, more porous coarse LWA tends to reduce the resistance to water and chloride ion penetration of concrete.

The experimental results show that the water absorption and resistance of concrete to chloride ion penetration are strongly correlated to their water accessible porosity. The sorptivity, total charge passed, and migration coefficient of the concrete were all increased with an increase in the water accessible porosity. In addition, unit weight of the concrete also has influence on the sorptivity, total charge passed, and

migration coefficient. Based on the experimental results and regression analyses, empirical relationships of the transport properties including water sorptivity, charge passed, and chloride migration coefficient (generalized with symbol μ) versus the water accessible porosity (P_w) and oven dry unit weight (D) of the concrete are established:

$$\mu = a_0 + a_1 P_w^2 + a_2 \frac{P_w^2}{D}$$

Coefficient a_0, $a_1$and a_2 are all constant which can be found in Chapter 6. These empirical models help to achieve the target to estimate the transport properties of concrete using some basic material properties as set in the fourth objective in Chapter 1.

7.2 Research significance

1. Pre-soaked LWA is commonly incorporated into concrete for internal curing to reduce/eliminate autogeneous shrinkage and potential cracking. Based on published information, the efficiency of the internal curing and reduction in the autogenous shrinkage was affected by the size of LWA incorporated. Smaller size LWAs are more efficient in reducing autogenous shrinkage. However, no information is available on how the use of such porous LWA affects the transport properties of concrete and how the fine LWAs influence the concrete permeability compared with coarse ones. Only limited information on charge passed determined by ASTM C 1202 is available for concrete with w/c of 0.35. For structures exposed to severe environment, such information is essential to design structures with good long term durability. This study

provides the information that allows engineers and designers to select concrete mixtures for exposure in severe environment to reduce autogenous shrinkage, cracking, and improve long term durability.

2. There are contradicting opinions on the effect of LWA on the transport properties of concrete. By carefully analyzing the published information, it seems that the amount, size, and porosity of LWA and w/c of concrete all play important roles. A comprehensive research was thus carried out to investigate the influence of cumulative LWA contents, porosity and surface textures of LWA, and w/c of concrete on the transport properties of LWC. The results clarify the effect of LWA on the transport properties of concrete, and provide a general guideline for design of lightweight and durable concrete.
3. Most LWC used for long-span bridges and floating structures built in the last 30 years incorporated only coarse LWA and had unit weight generally more than 1700 kg/m^3. In the present study, LWC with very low unit weight about 1300 kg/m^3 but high resistance to water and chloride ion penetration was developed by using low w/cm, silica fume, and LWA with very low density. Such low unit weight has opened up a new avenue for potential use of LWC in marine environment for floating structures.
4. Empirical equations have been established between the transport properties of the concrete including sorptivity, total charge passed, and migration coefficient and their water accessible porosity and oven dry unit weight. For both LWC and NWC, physical properties of water accessible porosity and unit weight can be easily determined in

laboratory. Using the empirical equations, the transport properties of concrete can be estimated for quality control and for estimating durability of concrete.

7.3 Recommendations for further research

1. In the present study, the water permeability test was conducted on concretes moisture cured for 7 days and the test duration was 14 days due to the low pressure achievable by the equipment available in the laboratory. The young concrete at 7days experienced further hydration during the test period which may influence the results. Therefore, the water permeability coefficient obtained may be higher than that of the concrete cured for 28 days as other specimens. No clear relation between the water permeability and water accessible porosity and unit weight of concrete was found. Equipment with high pressure leading to axial flow which can produce measurable flow through the specimens is recommended for further research.
2. Experimental investigations carried out in this study were restricted to short-term test. For concrete resistance to chloride ion penetration, long-term test and monitoring of chloride-ion diffusion in LWC are recommended.
3. This study used expanded glass aggregates to achieve the very low unit weight of LWC. The fine expanded glass aggregates may react with alkalis from cement and cause potential damages in concrete. Therefore, the short and long term chemical reaction and change in microstructure

between the expanded glass aggregate particles and alkalis from cement paste need to be further investigated.

REFERENCES

FIP manual of lightweight aggregate concrete, Glasgow ; New York: : Surrey University Press : Halsted Press. 1983.

Report on autogenous Shrinkage of concrete. Japan Concrete Institute Committee, Hiroshima, Japan. 1999.

AASHTO T259, Standard Method of Test for Resistance of Concrete to Chloride Ion Penetration, American Association of State Highway and Transportation Officials. 2002.

AASHTOT260 Standard Method of Test for Sampling and Testing for Chloride Ion in Concrete and Concrete Raw Materials, American Association of State Highway and Transportation Officials. 1994.

ACI-201.2R-08 Guide to Durable Concrete, American Concrete Institute. 2008.

ACI-213R Guide for Structural LIghtweight Aggregate Concrete, American Concrete Institute. 2003.

Al-Khaiat, H. and Haque, N. Strength and durability of lightweight and normal weight concrete. Journal of Materials in Civil Engineering, 11(3), pp. 231-235. 1999.

Andrade, C. Calculation of Chloride Diffusion Coefficients in Concrete from Ionic Migration Measurements. Cement and Concrete Research, 23, pp. 724-742. 1993.

Andrade, C. and Sanjuan, M. A. Experimental Procedure for the Calculation of Diffusion Coefficients in Concrete from Migration Tests. Advances in Cement Research, 6, pp. 127-134. 1994.

Arya, C., et al. Factors Influencing Chloride-Binding in Concrete. Cement and Concrete Research, 20, pp. 291-300. 1990.

Arya, C. and Newman, J. B. An assessment of four methods of determining the free chloride content of concrete. Materials and Structures, 23, pp. 319-330. 1990.

ASTM C 33-03, Standard Specification for Concrete Aggregates, West Conshohocken, PA: ASTM International. 2006a.

ASTM C 128-04a, Standard Test Method for Density, Relative Density (Specific Gravity), and Absorption of Fine Aggregate, West Conshohocken, PA: ASTM International. 2006b.

ASTM C 143/C 143M-05a, Standard Test Method for Slump of Hydraulic-Cement Concrete, West Conshohocken, PA: ASTM International. 2006c.

ASTM C 330-05, Standard Specification for Lightweight Aggregates for Structural Concrete, West Conshohocken, PA: ASTM International. 2006d.

ASTM C 1202-05, Standard Test Method for Electrical Indication of Chloride's Ability to Resist Chloride, West Conshohocken, PA: ASTM International. 2006e.

ASTM C 150, Standard Specification for Portland Cement, West Conshohocken, PA: ASTM International. 2008.

ASTMC403 /C403M-05 Standard Test Method for Time of Setting of Concrete Mixtures by Penetration Resistance, West Conshohocken, PA: ASTM International. 2006.

ASTMC1218 /C1218M-99, Standard Test Method for Water-Soluble Chloride in Mortar and Concrete, West Conshohocken, PA: ASTM International. 2006.

Ballim, Y. and Alexander, M. G. Towards a performance-based specification for concrete durability. In African Concrete Code Symposium, Tripoli, Libya, pp. 206-218.

Banthia, N. and Mindess, S. Water permeability of cement paste. Cement and Concrete Research, 19, pp. 727-736. 1989.

Barneyback, R. S. and Diamond, S. Expression and analysis of pore fluids from hardened cement pastes and mortars. Cement and Concrete Research, 11(2), pp. 279-285. 1981.

Basheer, L., et al. Influence of coarse aggregate on the permeation, durability and the microstructure characteristics of ordinary Portland cement concrete. Construction and Building Materials, 19(9), pp. 682-690. 2005.

Basheer, P. A. M. Clam' permeability tests for assessing the durability of concrete, PhD Thesis, The Queen's University of Belfast, 1991.

Basheer, P. A. M. and Nolan. Near-surface moisture gradients and in situ permeation tests. Construction and Building Materials, 15(2-3), pp. 105-114. 2001.

Bentz, D. P. Influence of silica fume on diffusivity in cement-based materials II. Multi-scale modeling of concrete diffusivity. Cement and Concrete Research, 30(7), pp. 1121-1129. 2000.

Bentz, D. P. Influence of internal curing using lightweight aggregates on interfacial transition zone percolation and chloride ingress in mortars. Cement and Concrete Composites, 31(5), pp. 285-289. 2009.

Bentz, D. P., et al. On the Mitigation of Early Age Cracking. The Third International Seminar on Self-Desiccation, B. Persson and G. Fagerlund, eds., Lund, Sweden, pp. 195-203. 2002.

Bentz, D. P., et al. Mixture Proportioning for Internal Curing. Concrete Internaltional, 27(2), pp. 35-40. 2005.

Bentz, D. P. and Snyder, K. A. Protected paste volume in concrete Extension to internal curing using saturated lightweight fine aggregate. Cement and Concrete Research, 29, pp. 1863-1867. 1999.

Berke, N. S. and Hicks, M. C. Estimating the life cycle of reinforced concrete decks and marine piles using laboratory diffusion and corrosion data. In Corrosion Forms and Conctrol for Infrastructure, ASTM Philadelphia. 1992.

Berke, N. S. and Hicks, M. C. Techniques to Assess the Corrosion Activity of Steel Reinforced Concrete Structures. In ASTM STP 1276, ASTM International. 1996.

Bisaillon, A. and Malhotra, V. M. Permeability of concrete using a uniaxial water-flow method", ACI SP 108, Permeability of Concrete. In ACI SP 108, Permeability of Concrete, D. Whiting and A. Walitt, eds., Detroit, American Concrete Institute. 1988.

Bouguerra, A., et al. Water sorptivity and pore structure of wood-cementitious composites. Magazine of Concrete Research, 54(2), pp. 103-112. 2002.

Bourdette, B. and Ollivier, J. P. Durabilité du mortier: prise en compte des auréoles de transition dans la caractérisation et la modélisation des processus physiques et chimiques d'altération (The durability of mortar: consideration of interfacial transition zones to characterize and to model the physicals and chemicals mecanisms involved in mortar corrosion), PhD Thesis, Université de soutenance, 1994.

Bretton, D., et al. Diffusivite des ions chlore dans la zone de transition entre pate de ciment et roche granitique. In Interfaces in cementitious composites : proceedings of the international conference held by RILEM (the International Union of Testing and Research Laboratories for Materials and Construction) at the Université Paul Sabatier, Toulouse, and organised by RILEM Technical Committee 108 and the Laboratory for Materials and Durability of Constructions (LMDC), INSA-UPS, Toulouse, France : Toulouse, October 21-23, 1992, J. C. Maso, International Union of Testing and Research Laboratories for Materials and Structures., RILEM Technical Committee 108., and Laboratory for Materials and Durability of Constructions., eds., London ; New York, E & FN Spon. 1993.

Breugel, K. v. and Vries, J. Mixture optimization of HPC in view of autogenous shrinkage. Proceedings of fifth international symposium on utilization of high strength/high performance concrete, Vol. II, Sandefjord, Norway, pp. 1041-1050. 1999.

Brown, P. W. Porosity/permeability relationships. In Materials Science of Concrete II, P. Skalny and S. Mindess, eds., Westerville, Ohio, American Ceramic Society. 1991.

BS 1881, Methods of Testing Concrete, Part 121: Methods for Determination of Static Modulus of Elasticity in Compression. London: British Standards Institution. 1983.

BS 1881-124, Methods of Testing Concrete Part 124: Methods for Analysis of Hardened Concrete, London: British Standards Institution. 1988.

BS EN 12390, Testing hardened concrete, Part 7: Density of hardened concrete. London: British Standards Institution. 2000a.

BS EN 12390, Testing hardened concrete, Part 3: Compressive strength of test specimens. London: British Standards Institution. 2000b.

BS EN 12390, Testing hardened concrete, Part 8: Depth of penetration of water under pressure. London: British Standards Institution. 2000c.

Buenfeld, N. R. and Newman, J. B. Examination of Three Methods for Studying Ion Diffusion in Cement Pastes, Mortar, and Concrete. Materials and Structures, 20, pp. 3-10. 1987.

Buyle-Bodin, F. and Hadjieva-Zaharieva, R. Influence of industrially produced recycled aggregates on flow properties of concrete. Materials and Structures/Materiaux et Constructions, 35(252 SPEC.), pp. 504-509. 2002.

Chia, K. S. and Zhang, M. H. Water permeability and chloride penetrability of high-strength lightweight aggregate concrete. Cement and Concrete Research, 32(4), pp. 639-645. 2002.

CPC11.3. Absorption of water by concrete by immersion under vacuum. In RILEM Recommendations for the Testing and Use of Constructions Materials, RILEM, ed., E & FN SPON. 1984.

Darcy, H. P. G. The Public Fountains in the Town of Dijon. V. Dalmont, Paris. 1856.

Delagrave, A., et al. Influence of the interfacial zone on the chloride diffusivity of mortars. Advanced Cement Based Materials, 5(3-4), pp. 86-92. 1997.

Detwiler, R. J. and Fapohunda, C. A. A comparison of two methods for measuring the chloride ion permeability of concrete. Cement, Concrete and Aggregates, 15(1), pp. 70-73. 1993.

Detwiler, R. J., et al. Preparing Specimens for Microscopy. Concrete Internaltional. 2001.

Dhir, R. K., et al. Near surface characteristics of concrete: intrinsic permeability. Magazine of Concrete Research, 47, pp. 87-97. 1989.

Dhir, R. K., et al. Rapid estimation of chloride diffusion coefficient in concrete. Magazine of Concrete Research, 42(152), pp. 177-185. 1990.

Dhir, R. K., et al. Role of cement content in specifications for concrete durability: aggregate type influences. In Proceedings of the Institution of Civil Engineers, Structures and Buildings. 2006.

Diamond, S. Effects of microsilica (silica fume) on pore solution chemistry of cement pastes. Journal of the American Ceramic Society 66(5), pp. C82-C84. 1983.

Duchesene, J. and Berube, M. A. The effectiveness of supplementary cementing materials in suppressing expansion due to ASR: another look at the reaction mechanism. Part 2. Pore solution chemistry. . Cement and Concrete Research, 24(2), pp. 221-230. 1994.

Elkey, W. and Sellevold, E. J. Electrical resistivity of concrete. Publication No. 80. 1995.

Elsharief, A., et al. Influence of lightweight aggregate on the microstructure and durability of mortar. Cement and Concrete Research, 35(7), pp. 1368-1376. 2005.

EuroLightCon. Definitions and International Consensus Report. European Union - Brite EuRam. III. 1988.

EuroLightCon. LWAC Material Properties State-of-the-Art. Brite-EuRam III. 1998.

Eyres, D. J. Ship Construction, Oxford: Butterworth-Heinemann. 2007.

FIB Lightweight Aggregate Concrete, Recommended Extension to Model Code 90. Föderation International du Beton, Bulletin 8. 2000.

Frederiksen, J. M. HETEK-Chloride penetration into concrete. Copenhagen. 1996.

Garboczi, E. J. PERMEABILITY, DIFFUSIVITY, AND MICROSTRUCTURAL PARAMETERS - A CRITICAL-REVIEW. Cement and Concrete Research, 20(4), pp. 591-601. 1990.

Gautefall, O., et al. Modified Portland cement, Part 8, Chloride Diffusion, Sintef Report, No. STF65 A86014. No. STF65 A86014. 1986.

Gjørv, O. E. Durability design of concrete structures in severe environments, London ; New York: Taylor & Francis. 2009.

Glass, G. K., et al. An Investigation of Experimental Methods to Determine Free and Total Chloride Contents. Cement and Concrete Research, 26, pp. 1443-1449. 1996.

Glasser, F. P., et al. Modification of cement pore fluid compositions by pozzolanic additives. Cement and Concrete Research, 18(2), pp. 165-178. 1988.

Gummerson, R. J., et al. Unsaturated water flow with porous materials observed by NMR imaging. Nature, 281(5726), pp. 56-7. 1979.

Hall, C. Water sorptivity of mortars and concretes - a review. Magazine of Concrete Research, 41(147), pp. 51-61. 1989.

Hall, C. and Hoff, W. D. Water transport in brick, stone and concrete, London: Spon Press. 2002.

Hammer, T. A. High strength LWA concrete with silica fume - Effect of water content in the LWA on mechanical properties. Supplementary papers in the 4th CANMET/ACI Int. Conf. on Fly Ash, Silica Fume, Slag and natural Pozzolans in Concrete, Turkey, pp. 314-330. 1992.

Hammer, T. A. The maturation of mechanical properties of high strength concrete exposed to different moisture conditions. Proceedings of the intrernational symposium on utilization of high strength concrete, I. Holand and E. Sellevold, eds., Lillehammer, Norway pp. 1084-1091. 1993.

Ho, D. W. S. and Lewis, R. K. Qualité du béton mesurée par l'adsorptivité de l'eau (Concrete quality as measured by water sorptivity). Transactions of the Institution of Engineers, Australia. Civil engineering 26(4), pp. 306-313. 1984.

Hoff, G. C. Internal Curing of Concrete Using Lightweight Aggregates. Theodore Bremner Symposium, Sixth CANMET/ACI, International Conference on Durability of Concrete, Thessaloniki, Greece, pp. 185-204. 2003.

Holt, E. and Leivo, M. Cracking risks associated with early age shrinkage. Cement and Concrete Composites, 26(5), pp. 521-530. 2004.

Hughes, D. C. Pore structure and permeability of hardened cement paste. Magazine of Concrete Research, 37(133), pp. 227-233. 1985.

Izquierdo, D., et al. Potentiostatic determination of chloride threshold values for rebar depassivation experimental and statistical study. Electrochimica Acta, 49(17-18), pp. 2731-2739. 2004.

Jensen, O. M. and Hansen, P. F. Autogenous deformation and change of the relative humidity in silica fume-modified cement paste. ACI Materials Journal, 93(6), pp. 539-543. 1996.

Jiang, L., et al. Evaluation of test methods for determining the resistance of concrete to chloride-ion penetration. Eighth CANMET/ACI International Conference on Fly Ash, Silica Fume, Slag and Natural Pozzolans in Concrete, V. M. Malhotra, ed., Las Vegas, USA, pp. 1-27. 2004.

Kada, H., et al. Determination of the coefficient of thermal expansion of high performance concrete from initial setting. Materials and Structures, 35(245), pp. 35-41. 2002.

Kaufmann, J., et al. Analysis of cement-bonded materials by multi-cycle mercury intrusion and nitrogen sorption. Journal of Colloid and Interface Science, 336, pp. 730-737. 2009.

Khan, M. I. Isoresponses for strength, permeability and porosity of high performance mortar. Building and Environment, 38(1051-1056). 2003.

Khatri, R. P. and Siriviatnanon, V. Methods for the determination of water permeability of concrete. ACI Materials Journal, 94(3), pp. 257-261. 1997.

Kropp, J. and Hilsdorf, H. K. Performance Criteria for Concrete Durability. Proceedings. State of the Art Report prepared by RILEM Technical Committee TC 116-PCD, Performance of Concrete as a Criterion of Its Durability. . In, pp. 198-212.

Kyaw, M. L. Early Age Shrinkage and Bond at Interface between Repair Material and Concrete Substrate, PhD Thesis, National University of Singapore, 2007.

Lam, H. and Hooton, R. D. Effects of internal curing methods on restrained shrinkage and permeability. In Proceedings of the Fourth International Research Seminar, Self-Desiccation and Its Importance in Concrete Technology, Lund, Sweden, pp. 210-228.

Lee, H. K., et al. Autogenous shrinkage of high-performance concrete containing fly ash. Magazine of Concrete Research, 55(6), pp. 507-515. 2003.

Liu, X. M., et al. Development of lightweight aggregate concrete with high resistance to water and chloride-ion penetration. Submitted to Cement and Concrete Composites. 2009a.

Liu, X. M., et al. Water absorption, Permeability, and Resistance to Chloride-ion Penetration of Lightweight Aggregate Concrete. submitted to Construction & Building Materials. 2009b.

Liu, X. M. and Zhang, M. H. Permeability of High-Performance Concrete Incorporating Presoaked Lightweight Aggregates for Internal Curing. Magazine of Concrete Research, Accepted for publication. 2009.

Lo, T. Y., et al. The effects of air content on permeability of lightweight concrete. Cement and Concrete Research, 36(10), pp. 1874-1878. 2006.

Lu, X. Y., et al. Relationship between the free and total chloride diffusivity in concrete. Cement and Concrete Research, 32(2), pp. 323-326. 2002.

Lura, P. Autogenous deformation and internal curing of concrete, Ph.D Thesis, Technical University of Delft, 2003.

Mangat, P. and Molloy, B. Prediction of long term chloride concentration in concrete. Materials and Structures, 27(6), pp. 338-346. 1994.

McCarter, W. J. Influence of Surface Finish on Sorptivity. Journal of Materials in Civil Engineering, 5(1), pp. 7. 1993.

McGrath, P. F. and Hooton, R. D. Re-evaluation of the AASHTO T259 90-day salt ponding test. In, Jul 05-10, Banff, Canada, pp. 1239-1248.

Mehta, P. K. and Monteiro, P. Concrete : Microstructure, Properties, and Materials, New York: McGraw-Hill. 2005.

Mindess, S., et al. Concrete, Upper Saddle River, NJ: Prentice Hall. 2003.

Mladenovič, A., et al. Alkali-silica reactivity of some frequently used lightweight aggregates. Cement and Concrete Research, 34(10), pp. 1809-1816. 2004.

Montgomery, D. C. and Runger, G. C. Applied Statistics And Probability for Engineers, NY: John Wiley & Sons, Inc. 2002.

Neville, A. and Aitcin, P. C. High performance concrete - An overview. Materials and Structures, 31(206), pp. 111-117. 1998.

Neville, A. M. Properties of concrete, Harlow, Essex: : Longman. 1995.

NT BUILD 443, Concrete, Hardened: Accelerated chloride penetration, Espoo, Finland: NordTest. 1995.

NTBUILD492 Concrete, Mortar and Cement-Based Repair Materials: Chloride migration coefficient from non-steady-state migration experiments, Espoo, Finland: NordTest. 1999.

Nyame, B. K. Permeability of normal and lightweight mortars. Magazine of Concrete Research, 37(130), pp. 44-48. 1985.

Oh, W. C. Effects of exposure conditions on the penetration of chloride ions into concrete, B. Eng. Thesis, National University of Singapore, 2003.

Ollivier, J. P., et al. Interfacial transition zone in concrete. Advanced Cement Based Materials, 2(1), pp. 30-38. 1995.

Olorunsogo, F. T. and Padayachee, N. Performance of recycled aggregate concrete monitored by durability indexes. Cement and Concrete Research, 32(2), pp. 179-185. 2002.

Otsuki, N., et al. Evaluation of $AgNO_3$ solution spray method for measurement of chloride penetration into hardened cementitious matrix materials. ACI Materials Journal, 89(6), pp. 587-592. 1992.

Otsuki, N., et al. Experimental study on influence of ITZ around aggregate on Cl^- diffusivity of concrete. Journal of the Society of Materials Science, 55(10), pp. 899-904 [in Japanese]. 2006.

Page, C. and Vennesland, Ø. Pore solution composition and chloride binding capacity of silica-fume cement pastes. Materials and Structures, 16(1), pp. 19-25. 1983.

Persson, B. Self-desiccation and its importance in concrete technology. Materials and Structures, 30(199), pp. 293-305. 1997.

Philip, J. R. The theory of infiltration: 4. Sorptivity and algebraic infiltration equations. Soil Science, 84, pp. 257-264. 1957.

Philleo, R. Concrete science and reality. Materials Science of Concrete II J. SKALNY and S. MINDESS, eds., American Ceramic Society, Westerville, OH, pp. 1991.

Powers, T. C. Structure and Physical Properties of Hardened Portland Cement Paste. Journal of the American Ceramic Society, 41(1), pp. 1-6. 1958.

Quenard, D., et al. Microstructure and transport properties of porous building materials. Materials and Structures, 31(5), pp. 317-324. 1998.

Rasheeduzzafar and Ehtesham Hussain, S. Effect of microsilica and blast furnace slag on pore solution composition and alkali-silica reaction. Cement and Concrete Composites, 13(3), pp. 219-225. 1991.

Ries, J. P. and Holm, T. A. A Holistic Approach to Sustainability For the Concrete Community - Lightweight concrete-Two Millennia of Proven Performance. ESCSI, Salt Lake City, UT. 2004.

RILEM TC 178-TMC: Testing and modelling chloride ingress into concrete, 4th Meeting. Bremen, Germeany: 1999.

Rindal, J., et al. Høvingen Sewage Plant: Documentation of Achieved Concrete Construction Quality. Department of Building Materials, Norwegian University of Science and Technology - NTNU, Trondheim. 2000.

Russell, H. G. ACI defines high-performance concrete. Concrete Internaltional, 21(2), pp. 56-57. 1999.

Sabir, B., et al. A water sorptivity test for martar and concrete. Materials and Structures, 31(8), pp. 568-574. 1998.

Samples, L. M. and Ramirez, J. A. Methods of corrosion protection and durability of concrete bridge decks reinforced with epoxy-coated bards phase 1. Final Report, FHWA/IN/JTRP-98/15, Purdue University College of Engineering. 1999.

Scrivener, K. L. Use of back scattered electron microscopy and image analysis to study the porosity of cement paste. In Proceedings of pore structure and permeability of cementitious materials, Boston, Massachusetts, U.S.A. , pp. 129-140.

Shane, J. D. and Jennings, H. M. Conductivity and microstructure of the interfacial transition zone measured by impedance spectroscopy. In RILEM Report 20, Engineering and Transport Properties of the Interfacial Transition Zone in Cementitious Composites. 1999.

Shehata, M. H., et al. The effects of fly ash composition on the chemistry of pore solution in hydrated cement pastes. Cement and Concrete Research, 29(12), pp. 1915-1920. 1999.

Stanish, K. D., et al. Testing the Chloride Penetration Resistance of Concrete: A Literature Review. FHWA Contract DTFH61-97-R-00022. 1997.

Stutzman, P. E. and Clifton, J. R. Sample preparation for scanning electron microscopy. 21st International Conference on Cement Microscopy, Las Vegas, Nevada, pp. 10-22. 1999.

Takada, K., et al. Experimental evaluation of autogenous shrinkage of lighweight aggregate concrete. Proceedings of international workshop Autoshrink'98, E. I. Tazawa, ed., E&FN Spon, London, Hiroshima, Japan, pp. 221-230. 1999.

Tang, L. Electrical accelerated methods for determining chloride diffusivity in concrete-current development. Magazine of Concrete Research, 48, pp. 173-179. 1996.

Tang, L. and Sørensen, H. E. Evaluation of the rapid test methods for measuring the chloride diffusion coefficients of concrete. SP Report 1998:42, Borås, Sweden. 1998.

Tang, L. P. and Nilsson, L. O. Rapid-determination of the chloride diffusivity in concrete by applying an electrical-field. ACI Materials Journal, 89(1), pp. 49-53. 1992.

Taylor, H. F. W. Cement chemistry, San Diego, CA: Academic Press. 1990.

Thomas, M. D. A. Chloride diffusion in High-performance lightweight aggregate concrete. Durability of Concrete, Proceedings 7th CANMET/ACI International Conference, SP234, Montreal, Canada, pp. 797-812. 2006.

Torgal, F. P. and Castro-Gomes, J. P. Influence of physical and geometrical properties of granite and limestone aggregates on the durability of a C20/25 strength class concrete. Construction and Building Materials, 20, pp. 1079-1088. 2006.

Valenta, O. The permeability and durability of concrete in aggressive conditions. Proceedings of 10th International Congress on Large Dams, Montreal, pp. 103-117. 1970.

Vaysburd, A. M. Durability of lightweight concrete bridges in severe environments. Concrete Internaltional, 18, pp. 33-38. 1996.

Vuorinen, J. APPLICATIONS OF DIFFUSION THEORY TO PERMEABILITY TESTS ON CONCRETE. PART I: DEPTH OF WATER PENETRATION INTO CONCRETE AND COEFFICIENT OF PERMEABILITY. Magazine of Concrete Research, 37(132), pp. 145-152. 1985.

Washburn, E. W. Note on method of determining the distribution of pore sizes in porous materials. In Proceeding of the National Academy of Science, USA, pp. 115-116.

Watson, A. J. and Oyeka, C. C. Oil permeability of hardened cement pastes and concrete. Magazine of Concrete Research, 33(115), pp. 85-95. 1982.

Weber, S. and Reinhardt, H. W. A New Generation of High Performance Concrete: Concrete with Autogenous Curing. Advanced Cement Based Materials, 6(2), pp. 59-68. 1997.

Whiting, D. Rapid determination of the chloride permeability of concrete. FHWA/RD-81119. 1981.

Wiens, U., et al. Influence of high Silica Fume and High Fly Ash Contents on Alkalinity of Pore Solution and Protection of Steel Against Corrosion In Proceedings of Fifth International Conference on the Use of Fly Ash, Silica Fume, Slag and Natural Pozzolan in Concrete, SP-153, Vol. 2, MI, USA pp. 741-762.

Zaharieva, R., et al. Assessment of the surface permeation properties of recycled aggregate concrete. Cement and Concrete Composites, 25(2), pp. 223-232. 2003.

Zhang, M.-H. Microstructure and Properties of High Strength Lightweight Concrete, PhD Thesis, The Norwegain Institute of Technology, 1989.

Zhang, M. H. and Gjørv, O. E. Microstructure of the interfacial zone between lightweight aggregate and cement paste. Cement and Concrete Research, 20(4), pp. 610-618. 1990.

Zhang, M. H. and Gjørv, O. E. Permeability of high-strength lightweight concrete. ACI Materials Journal, 88(5), pp. 463-469. 1991.

ZhangT, W. and Gjorv, O. E. An electrochemical method for accelerated testing of chloride diffusivity in concrete. Cement and Concrete Research, 24(8), pp. 1534-1548. 1994.

Zhutovsky, S., et al. Influence of cement paste matrix properties on the autogenous curing of high-performance concrete. Cement and Concrete Composites, 26, pp. 499-507. 2004.

PAPERS PUBLISHED, ACCEPTED AND SUBMITTED FOR PUBLICATION

Papers published or submitted to Journals for publication:

- Liu, X.M. and M.H. Zhang, Permeability of High-Performance Concrete Incorporating Presoaked Lightweight Aggregates for Internal Curing. Magazine of Concrete Research, 2010 62(2):79-89.

- Liu, X.M., K.S. Chia, and M.H. Zhang, Development of lightweight aggregate concrete with high resistance to water and chloride-ion penetration. Accept for publication to Cement and Concrete Composites, February 2010.

- Liu, X.M., K.S. Chia, and M.H. Zhang, Water absorption, Permeability, and Resistance to Chloride-ion Penetration of Lightweight Aggregate Concrete. Submitted to Construction and Building Materials in June 2009.

Papers published or accepted for publication in international conferences:

- Liu, X.M. and M.H. Zhang. Effect of cumulative lightweight aggregate volume in concrete on its resistance to chloride-ion penetration. in Excellence in concrete construction through innovation, Proceedings of the international conference on concrete construction. Kingston University, London, UK: CRC Press/Balkema. 9-10 September 2008.

- Liu, X.M., K.S. Chia, and M.H. Zhang, Development of lightweight aggregate concrete with high resistance to water and chloride-ion penetration, in sixth International Conference: Concrete under Severe Conditions Environment and Loading. Merida, Yucatan, Mexico. June 7-9, 2010.